MICROREGULATION OF ZEBRAFISH SKELETAL SYSTEM DEVELOPMENT BY MICRORNAS

by

XINJUN HE

A DISSERTATION

Presented to the Department of Biology
and the Graduate School of the University of Oregon
in partial fulfillment of the requirements
for the degree of
Doctor of Philosophy

September 2010

University of Oregon Graduate School

Confirmation of Approval and Acceptance of Dissertation prepared by:

Xinjun He

Title:

"Microregulation of Zebrafish Skeletal System Development by MicroRNAs"

This dissertation has been accepted and approved in partial fulfillment of the requirements for the Doctor of Philosophy degree in the Department of Biology by:

Judith Eisen, Chairperson, Biology
John Postlethwait, Advisor, Biology
Charles Kimmel, Member, Biology
William Cresko, Member, Biology
J. Andrew Berglund, Outside Member, Chemistry

and Richard Linton, Vice President for Research and Graduate Studies/Dean of the Graduate School for the University of Oregon.

September 4, 2010

Original approval signatures are on file with the Graduate School and the University of Oregon Libraries.

An Abstract of the Dissertation of

Xinjun He for the degree of Doctor of Philosophy

in the Department of Biology to be taken September 2010

Title: MICROREGULATION OF ZEBRAFISH SKELETAL SYSTEM DEVELOPMENT BY MICRORNAS

Approved: _____
Dr. John Postlethwait

MicroRNAs are small regulatory RNAs that control various developmental and physiological processes in animals and plants. To study the involvement of microRNAs in skeletal development, I manipulated the expression of miR-140, which is strongly expressed in the developing skeleton, and miR-196, which is located among the body patterning *Hox* cluster genes. I found that miR-140 regulates zebrafish palate formation by interfering with neural crest cell migration through the inhibition of the expression of the *platelet derived growth factor receptor alpha* (*pdgfra*) gene. I also found that miR-196 regulates zebrafish pectoral fin initiation by regulating the expression of the *retinoic acid receptor alpha b* (*rarab*) gene and that miR-196 is involved in the patterning of zebrafish pharyngeal arches and vertebrae. These results illuminate previously unknown regulatory mechanisms of skeletal development. I also reviewed current knowledge concerning microRNAs in skeletal development and evolution and discussed potential

relationships between microRNAs and skeletal disease.

This dissertation includes previously published and unpublished coauthored material.

CURRICULUM VITAE

NAME OF AUTHOR: Xinjun He

GRADUATE AND UNDERGRADUATE SCHOOLS ATTENDED:

University of Oregon, Eugene, Oregon
Tsinghua University, Beijing, China

DEGREES AWARDED:

Doctor of Philosophy, Biology, 2010, University of Oregon
Bachelor of Science, Biology, 2005, Tsinghua University

AREAS OF SPECIAL INTEREST:

Development of skeletal system in vertebrates
Biogenesis and function of microRNAs during development

PROFESSIONAL EXPERIENCE:

Graduate research assistant, Institute of Neuroscience, University of Oregon, Eugene, Oregon 2006-2010

Graduate teaching assistant, Department of Biology, University of Oregon, Eugene, Oregon 2005-2006

GRANTS, AWARDS AND HONORS:

Facebase Research grant, National Center for Research Resources, 2009-2011

Integrative Graduate Education and Research Traineeship (IGERT) Research Fellowship through the University of Oregon, 2009-2010

Genetics Training Grants, University of Oregon, 2009-2010

German "Deutscher Akademischer Austausch Dienst" (DAAD) grant through the graduate school of the University of Würzburg, Germany, 2009

Chinese Outstanding Self-financed Graduate Student Abroad Fellowship, Consulate General of the People's Republic of China in San Francisco, 2009

International Understanding Award, University of Oregon, 2008

PUBLICATIONS:

He, X., Yan, Y. L., Eberhart, J. K., Wagner, T. U., Herpin, A., Manfred, S. and Postlethwait, J. H. (2010). miR-196 regulates axial patterning and pectoral appendage initiation. *Dev Biol* Submitted.

Delaurier, A., Eames, B. F., Blanco-Sanchez, B., Peng, G., He, X., Swartz, M. E., Ullmann, B., Westerfield, M. and Kimmel, C. B. (2010). Zebrafish sp7:EGFP: A transgenic for studying otic vesicle formation, skeletogenesis, and bone regeneration. *Genesis* 2010 May 4.

Eames, B. F., Singer, A., Smith, G. A., Wood, Z. A., Yan, Y. L., He, X., Polizzi, S. J., Catchen, J. M., Rodriguez-Mari, A., Linbo, T. et al. (2010). UDP xylose synthase 1 is required for morphogenesis and histogenesis of the craniofacial skeleton. *Dev Biol* 341, 400-15.

Jovelin, R., Yan, Y. L., He, X., Catchen, J., Amores, A., Canestro, C., Yokoi, H. and Postlethwait, J. H. (2010). Evolution of developmental regulation in the vertebrate FgfD subfamily. *J Exp Zool B Mol Dev Evol* 314, 33-56.

He, X., Eberhart, J. K. and Postlethwait, J. H. (2009). MicroRNAs and micromanaging the skeleton in disease, development and evolution. *J Cell Mol Med* 13, 606-18.

Titus, T. A., Yan, Y. L., Wilson, C., Starks, A. M., Frohnmayer, J. D., Bremiller, R. A., Canestro, C., Rodriguez-Mari, A., He, X. and Postlethwait, J. H. (2009). The Fanconi anemia/BRCA gene network in zebrafish: embryonic expression and comparative genomics. *Mutat Res* 668, 117-32.

Eberhart, J. K., He, X., Swartz, M. E., Yan, Y. L., Song, H., Boling, T. C., Kunerth, A. K., Walker, M. B., Kimmel, C. B. and Postlethwait, J. H. (2008). MicroRNA Mirn140 modulates Pdgf signaling during palatogenesis. *Nat Genet* 40, 290-8.

Jovelin, R., He, X., Amores, A., Yan, Y. L., Shi, R., Qin, B., Roe, B., Cresko, W. A. and Postlethwait, J. H. (2007). Duplication and divergence of fgf8 functions in teleost development and evolution. *J Exp Zool B Mol Dev Evol* 308, 730-43.

Zhao, C., He, X., Tian, C. and Meng, A. (2006). Two GC-rich boxes in huC promoter play distinct roles in controlling its neuronal specific expression in zebrafish embryos. *Biochem Biophys Res Commun* 342, 214-20.

ACKNOWLEDGMENTS

I wish to express sincere appreciation to Prof. John Postlethwait for his help with my graduate study and the assistance in the preparation of this manuscript. In addition, special thanks are due to Dr. Yi-Lin Yan and other members in the Postlethwait lab, who were there to help on most of the research I have done for this manuscript. I thank the members of my committee for their valuable input for my research and dissertation writing. I also thank my wife for her help on this manuscript formating. The research was supported in part by grants from the National Center for Research Resources (NCRR) (R01 RR10715 and R01 RR020833 to Prof. John Postlethwait); the National Institutes of Health (NIH) (5 P01 HD22486, 1 R01 RR020833, and 1 U01 DE020076 to Prof. John Postlethwait, P01 HD22486 to Profs. Charles Kimmel and John Postlethwait; 5 K99 DE018088 to Dr. Johann Eberhart); the National Institute of Child Health and Human Development (NICHD) (R00 DE018088 to Dr. Johann Eberhart). The work is also supported by the Deutsche Forschungsgemeinschaft (GRK 1048 to Prof. Manfred Schartl), Alexander von Humboldt Foundation to Prof. John Postlethwait; by the DAAD (German Academic Exchange Services) through the Graduate School of Life Sciences, University of Würzburg to myself, by Genetics Training Grant from the University of Oregon, and by the IGERT Research Fellowship from National Science Foundation through the University of Oregon.

To my parents, who supported me of my every decision,
and my wife, who always accompanies me wherever I go and whatever happens.

TABLE OF CONTENTS

Chapter Page

Chapter Page

Chapter Page

Chapter Page

LIST OF FIGURES

Figure Page

Figure Page

LIST OF TABLES

Table Page

CHAPTER I

INTRODUCTION

A variety of mechanisms regulate skeletal system development. Mis-regulation of many genes involved in skeletogensis result in failure or malformation of the skeleton. microRNAs (miRNAs) have been shown to provide an important additional layer of regulation in various aspects of development, raising the question of the role of miRNAs in skeletal system development. Here I explore the following questions: (1) Do miRNAs regulate skeletogensis? (2) If so, which miRNAs regulate skeletogenesis? (3) What genes are the targets of skeletal miRNAs? And (4), how do miRNAs regulate their target genes to control skeletogenesis?

This chapter provides general background information about miRNAs and skeletogenesis. In addition, it provides related background information specifically about two miRNAs on which I focused to understand their function during zebrafish skeletal system development: miR-140 and miR-196.

1.1. MicroRNA and Development

MicroRNAs (miRNAs) are small non-coding RNAs that are about 22 nucleotides (nts) long. These miRNA genes usually are processed from long primary transcripts (pri-miRNAs) (Denli et al., 2004; Gregory et al., 2004; He and Hannon, 2004; Lee et al., 2003). Based on their genomic contexts and the nature of their biogenesis, miRNAs are largely categorized into two different groups. One group is intergenic miRNAs that are usually found between protein coding genes and they are predicted to utilize their own transcriptional machineries to produce pri-miRNAs (Lee et al., 2004). The other group are intronic miRNAs that are believed to be the byproducts of spliced introns from their

host genes (Ruby et al., 2007). Pri-miRNAs form local stem-loop structures *in vivo* at the miRNA sequence. The primary transcripts of both intergenic and intronic miRNAs are then sequentially processed in the nucleus by the Drosha/DGC8 complex into 80-100 nts long miRNA precursors (pre-miRNAs) by cutting out the hairpin structures of miRNAs (Lee et al., 2003). Then, with the help from the cytoplasmic membrane-binding protein Transportin-5 (Kim, 2004), pre-miRNAs exit the nucleus and are further processed by Dicer into about 22 nts long mature miRNA duplexes by cutting off the loop region (Jaskiewicz and Filipowicz, 2008). In the cytoplasm, with the help from miRNA-induced silencing complex (miRISC), miRNA duplexes release their passenger strands (the strands without coding miRNAs) while keep the guide strands (the working strands, which has the miRNA mature sequences) (Rand et al., 2005). In the miRISC complexes, the guide strands then recognize their target genes by base-pairing with the targeted messenger RNA sequences to either induce target messenger cleavage or protein production inhibition to regulate target gene expression (Rand et al., 2005). Thus, miRNAs act as a negative regulator on the post-transcriptional level to regulate gene expression.

MiRNAs can regulate a large portion of gene expression *in vivo*. There are hundreds of miRNAs identified experimentally in each genome, ranging from nematodes to human (Aboobaker et al., 2005; Boehm and Slack, 2005; Giraldez et al., 2005; Kidner and Martienssen, 2005). For example, the human genome has 939 and the zebrafish genome has 352 miRNAs (miRBase, http://www.miRBase.org, Release 15, April, 2010) (Griffiths-Jones et al., 2006; Griffiths-Jones et al., 2008). However, the miRNA collection at miRBase database contains 14197 pre-miRNAs and 15632 mature miRNA entries in release 15, and this increased 3377 pre-miRNA in release 14 (June, 2009). These miRNAs in the miRBase database were deposited from 133 species ranging from virus to human (http://www.miRBase.org). Target prediction based on base-pairing algorithms often predict up to a thousand target genes for each miRNA. Although computer programs can predict miRNA target genes, functional studies are required to validify and to fully understand miRNA functions during development and physiology.

It is predicted that at least 60% of human genes are regulated by miRNAs (Friedman et al., 2009), implying the importance of miRNA regulation. The *dicer* mutation that ablates all miRNA production in nematodes causes sterility, while knockout of *Dicer* in mice results in early embryonic lethality (Bernstein et al., 2003). Furthermore, studies by over-expression or knockdown of individual miRNA showed that miRNAs are widely involved in various aspects of development and physiology (Boehm and Slack, 2005; Chen et al., 2006; Eberhart et al., 2008; Hornstein et al., 2005; Jiang et al., 2006; Tuddenham et al., 2006; Wang et al., 2009; Zhang et al., 2009). Thus, miRNAs impose another layer of gene regulation at the post-transcriptional level.

In zebrafish, 352 miRNAs have been identified so far and most of these miRNAs are conserved across vertebrates (Ason et al., 2006; Wienholds et al., 2005). An expression study that investigated 115 Zebrafish miRNAs showed that most of these miRNAs were expressed in a tissue- and time-specific manner (Wienholds et al., 2005). Zebrafish with mutation in *dicer* have developmental delay, finally dying in two to three weeks after fertilization (Giraldez et al., 2006). Detailed study showed that zebrafish mutant embryos undergo abnormal morphogenesis of the brain, heart, and other organs, although they can pass the early embryonic stage, suggesting that most aspects of differentiation are under the control of Dicer (Kanellopoulou et al., 2005). Thus, zebrafish has very similar miRNA biology as other vertebrate species.

1.2. Zebrafish Skeletogenesis

The skeletal system is a novel invention for animals. It makes the animal body strong but with enough freedom for locomotion. The skeletal system also supports the body weight and protects soft tissues from impacts. There are cartilage and bone in the vertebrate skeleton system. In cartilage, cartilage cells are surrounded by thick extracellular matrix that includes big extra celluar matrix protein and sugars; bone is a calcium matrix with only a few living cells. Cartilage and bone both develop from mesenchyme that derives from various origins. Mesenchyme derived from neural crest

forms palate and pharyngeal arches; paraxial mesoderm derived mesenchyme differentiates and builds ribs and vertebral column; and lateral plate mesoderm derived mesenchyme gives rise to limb bones. During embryogenesis, there are two major processes through which bones are formed. Some bones form through endochondral ossification and others by intramembranous ossification (Huysseune and Sire, 1992; Javidan and Schilling, 2004; Lefebvre and Smits, 2005). Mesenchyme forms cartilage first in the endochondral skeleton, then bone forms on a cartilage model and finally replaces cartilage. This includes bones of lower jaw, the limbs in tetrapods and paired fins in fish. Intramembranous ossification forms most part of the flat bone of the skull. In intramembranous ossification, mesenchymal cells bypass the cartilage model and differentiate directly into osteoblasts, which secrete extracellular matrix that becomes mineralized, thus forming bone.

Like human and other vertebrate species, zebrafish develops its skeletal system during the embryonic stage (Fisher and Halpern, 1999; Westerfield, 1995). Cartilage forms as early as 2 days post-fertilization (dpf) and continues to adulthood. The earliest observed structure positive for Alcian blue, which stains cartilage, is the palate of zebrafish, which is a single layer of cartilage cells that are derived from post-migratory neural crest cells (Eberhart et al., 2008; Wada et al., 2005). At 1 dpf, neural crest cells from midbrain and hindbrain migrate anteriorly to beneath the brain and upper region of the oral cavity (Eberhart et al., 2008; Wada et al., 2005). There, these neural crest cells differentiate into cartilage cells and start to secrete cartilage specific collagens, including collagen type II. Then starting from 3 dpf, cartilages in pharyngeal arches and paired pectoral fins start to differentiate. Cleithrum and opercular bone are intramembranous bones first visible at 3 dpf. At about 5 dpf, the Meckels cartilage, the first pharyngeal arch that is derived from neural crest, starts to ossify. The whole process of zebrafish skeletogenesis continues until two to three months after birth (Bird and Mabee, 2003; Fisher and Halpern, 1999; Neuhauss et al., 1996; Rebagliati et al., 1998).

Skeletogenesis is a tightly regulated process. Mis-regulation of genes involved in skeletogenesis can result in failure or malformation of the skeletal system. Several genetic pathways have been shown to regulate the developmental programs that specify the type, size and shape of each skeletal element. Sox9 and Runx2 transcription factors are the two master genes that together regulate the specification and differentiation of cartilage and bone (Depew et al., 2005; Kawakami et al., 2006; Komori, 2003; Okazaki and Sandell, 2004; Samee et al., 2007). Other signal pathways, including Bmp, Hh, Wnt and Fgf and some extra cellular matrix components including collagens, Sparc, and glycosaminoglycans are also extensively involved in the skeletal morphogenesis (Blair et al., 2002; Cancedda et al., 2000; Chen and Deng, 2005; Day and Yang, 2008; Ehlen et al., 2006; Goldring et al., 2006; Holmbeck, 2005; Kronenberg, 2006; Ornitz, 2005; Velleman, 2000; Wu et al., 2007).

Due to the small size of the miRNA binding sites on miRNA targets, in principle, members of any or all of genetic pathways are potentially subject to miRNA regulation. Thus, it provides numerous genetic inroads to understand the roles of miRNAs in skeletal development, morphological evolution, and skeletal diseases. To date, however, there has been limited study to understand the regulation of skeletal development by miRNAs, in spite of the importance of miRNAs during development. To understand the regulation of skeletal system development, I overexpressed and knocked down miRNAs and found that miR-140 is important for palatogenesis, while miR-196 is involved in skeletal system patterning.

1.3. *Mir140* and Palatogenesis

From the study of Wienholds group and research results from medaka, chicken (Ason et al., 2006; Hicks et al., 2008; Wienholds et al., 2005), as well as my preliminary study, I found that microRNA miR-140 (*mir140*, *mirn140*) is strongly and specifically expressed in developing cartilage tissues. With the skeletal study expertise in the Postlethwait lab,

this miRNA fits as a good tool to understand miRNA function during skeletal development. Thus, I chose miR-140 to start with to investigate the regulation of zebrafish skeletogenesis by miRNAs. I found that miR-140 is involved in the regulation of palatogenesis in zebrafish by regulating the *platelet derived growth factor alpha* (*pdgfra*) gene expression. Mis-regulation of miR-140 as well as mutation of *pdgfra* induces cleft lip and palate in zebrafish. The importance of miR-140 and *pdgfra* is conserved among fish and human. Mutation of *pdgfra* gene in mice or human both result in cleft lip and palate disease. Thus, studying of zebrafish miR-140 provides a good example to understand the role of miRNAs in development of skeletal systems and imply the possibility to understand miRNA function in disease model study.

Cleft palate and other craniofacial diseases are common in humans and have complex cellular and genetic etiologies. In amniotes, the palate serves to separate the nasal cavity from the oral cavity and is generated through an intricate series of morphogenic events that include early neural crest cell migration and cell-cell signaling during the formation of facial prominences, as well as later generation and fusion of palatal shelves. While later events involving palatal shelves have not been described in zebrafish, palatal precursors follow homologous migratory pathways rostral and caudal to the eye to condense upon the oral ectoderm in amniotes (Osumi-Yamashita et al., 1994) as well as zebrafish (Trainor, 2003; Wada et al., 2005). Evidence continues to accumulate that the early signaling environment governing palatogenesis is also largely homologous (Eberhart et al., 2006; Hilliard et al., 2005; Hurria et al., 2003; Wada et al., 2005). For instance, disruption of Hh signaling causes cleft palate in humans and zebrafish (Eberhart et al., 2006; Roessler et al., 1996; Wada et al., 2005), and palatogenesis in zebrafish and amniotes involves shared expression patterns of genes whose disruption causes cleft palate, such as *Fgf8* (Bachler and Neubuser, 2001; Eberhart et al., 2006; Riley et al., 2007) and *Pdgf receptor a* (Liu et al., 2002; Soriano, 1997b; Tallquist and Soriano, 2003a).

In mouse, the Pdgf family consists of four soluble ligands, Pdgfa, Pdgfb, Pdgfc, and Pdgfd as well as two receptor tyrosine kinases, Pdgfra and Pdgfrb (Betsholtz et al., 2001). Pdgf signaling regulates a myriad of biological processes as demonstrated by analyses of mouse Pdgf ligand and receptor mutants (Betsholtz et al., 2001). Mice null for *Pdgfra* have a facial clefting phenotype that includes cleft palate (Soriano, 1997b; Tallquist and Soriano, 2003a). This facial phenotype is fully recapitulated in mice doubly mutant for *Pdgfa* and *Pdgfc* (Ding et al., 2004), although most *Pdgfc* mutants have cleft palate (Ding et al., 2004). *Pdgfa* mutants exhibit either severe phenotypes, dying before palatogenesis, or less severe phenotypes without cleft palate (Bostrom et al., 1996), but most *Pdgfc* mutants have cleft palate. The inability to examine the severe phenotypic class for defects in palatogenesis makes it unclear whether *Pdgfa* only interacts synergistically with *Pdgfc* during palatogenesis or whether *Pdgfa* has input into palatogenesis separate from *Pdgfc*. While neural crest require the reception of Pdgf signaling during palatogenesis in mouse (Tallquist and Soriano, 2003a), the palatogenic cell behaviors regulated by Pdgf signaling or how Pdgf signaling is modulated during palatogenesis are unknown.

MicroRNAs provide a unique mechanism for modulating signaling pathways (Hornstein and Shomron, 2006; Lee et al., 2006; Shalgi et al., 2007; Song and Tuan, 2006). Skeletogenic, including palatal, precursors express miR-140 (mirn140) in teleosts (Wienholds et al., 2005) and amniotes (Ason et al., 2006; Darnell et al., 2006; Tuddenham et al., 2006), suggesting that miR-140 may modulate signaling during palatogenesis across vertebrate species. Despite the function of miRNAs in development and the importance of neural crest cells in evolution and disease, no miRNA has yet been shown to regulate neural crest development or cellular behaviors.

One of the most important neural crest cell behaviors is their migration along highly stereotyped pathways to give rise to a diverse array of differentiated cell types. Across vertebrate species, neural crest cells at cranial levels migrate in one of three neural crest streams and the most anterior, or first, stream will migrate rostrally and caudally around the eye into the first pharyngeal arch and contribute to the jaw and palatal skeleton

(Trainor and Krumlauf, 2001). While research in zebrafish and amniotes have uncovered cues that regulate migration of cranial neural crest cells in all neural crest streams (Gammill et al., 2007; McLennan and Kulesa, 2007; Yu and Moens, 2005), nothing is known of what cues specifically guide neural crest-derived palatal precursors to the first pharyngeal arch.

In Chatper II of this manuscript I show that miR-140 attenuates Pdgf-mediated attraction of neural crest-derived palatal precursors. Embryos injected with miR-140 duplex and *pdgfra* mutants shared craniofacial phenotypes, including cleft palate and loss of oral ectoderm gene expression, suggesting an interaction between miR-140 and *pdgfra*. Binding sites for miR-140 are conserved in the 3' untranslated region (UTR) of *pdgfra* across vertebrate species and miR-140 interacts with the 3'UTR of *pdgfra* transcript to negatively-regulate Pdgfra protein production. Migratory neural crest cells co-expressed miR-140 and *pdgfra*, while palatal precursors follow a migratory pathway delimited by expression of the ligand, *pdgfaa*. Pdgf is an attractant cue for neural crest, as demonstrated by implantation of Pdgfa coated beads. Pdgf loss of function experiments showed that neural crest cell dispersion and migration of rostral neural crest cells around the optic stalk required Pdgf signaling. Attenuation of Pdgf signaling via miR-140 is critical for rostrally migrating neural crest to migrate beyond the optic stalk, a source of Pdgfaa, onward to the oral ectoderm, another Pdgfaa source. These results demonstrate how carefully orchestrated modulation of Pdgf signaling regulates palatal morphogenesis.

This part of the dissertation includes previously published co-authored material.

1.4. *Mir196* and Zebrafish Body Patterning

Zebrafish genome contains five copies of miR-196 gene, derived from whole genome duplication events (Amores et al., 1998). Expression studies by Wienholds et al. (Wienholds et al., 2005) showed that miR-196 is expressed in a pattern like its neighbor *hox* genes, *hox8* and *hox9,* in the central nerve system of developing zebrafish. In mice

and chicken, others have shown that miR-196 can regulate multiple *hox* cluster protein coding genes including *hoxB8*, indicating the complexity of miR-196 regulation and its function (Hornstein et al., 2005; McGlinn et al., 2009b; Yekta et al., 2004). My preliminary survey of the binding sites in the zebrafish *hox* gene 3'UTR by miR-196 have identified multiple *hox* genes as potential targets for miR-196 in zebrafish. Then, I did overexpression and knockdown analyses of miR-196 in zebrafish at the early embryonic stage and found that miR-196 controls zebrafish pharyngeal arch segmentation, controls anterior axial skeletal segmentation and, miR-196 overexpression inhibits pectoral fin initiation by reducing *retinoic acid receptor alpha-b* (*rarab*) expression through which miR-196 interacts with retinoic acid (RA) signal. These findings indicate that miR-196 is acting as an embryonic patterning gene during the early embryonic development stage.

Hox cluster genes control animal body patterning in radiata and in both protosotome and deuterostome bilateria (Finnerty et al., 2004; Postlethwait and Schneiderman, 1969; Wellik, 2009). In vertebrates, *Hox* cluster genes control the anterior-posterior body axis, including the identity of vertebrae and pharyngeal arches and the axes of body appendages, and they are important for the development of other organ systems, including blood cells and the vasculature (Antonchuk et al., 2001; Hunt et al., 1998; Pearson et al., 2005; Pruett et al., 2008). *Hox* clusters evolved initially by tandem gene duplication followed by a series of whole genome duplication events in vertebrates that provided tetrapods with four *Hox* clusters and most teleost fish with seven or eight *Hox* clusters (Amores et al., 1998; Gehring et al., 2009).

Hox genes are expressed in a collinear fashion along the anterior-posterior body axis during early development, with 3' genes controlling anterior and 5' genes regulating more posterior organ development (Duboule and Morata, 1994); as a result, *Hox* gene mutations can delete vertebrae or transform vertebral identity and remove or reduce limb skeletal elements (Chen and Capecchi, 1997; Davis et al., 1995). *Hox* genes act by controlling downstream transcription factors that regulate signaling events controlling body segmentation and organ initiation. Some *Hox* genes are themselves directly

regulated by the extracellular signaler retinoic acid (RA), which regulates axis and limb development (Grandel et al., 2002; Nolte et al., 2003).

Bilaterian *Hox* clusters contain genes encoding microRNAs (miRNAs), small non-coding RNAs that generally bind to 3' untranslated regions (UTRs) of messenger RNAs and regulate their stability or translation (Vella et al., 2004). For the three human *HOX* cluster miRNAs, *Mir10* is broadly distributed among bilaterians, *Mir196* is conserved among vertebrates, and *Mir615* appears to be limited to mammalian genomes [see miRBase collection at http://www.miRBase.org (Griffiths-Jones et al., 2008)]. In zebrafish, the *hoxdb* cluster lost all of its protein-coding genes, but surprisingly, *mir10* persisted as the only vestige of this *hox* cluster (Woltering and Durston, 2006). The similarity of *hox*-cluster miRNA expression patterns to those of nearby *hox* genes suggested the hypothesis that *hox*-cluster miRNAs and *hox*-cluster genes share regulatory mechanisms (Wienholds et al., 2005). Furthermore, the discovery that the 3' UTRs of several *hox*-cluster genes contain predicted binding sites for either miR-196 or miR-10 suggested the hypothesis that some *hox* genes might be regulated by *mir10* and/or *mir196* (He et al., 2009a; Hornstein et al., 2005; Kawasaki and Taira, 2004; Woltering and Durston, 2008; Yekta et al., 2004; Yekta et al., 2008). For example, *Mir10* is involved in the regulation of metastasis by regulating *Hoxd10* in cell culture and *hoxb1a* and *hoxb3a in vivo* (Lund, 2009; Ma et al., 2007; Woltering and Durston, 2008). MiR-196 binds to *HoxB8* mRNA, thereby accelerating its cleavage. This interaction has been hypothesized to be important for the outgrowth of hindlimb buds (Hornstein et al., 2005; Kawasaki and Taira, 2004; Yekta et al., 2004). MiRNA-196 can also repress *BACH1* expression in human liver cells (Hou et al., 2009). Knockdown of miR-196 in chick embryos leads to a homoeotic transformation of a cervical vertebra to thoracic identity (McGlinn et al., 2009a). Because no phenotype has yet been described for the over-expression of *mir196* in embryos and no phenotype has been described in other tissues where *mir196* is also expressed, we do not yet fully understand its roles in development or the mechanisms by which it acts.

In this manuscript I show that precise levels of *mir196* are required to initiate development of the pectoral appendage, to develop the correct number of pharyngeal arches, and to specify correct number and identity of rostral vertebrae and ribs. I show that miR-196 acts on pectoral appendage development by altering retinoic acid signaling via fine-tuning the expression of retinoic acid receptor Rarab.

This part of the dissertation includes previously unpublished co-authored material.

CHAPTER II

MICRORNA MIRN140 MODULATES PDGF SIGNALING DURING PALATOGENESIS

This chapter includes previous published co-authored material. This work was published in volume 40 of the journal *Nature Genetics* in March 2008. I performed functional study of *mirn140* (miR-140, *mir140*); Dr. Johann Eberhart initially identified allele $pdgfra^{b1059}$ ($pdgfra^{-/-}$) and performed functional study of *pdgfra* gene; Mary Swartz, Yi-Lin Yan, Hao Song, Taylor Boling, Allison Kunerth and Macie Walker helped Dr. Johann Eberhart and me to perform and analyze experiments and results; Profs. Charles Kimmel and John Postlethwait supervised and helped on experimental design, data analysis and manuscript writing; Prof. John Postlethwait was the principal investigator for this work. This work is the first major project for my Ph.D. dissertation.

2.1. Palatogenesis and MicroRNAs

As discussed in Chapter I, palatogenesis is a complex process in development. Misregulation of any step during palatogenesis may result in malformation of palate structure. However, even with extensive efforts to uncover the regulation of palatogenesis, we still do not fully undertand how palate is formed and which signals have been involved. The expression specificity of *mirn140* (*mir140*, miR-140) in the developing palate intrigued me to study the function of miR-140 and try to answer the question if this microRNA is involved in and play a role during zebrafish palatogenesis.

2.2. Results

2.2.1. *Mirn140* and Pdgf Signaling Regulate Palatal Development

Skeletal precursors across vertebrate species express *mirn140* (Ason et al., 2006; Darnell et al., 2006; Tuddenham et al., 2006; Wienholds et al., 2005) and *mirn140* occupies the orthologous intron in *wwp2* of zebrafish, human, and other vertebrates, prompting the hypothesis that Mirn140 plays a conserved role in craniofacial skeletogenesis across vertebrate species. To determine the *in vivo* role of *mirn140* during zebrafish craniofacial skeletogenesis, we injected embryos with active *mirn140* duplex. At 4 days post-fertilization (dpf), *mirn140* duplex injected embryos had a profound facial phenotype, including cranial hemorrhaging and a hypoplastic roof of the mouth (**Fig. 2.1a, b, d, e**). This hypoplasia suggested that the zebrafish skeletal palate was malformed and alcian/alizarin staining confirmed the presence of palatal defects, including cleft palate, in *mirn140* duplex injected embryos (**Fig. 2.1g, h, j, k**).

A clue to the target of Mirn140 during palatogenesis came from the fact that the array of facial defects seen in *mirn140* duplex injected embryos precisely phenocopy those observed in *pdgf receptor alpha*^{b1059} (*pdgfra* ^{b1059} or *pdgfra*$^{-/-}$) mutants (**Fig. 2.1c, f, i, l**), identified in our forward genetic screen for craniofacial mutants (**Fig. 2.1m**). The *pdgfra*^{b1059} allele is likely hypomorphic since, unlike mouse *Pdgfra* mutants (Soriano, 1997b) and *mirn140* duplex injected zebrafish embryos, zebrafish *pdgfra* mutants had normal somites and were typically of similar size to their wild-type siblings (data not shown). The molecular nature of the *pdgfra*^{b1059} allele is also supportive of *b1059* being hypomorphic. In *pdgfra*^{b1059} an I to N mis-sense mutation is present near the activation loop of the second tyrosine kinase domain of the receptor. The sequence of this kinase core is highly conserved in Pdgfra across species and even across other related tyrosine kinase receptors such as Pdgfrb and Kit (**Fig. 2.1m**). Therefore the non-conservative hydrophobic to hydrophilic amino acid substitution is likely to greatly attenuate receptor signaling. Pharmacologic inhibition of Pdgf receptor signaling, via Pdgfr inhibitor V, phenocopies the *b1059* allele and injection of *pdgfra* mRNA can rescue the palate of

b1059 embryos, providing confirmation that *b1059* lesions *pdgfra*. It is noteworthy that injection of *pdgfra* mRNA occasionally caused palatal defects in wild-type embryos (see below), suggesting that the overall level of Pdgf signaling must be strictly regulated for proper development of the palatal skeleton.

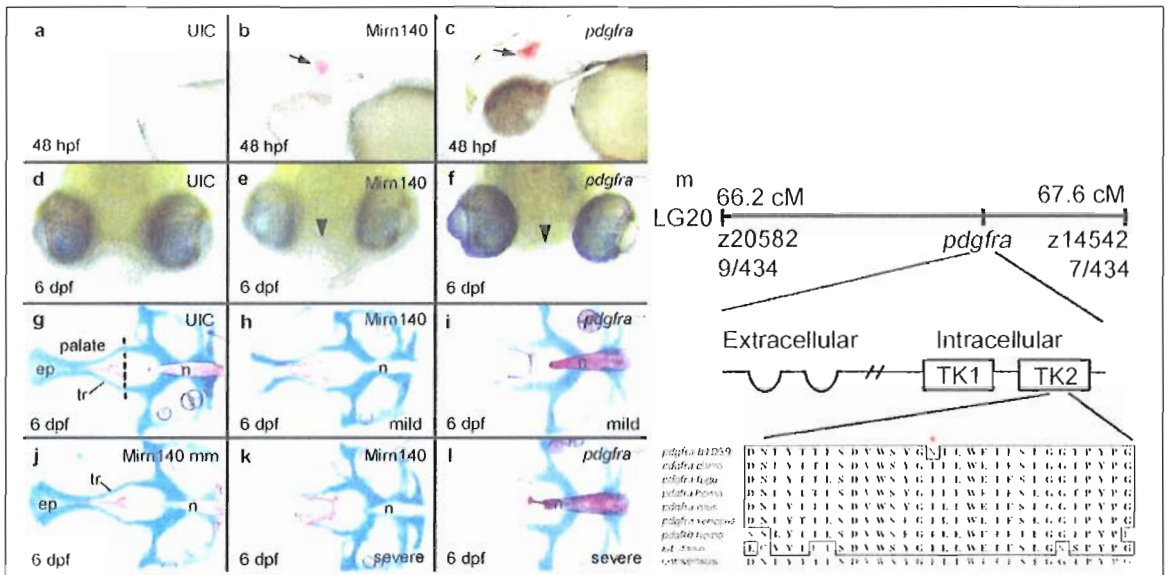

Fig. 2.1. Overexpression of *Mirn140* Phenocopies *Pdgfra* Mutants. (**a-c**) Compared to uninjected controls (UIC) (**a**), animals injected with *mirn140* duplex had cranial hemorrhaging at 48 hpf (**b**), mimicking the phenotype of zebrafish (**c**) and mouse *pdgfra* mutants (Soriano, 1997a; Tallquist and Soriano, 2003b). (**d-f**) Lateral views of 144 hpf larvae show that, compared to UIC (**d**), *mirn140* duplex injected (**e**) and *pdgfra* mutant (**f**) animals develop similarly shaped faces (**g-l**) Alcian/Alizarin-stained palates of 144 hpf uninjected controls (UIC) (**g**) or *mirn140* mis-match control injected embryos (**j**) are fused in the midline, but Mirn140 duplex injected (**h,k**) and *pdgfra* mutants (**i,l**) show both mild (**h,i**) and severe (**k,l**) phenotypes that include complete clefting of the palatal skeleton. The *b1059* allele mutates *pdgfra* (**m**). *b1059* was genetically mapped to linkage group 20 (LG20) between the polymorphic markers z20582 and z14542, with 9 cross-overs and 7 cross-overs, respectively, out of 434 meioses. Sequence analysis of wild-type and *b1059* mutant embryos revealed a missense mutation in the second tyrosine kinase (TK) domain of *pdgfra*. Protein sequence alignment of this region of the second tyrosine kinase domain (amino acids 841-870) of Pdgfra and related receptors shows isoleucine 855 to asparagine missense mutation (asterisk) in the second tyrosine kinase domain. ep=ethmoid plate, n=notochord, tr=trabeculae. Scale bar=50μm.

As in amniotes, the zebrafish palatal skeleton rests on the roof of the oral ectoderm. In addition to their skeletal defect, the oral ectoderm of both *mirn140* duplex injected embryos and *pdgfra* mutant embryos failed to express regulatory genes such as *pitx2*

(**Fig. 2.2a-c**) and *shha* (formerly called *shh*; **Fig. 2.2d-f**). The oral ectoderm is also misshapen in *mirn140* duplex injected embryos and *pdgfra* mutants (compare **Fig. 2.2a to 2.2b, c**). This morphological defect is not due to a developmental delay because *mirn140* duplex injected embryos and *pdgfra* mutants as old as 6 dpf, the latest stage examined, display this defect. The underlying mechanism of this lip defect is unclear; we do not detect elevated levels of cell death or loss of cell proliferation in the oral ectoderm (data not shown). Additionally, the epithelium is present and its fate map is not altered as determined by anti-pan-cadherin antibody staining and Kaede photoconversion, respectively. Collectively, the similarity of defects observed in *mirn140* duplex injected embryos and *pdgfra* mutants suggest a model where Mirn140 modulates Pdgf signaling, coordinating development of the palatal skeleton and the oral ectoderm.

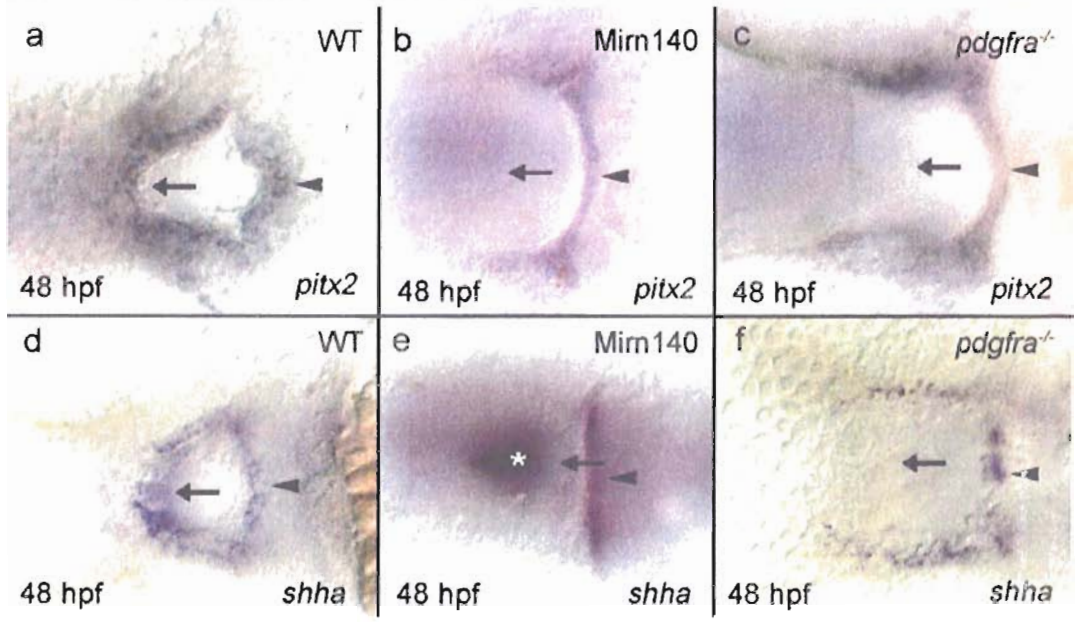

Fig. 2.2. The Oral Ectoderm is Similarly Disrupted in Mirn140 Duplex Injected Embryos and *Pdgfra* Mutants. Ventral views, anterior to the left, of oral ectoderm labeled with *pitx2* (**a-c**) and *shha* (**d-f**) riboprobe in wild-type (**a, d**), *mirn140* duplex injected embryos (**b,e**) and *pdgfra* mutants (**c,f**). The roof of the oral ectoderm (arrows), adjacent to the normal location of palatal precursors, expressed neither gene in *mirn140* duplex injected embryos or *pdgfra* mutants. Loss of gene expression was specific to the roof of the oral ectoderm as the floor of the oral ectoderm expressed both *pitx2* and *shha* (arrowheads). Asterisk in **e** marks *shha* staining in the ventral brain.

2.2.2. *Mirn140* Regulates Pdgfra Protein Levels during Palatogenesis

If Mirn140 modulates Pdgf signaling, we expect to find Mirn140 binding sites in the 3' UTR of one or more members of the Pdgf signal pathway. Sequence comparisons of the Pdgf signaling family revealed Mirn140 binding sites in the 3' UTR of *pdgfra* in all sequenced vertebrate genomes examined (data not shown). In contrast to *pdgfra*, the zebrafish Pdgf ligands *pdgfaa*, *pdgfab*, *pdgfba*, and *pdgfbb* do not possess predicted Mirn140 binding sites and although *pdgfc* has a Mirn140 binding site, *pdgfc* is not expressed in the craniofacial region until 30 hpf, after the time during which we show

that Mirn140 has its effects on palatogenesis (see below). An alternative hypothesis, that Mirn140 has its effects on palatogenesis through inhibition of *hdac4*, as observed in mouse tissue culture cells (Tuddenham et al., 2006), is unlikely. Zebrafish *hdac4* does not have a good candidate Mirn140 binding site, nor does the scheduling or quantity of bone in *mirn140* over-expression or knockdown animals change as predicted by the tissue culture studies, suggesting that *hdac4* is not a significant *in vivo* target of Mirn140 in zebrafish embryos. These results suggest that Mirn140 has its effects on palatal morphogenesis through inhibition of Pdgfra.

To directly test whether Mirn140 negatively regulates Pdgfra, we fused *GFP* to the 3'UTR of zebrafish *pdgfra* (GFP-*pdgfra*, **Fig. 2.3b**). Embryos co-injected with Mirn140 duplex and GFP-*pdgfra* displayed a loss of GFP fluorescence (**Fig. 2.3c-e, g**), compared to controls. In contrast to GFP-*pdgfra*, reporter constructs fusing *GFP* to the 3'UTR of *nog3*, which lacks a Mirn140 binding site, failed to respond to *mirn140* duplex (data not shown). These results indicate that the 3'UTR of *pdgfra* carries a sequence that responds to Mirn140. To learn if endogenous Mirn140 acts via the *pdgfra* 3'UTR, we injected embryos with *mirn140* morpholino and tested expression of the *GFP-pdgfra* reporter. Knockdown of endogenous Mirn140 elevated GFP fluorescence compared to Mirn140 mismatch or morpholino uninjected animals (**Fig. 2.3c, f, g**). These experiments show that the 3'UTR of *pdgfra* is a target of Mirn140.

Because microRNAs have many predicted targets (Griffiths-Jones et al., 2006), we co-injected *mirn140* duplex along with a synthetic *pdgfra* mRNA lacking the Mirn140 binding site (*pdgfra**) to test if the effects of *mirn140* on craniofacial development are mediated by Pdgfra. Our results showed that the palates of embryos co-injected with *mirn140* duplex and *pdgfra** mRNA were more normal than animals injected with *mirn140* duplex alone (**Fig. 2.3h-k**), indicating that the cleft palate phenotype of *mirn140* duplex injected embryos is primarily due to loss of Pdgf signaling.

Our results show that Mirn140 attenuates Pdgf signaling and that Pdgf signaling is required for palatogenesis, but the cellular events mediated by Pdgf signaling during

palatogenesis are unknown. Examining neural crest migration in mouse *Pdgfra* mutants uncovered no defect (Tallquist and Soriano, 2003a), yet early phenotypic changes in zebrafish postmigratory crest (described below) were suggestive that migration of palatal precursors was abnormal. Therefore, we examined the expression of *mirn140* and Pdgf signaling components during crest migration to elucidate how Pdgf signaling may be involved in neural crest cell migration.

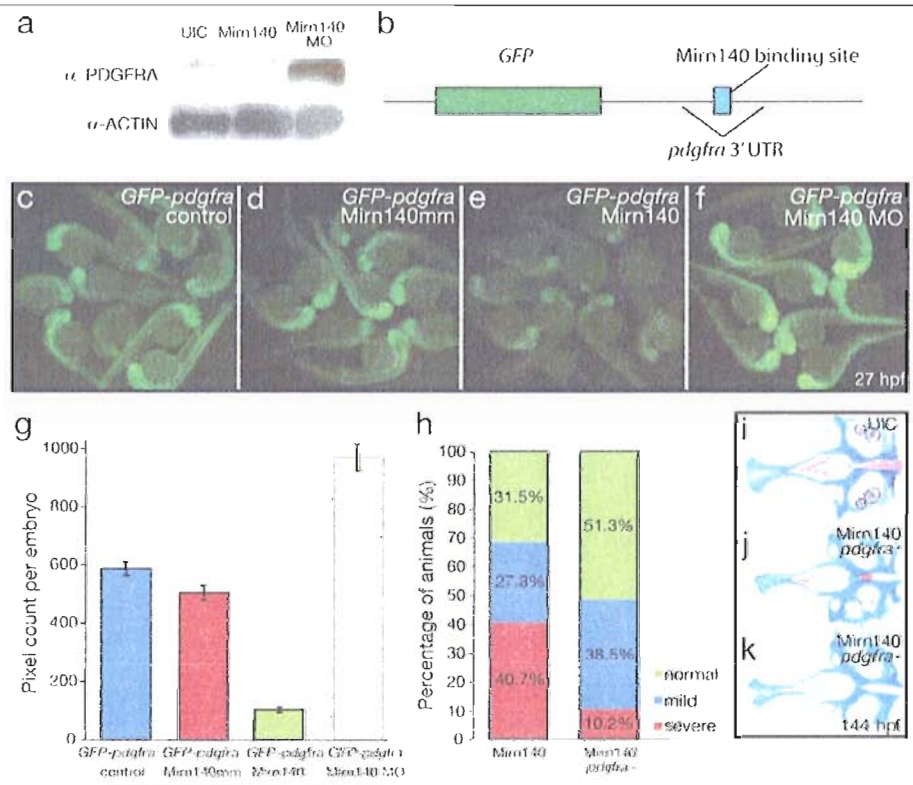

Fig. 2.3. *Mirn140* Decreases the Expression of Both Endogenous *Pdgfra* and a Synthetic *GFP*-mRNA Bearing the *Pdgfra* 3'UTR. (**a**) Compared to uninjected controls (UIC), Mirn140 duplex injection reduces endogenous Pdgfra protein in western blots probed with anti-human PDGFRA antibody. (**b**) Schematic of the *GFP* mRNA injected to test for interaction of Mirn140 with the *pdgfra* 3'UTR, which bears a predicted Mirn140 binding site. (**c-f**) Embryos (27 hpf) injected with the *GFP* construct alone (**c**) or with the *GFP* construct and the Mirn140-mismatch (Mirn140mm) duplex (**d**) fluoresce more strongly than animals injected with the *GFP* construct and Mirn140 duplex (**e**). Morpholino knockdown of Mirn140 with Dicer-inhibitor MO increased *GFP* fluorescence above controls (**f**). (**g**) Pixel density analysis of GFP fluorescence confirmed results of **c-f**; Error bars indicate standard deviations. (**h-k**) Synthetic *pdgfra* mRNA truncated to remove the Mirn140 binding site (*pdgfra**) rescued the cleft palate phenotype of *mirn140* over-expression, in three independent trials. (**h**) Distribution of animal phenotypes after embryo injection of Mirn140 duplex alone or after Mirn140 injection and *pdgfra** mRNA injection, in percent of animals. Mildly affected fish had near normal trabeculae and lateral ethmoid plate, but lacked the medial ethmoid plate like **Fig. 2.1m**; and severely affected fish lacked both the ethmoid plate and trabeculae like **Fig. 2.1n**. For Mirn140 duplex injection, N = 54; for Mirn140 duplex co-injection with *pdgfra** mRNA, N=117. (**i-k**) Alizarin/Alcian-stained palates of 144 hpf uninjected control (UIC) (**i**) and rescued animals (**j, k**) in the rescue experiment of **h**.

Consistent with previous reports (Liu et al., 2002), expression analyses showed that most, if not all, cranial neural crest cells express *pdgfra*. Crest-derived palatal precursors, fate mapped in previous studies (Eberhart et al., 2006; Wada et al., 2005), migrate around the eye to reach the oral ectoderm and those crest cells migrating rostrally to the eye must additionally migrate around the optic stalk (see below). Both rostrally and caudally migrating crest cells express *pdgfra* throughout migration to the oral ectoderm (**Fig. 2.4a, c, e, g**). We did not detect *pdgfra* expression in the oral ectoderm itself, even though the morphology of the oral ectoderm is altered in *pdgfra* mutants. This expression pattern suggests that Pdgfra mediates migration of palatal precursors to the oral ectoderm.

To determine what ligand Pdgfra utilizes during crest cell migration, we cloned and surveyed the expression of the zebrafish homologues of *Pdgfa* and *Pdgfc*, because mice doubly mutant for these genes recapitulate the mouse *Pdgfra* mutant phenotype (Ding et al., 2004; Soriano, 1997b). The zebrafish genome database at Sanger research center (http://www.ensembl.org/Danio_rerio/index.html) contains a single copy of *pdgfc* and duplicates of *pdgfa*, we designate these duplicates *pdgfaa* [formerly called *pdgf-a* (Liu et al., 2002)] and *pdgfab*. We found that only *pdgfaa* has spatiotemporal expression appropriate as a candidate guide for migrating crest cells. Just before migration initiates, the midbrain expresses *pdgfaa* in a pattern that predicts the location of *pdgfra*-expressing palatal skeleton precursor four hours later (**Fig. 2.4a-d**). Expression is dynamic, and shifts to include the optic stalk and oral ectoderm as rostral crest cells migrate around the eye and optic stalk to reach the oral ectoderm (**Fig. 2.4e-h**). The optic stalk maintains expression of *pdgfaa* well after palatogenic crest have reached the oral ectoderm. Later other Pdgf ligands begin to be expressed in the pharyngeal arches, but the expression of these genes occurs only well after migration has ceased. These expression patterns are expected under the hypothesis that Pdgfaa acts as an attractant cue guiding palatal precursors to the oral ectoderm, but the lingering expression of Pdgf in the optic stalk may require attenuation of Pdgf signaling for rostral crest to migrate past the optic stalk.

Because our reporter constructs demonstrated that Mirn140 functions by negatively regulating Pdgfra levels, we expect to see *mirn140* and *pdgfra* co-expressed. RT-PCR detected *mirn140* transcripts as early as 1 hpf and throughout crest cell migration (**Fig. 2.4i**) and *in situ* hybridization demonstrated that these transcripts were distributed broadly as late as 24 hpf (**Fig. 2.4j**). Following crest cell migration, transcripts for *mirn140* became localized to skeletogenic crest (**Fig. 2.4k,l**), similar to the later expression of *pdgfra* (Liu et al., 2002). This expression profile of *mirn140* supports the conclusion that it modulates Pdgfra levels during palatal development, including crest cell migration.

Together, these results suggest the hypothesis that *mirn140* modulates Pdgf-mediated attraction of palatal precursor cells, which are required for oral ectodermal gene expression.

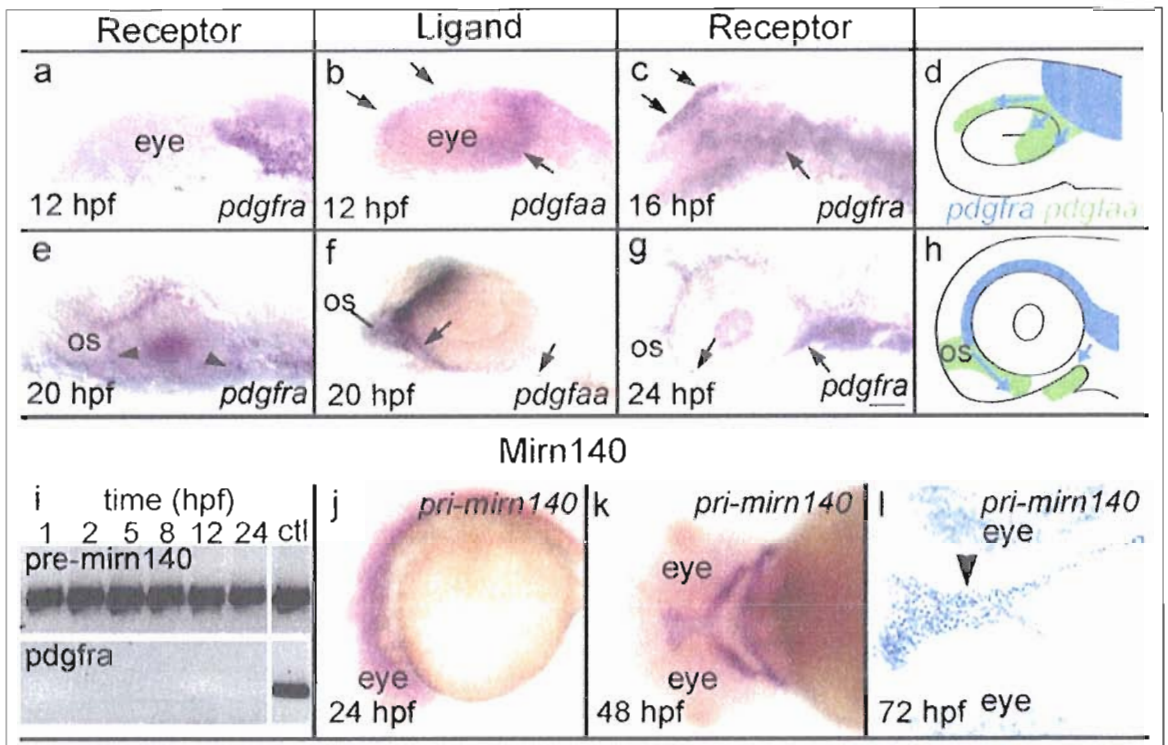

Fig 2.4. *Mirn140* Overlaps With *Pdgfra* During Crest Cell Migration. (**a-h**) The expression of *pdgfaa* predicts the migratory pathway of *pdgfra*-expressing palatal precursor cells. (**a-c**) Lateral views of embryos stained with riboprobe for *pdgfra* (**a,c**) or *pdgfaa* (**b**) at 12 hpf (**a,b**) and 16 hpf (**c**). At 12 hpf, pneural crest cells express *pdgfra* (**a**) and regions of the midbrain rudiment express *pdgfaa* (**b**, arrows). By 16 hpf, the position of *pdgfra*-expressing neural crest cells (**c**, arrows) closely resembles the 12 hpf distribution of *pdgfaa*-expressing cells (compare arrows in **b,c**). (**d**) Schematic showing the relative position of *pdgfaa* expressing cells (green) at 12 hpf relative to crest cell migration from 12 hpf to 16 hpf (blue arrows). (**e-g**) Neural crest cells migrating into the first pharyngeal arch encounter *pdgfaa*. Lateral views of 20 hpf (**e,f**) and 24 hpf (**g**) embryos stained with *pdgfra* (**e,g**) or *pdgfaa* (**f**) riboprobe. At 20 hpf, *pdgfra*-expressing neural crest cells have migrated to the optic stalk (os) and are near the oral ectoderm (**e**, arrowheads). At this same time the optic stalk, oral ectoderm, and a group of cells connecting these two tissues express *pdgfaa* (**f**). By 24 hpf, neural crest cells have migrated past the optic stalk and are condensing on the oral ectoderm (**g**, arrows). (**h**) Schematic depicting the expression of *pdgfaa* (green) relative to neural crest cells (blue) migrating to the oral ectoderm. *mirn140* is expressed where it could interact with *pdgfra*. (**i**) RT-PCR detects *mirn140* as early as one cell and throughout crest cell migration. (**j-l**) *mirn140* transcripts are broadly distributed during crest cell migration (**j**) and become restricted through development to post-migratory crest cells (**k,l**).

2.2.3. Pdgf Signaling Is an Attractant Cue for Palatal Precursor Cells

Our hypothesis predicts that palatal precursor migration (Eberhart et al., 2006; Wada et al., 2005) will be disrupted in *pdgfra* mutants. Palatal precursor cells normally disperse rapidly rostrally and caudally around the eye to reach the oral ectoderm, where they condense. Rostrally migrating cells must additionally migrate around the optic stalk before reaching the oral ectoderm (**Fig. 2.5a**). However, in *pdgfra* mutants, palatal precursors failed to disperse, rostral crest did not migrate around the optic stalk (**Fig. 2.5b**), and most crest cells never reached the oral ectoderm. Crest cells that reached the oral ectoderm in *pdgfra* mutants did so via a circuitous route, avoiding a cell-free region normally invaded by crest in wild-type embryos. In contrast to palatal precursors, most other neural crest cells in *pdgfra*$^{-/-}$*;sox10:EGFP* (crest-labeling) transgenics migrated appropriately, similar to findings in mouse (Tallquist and Soriano, 2003a). Hence, a subpopulation of neural crest cells, namely palatal precursors, requires Pdgfra function to migrate to the oral ectoderm.

Our hypothesis also predicts that both *pdgfaa* loss-of-function and *mirn140* overexpression should result in palatal precursor migration defects as observed in *pdgfra* mutants. Similar to *pdgfra* mutants, neural crest cells in *pdgfaa* morpholino injected or *mirn140* duplex injected, *sox10:EGFP* transgenic embryos failed to disperse properly and rostral crest cells stopped migrating at the optic stalk (**Fig. 2.5c, d)** resulting in clefting or reduction in the palatal skeleton (**Fig. 2.1h, k**). This effect on migration of *pdgfra*-expressing crest cells (**Fig. 2.5g, h**, arrowheads) in *mirn140* duplex injected embryos was not through loss of *pdgfra* transcripts (**Fig. 2.5g, h e, f**), suggesting that Mirn140 attenuates Pdgf signaling by blocking Pdgfra translation. Collectively, these results show that loss of Pdgf signaling either by blocking the ligand, by mutating the receptor, or by mirn140 overexpression, results in the failure of palatal precursors to reach the oral ectoderm.

Phenotype resulting from loss of Pdgf signaling and our expression analyses are consistent with Pdgf signaling being a positive guidance cue for cranial neural crest. To

directly test the nature of Pdgf signaling during crest migration, we implanted beads soaked in Pdgfa or BSA (bovine serum albumin) as a negative control into *pdgfaa* morpholino injected *sox10:EGFP* transgenic embryos. Neural crest cells accumulated next to Pdgfa beads, but not BSA beads (**Fig. 2.5g-i**, arrows). In mouse, the role that *Pdgfa* plays in palatogenesis is obscured by complex phenotypes and early lethality in a subset of mutant embryos (Bostrom et al., 1996). Our results demonstrate that Pdgfa is a positive cue, probably a chemoattractant as it is in oligodendrocyte migration (Adams et al., 2003), that guides crest to the oral ectoderm.

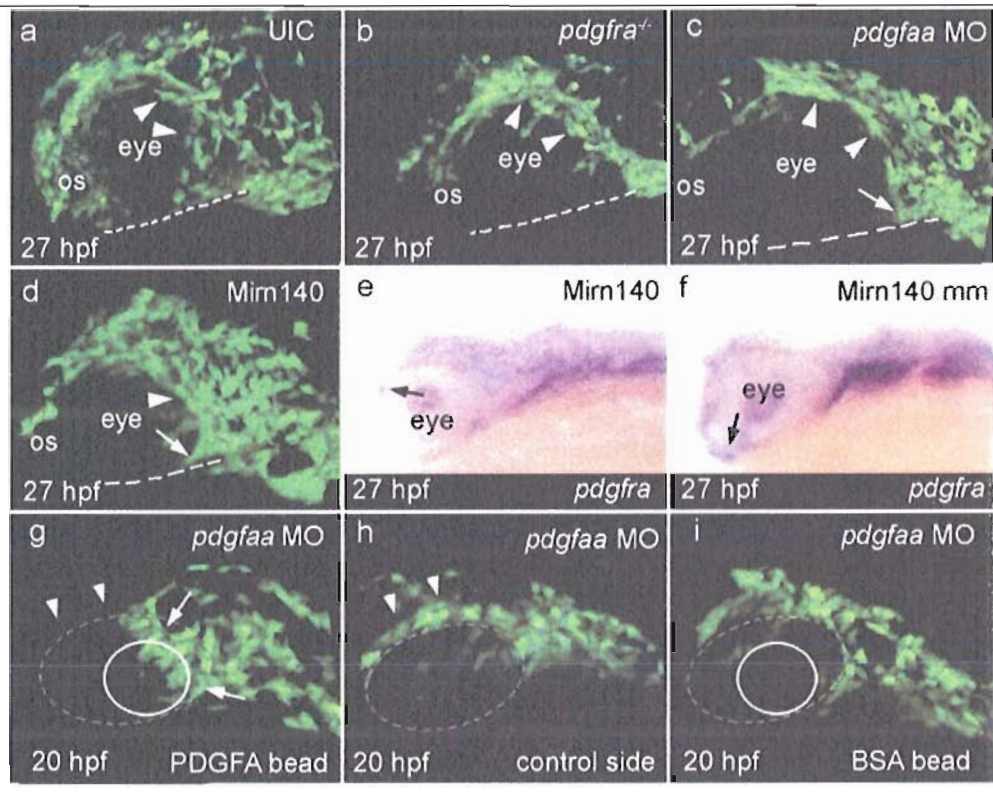

Fig. 2.5. Pdgf Signaling is Modulated by *Mirn140* and Guides Palatal Skeleton Precursors to the Oral Ectoderm. (**a**) Neural crest cells that have migrated over the eye and around the optic stalk (asterisk) in *pdgfra*$^{+}$ embryos have reached the oral ectoderm (dashed line) by 27 hpf. However, most palatal precursor cells do not migrate to the oral ectoderm in *pdgfra* mutants (**b**), *pdgfaa* morpholino injected embryos (**c**), or *mirn140* duplex injected embryos (**d**) In all three circumstances, rostrally migrating neural crest cells stop migrating at the optic stalk, within 50-60μm of the oral ectoderm. Caudally migrating crest is less severely effected in *pdgfaa* morpholino injected embryos and *mirn140* duplex injected embryos than in *pdgfra* mutants (arrows, **c,d**). Although, even in *pdgfra* mutants some caudally migrating neural crest cells reach the oral ectoderm (see Supplementary Figure 6). Transcripts for *pdgfra* are detected in neural crest cells of *mirn140* duplex injected embryos (**e**), as in control *mirn140* mismatch injected embryos (**f**). (**g-i**) Confocal projections of *pdgfaa* morpholino injected, *sox10:GFP* transgenic embryos implanted with a Pdgfa (**g,h**) or a BSA (**i**) loaded bead. The dashed outline represents the location of the eye and the solid circles depict the location of the bead, just medial to the eye. (**g**) Neural crest cells accumulated adjacent to beads preloaded with recombinant Pdgfa protein, in a region that is cell poor in controls (between the arrows, n=8). Additionally, fewer neural crest cells were present in the pathway over the eye (arrowhead), as compared to the control side of the same embryo (**h**) suggesting that crest cells were rerouted to the Pdgfa bead. (**i**) Control beads did not attract crest cells.

Loss of Pdgf signaling causes defects in both cranial neural crest cell migration and oral ectodermal gene expression. Our hypothesis and results from bead experiments predicts that Pdgf receptor function is required in migrating neural crest cells. Additionally, interspecific neural crest transplantation in avian species has shown that the oral ectoderm responds to crest-derived signals (Schneider and Helms, 2003), predicting that loss of oral ectodermal gene expression in *pdgfra* mutants is secondary to the failure of crest to reach the oral ectoderm. We tested both these predictions by transplanting wild-type crest into *pdgfra*$^{-/-}$ hosts and assaying neural crest migration and oral ectoderm gene expression. Neural crest cells from *pdgfra*$^{+/+}$; *sox10:EGFP* donors dispersed and migrated to the oral ectoderm normally in *pdgfra*$^{-/-}$ hosts (**Fig. 2.6a, b**). Not only did transplanted *pdgfra*$^{+/+}$ crest restore the palatal skeleton (**Fig. 2.6c-e**), but it also rescued gene expression (**Fig. 2.6f**) in the *pdgfra*$^{-/-}$ oral ectoderm. These neural crest cell transplants frequently contain non-neural crest cells, yet these cells were typically distant from the oral ectoderm (**Fig. 2.6d**, arrowheads) and thus unlikely to influence oral ectodermal development. Therefore, a crest migration defect is the primary cause of both the palatal skeleton and oral ectodermal phenotypes observed in embryos lacking functional Pdgf signaling.

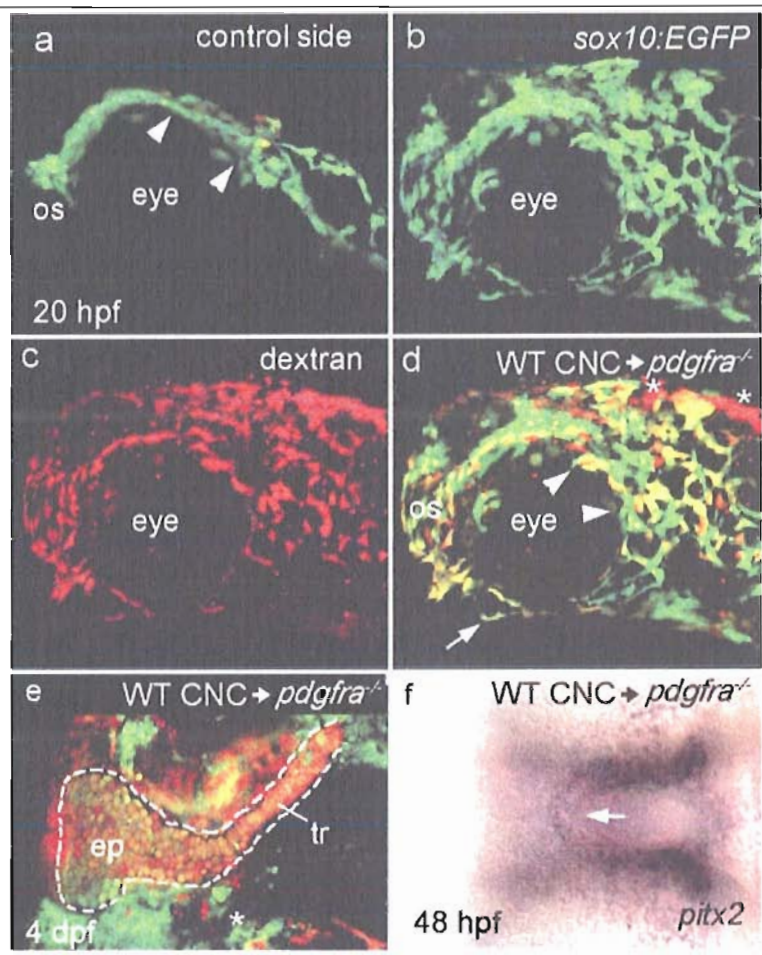

Fig. 2.6. *Pdgfra* is Required for Neural Crest Cell Migration, Palatal Skeleton Development and Proper Oral Ectoderm Specification. The control (**a**) and experimental side (**b-d**) of a 20 hpf *pdgfra* mutant embryo that received a neural crest cell transplantation from a *pdgfra*$^{+/+}$;*sox10:EGFP* embryo. (**a**) Mutant neural crest cells (green) are not dispersed and failed to migrate beyond the optic stalk (asterisk) on the control side of the embryo. (**b-d**) Donor *pdgfra*$^{+/+}$;*sox10:EGFP* transgenic cells (**b**), labeled with Alexa dextran 568 (**c**), have dispersed, migrated around the optic stalk (asterisk), and reached the oral ectoderm (arrow) in a *pdgfra*$^{-/-}$ environment (n=15). (**d**) Merged imaged of **b,c**. (**e**) Flat mounted palatal skeleton of another *pdgfra* mutant that received a neural crest cell transplant from a *pdgfra*$^{+/+}$;*fli1*:EGFP transgenic donor (n=5). *pdgfra*$^{+/+}$ crest-derived cartilage was present unilaterally in the ethmoid plate (ep) and trabeculae (tr) of the palatal skeleton (outlined). The trabecula and a portion of the ethmoid plate on the control side of the mutant embryo host were missing (asterisks). (**f**) Transplantation of *pdgfra*$^{+/+}$ neural crest cells restored the expression of *pitx2* in the oral ectoderm of *pdgfra* mutants (n=8). Ventral view of a 48 hpf *pdgfra* mutant embryo showing *pitx2* expression in the roof of the *pdgfra*$^{-/-}$ oral ectoderm (arrow). Scale bar=50μm. Anterior is left in all panels,

2.2.4. *Mirn140* Is Necessary for Rostrally Neural Crest Cells Migration

Collectively, these results demonstrate that Mirn140 negatively regulates Pdgf signaling, which is required for neural crest cells to migrate to the oral ectoderm. To further probe the normal function of *mirn140,* we utilized morpholinos to knockdown Mirn140 activity.

Loss of Mirn140 activity resulted in elevated levels of Pdgfra protein (**Fig. 2.3a,** inset) and caused alteration in the length-to-width ratio of the palatal skeleton (**Fig. 2.7a**). Co-injection of *mirn140* duplex rescues this palatal phenotype, showing specificity of the morpholino (**Fig. 2.7a**). Normally, caudally migrating neural crest cells give rise to the lateral ethmoid plate, while rostrally migrating crest cells fill in the medial ethmoid. Therefore, shape change after Mirn140 knockdown could be due to changes in the relative contributions of caudal versus rostral crest cells to the ethmoid plate.

Rostrally migrating crest cells must pass the optic stalk, a Pdgfaa source, to reach the oral ectoderm. Therefore, elevating Pdgf signaling by injections of either *mirn140* morpholino or *pdgfra** mRNA, which lacks the *mirn140* binding site, may alter the number of rostral crest cells migrating past the optic stalk. In *sox10:EGFP* transgenics, we found that many crest cells had migrated past the optic stalk (**Fig. 2.7f**) to the oral ectoderm by 24 hpf. In transgenics injected with either *mirn140* morpholino or *pdgfra** mRNA, however, neural crest cells enveloped the optic stalk, yet few had migrated on to the oral ectoderm (**Fig. 2.7g, h**). The palatal skeleton's morphology was altered in mirn140 morpholino injected embryos (**Fig. 2.7i-j**), but appeared fairly normal in *pdgfra** injected embryos (**Fig. 2.7k**). This difference could be due to the labile nature of mRNA allowing the embryo to recover by 6 days post injection. We conclude that elevation of Pdgf signaling causes alterations in the shape of the palatal skeleton by reducing the number of rostrally migrating crest cells that reach the oral ectoderm, although work remains to determine how this crest defect precisely correlates with the skeletal phenotype.

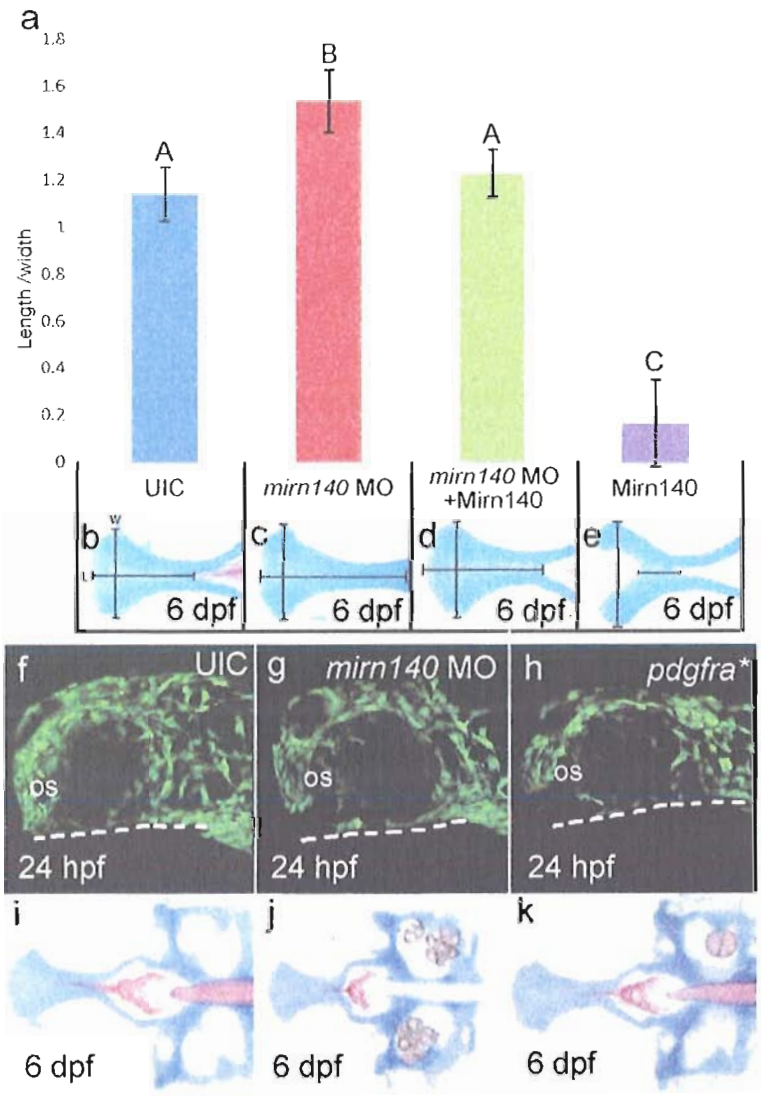

Fig. 2.7. Loss of *Mirn140* Alters Palatal Skeleton Morphology and Neural Crest Cell Migration. (**a-e**) The width of the ethmoid plate was compared to the length. Uninjected control (UIC), N=9; Mirn140 MO, N=8; Mirn140 duplex, N=11, Mirn140 MO plus Mirn140 duplex co-injection, N=13. Student two-tailed t-test. P= 8.405E-06, Error bars indicates standard deviation. Scale bar, 1mm. (**f-h**) Compared to controls (**f,** n=8) fewer rostrally migrating neural crest cells had migrated from the optic stalk (asterisk) to the oral ectoderm (dashed line) in *sox10:EGFP* transgenics injected with *mirn140* morpholino (**g**, n=10) or *pdgfra** mRNA (**h**, n=10). Neural crest cells did encircle the optic stalk in these embryos, unlike the effects of Pdgf loss-of-function (see **Fig. 5**). (**i-k**) The resultant palatal phenotypes in the same embryos imaged in **a-c**. Compared to controls (**i**) Palatal morphology was altered in the *mirn140* morpholino injected embryo (**j**) but not the *pdgfa** injected embryo (**k**).

2.3. *Mirn140* and Zebrafish Skeletogenesis

Here we show that precise control of Pdgf signaling is crucial for at least two separate events in crest migration. First, Pdgf signaling is necessary for neural crest cell dispersion (**Fig. 2.8a**). Most or all palatal precursors fail to disperse if Pdgf signaling levels are low, whether by *pdgfra* mutation, *pdgfaa* morpholino injection, or *mirn140* duplex injection. Our time-lapse analyses show that, after dispersion, caudally migrating neural crest cells quickly reach the oral ectoderm. Therefore, the severe loss of crest dispersion in embryos with reduced Pdgf signaling may directly account for why few caudally migrating crest cells reach the oral ectoderm. We find that more caudally migrating crest cells reach the oral ectoderm either in *pdgfaa* morpholino injected embryos or *mirn140* duplex injected embryos than in *pdgfra* mutants. This is likely due to the incomplete loss of Pdgfaa and Pdgfra protein in embryos injected with *pdgfaa* morpholino and *mirn140* duplex, respectively. Despite this diminution of crest dispersion, some rostrally migrating cells do reach the optic stalk, suggesting other guidance cues are also important in the early guidance of the neural crest cells.

Our results show, secondly, that modulated Pdgf signaling is critical for rostrally migrating cells to reach the oral ectoderm. In loss-of-Pdgf function experiments, rostrally migrating neural crest do not migrate around the optic stalk, while in embryos with elevated Pdgf signaling, crest cells encircle the optic stalk, but few migrate on to the oral ectoderm. Since the optic stalk continues to express *pdgfaa* while palatal precursors migrate to the oral ectoderm, we propose that Mirn140 acts to attenuate Pdgf signaling, allowing rostrally migrating crest cells to migrate past one source of Pdgfaa on to the next source, the oral ectoderm (**Fig. 2.8b**).

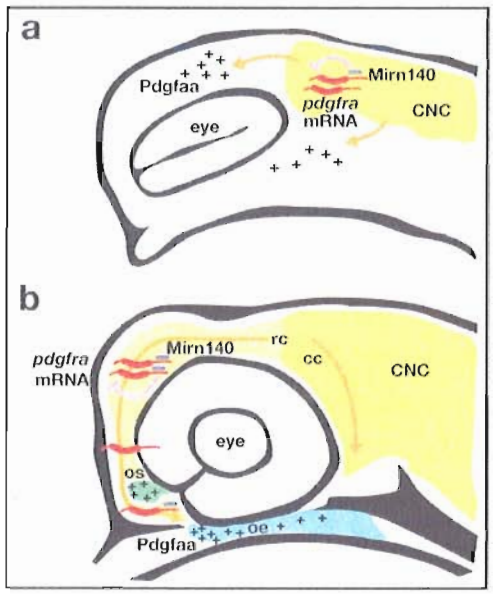

Fig. 2.8. *Mirn140* Modulates Pdgf Signaling During Palatogenesis. (**a**) Pdgfra signaling is required for neural crest cell dispersion. Neural crest cells (yellow), expressing *pdgfra* and *mirn140*, disperse into regions of *pdgfaa* expression. (**b**) At 20 hpf rostral crest cells have reached the optic stalk (green) and require Pdgf signaling to encircle the stalk. Attenuation of Pdgf signaling via *mirn140* allows crest cells to migrate past the stalk to the oral ectoderm.

Our results show that alterations to the normal modulation of Pdgf signaling affect the relative number of rostrally migrating crest that reach the oral ectoderm. In amniotes, snout length is associated with the relative contributions of the frontonasal prominence, derived from rostrally migrating cells, and the maxillary prominence, derived from caudally migrating cells, to the facial skeleton (Brugmann et al., 2007; Osumi-Yamashita et al., 1994). Therefore, the evolution of skull morphology could utilize miRNAs to tweak the number of crest cells arriving at an individual prominence within the first pharyngeal arch.

Cranial neural crest cells migrate to the pharyngeal arches in three crest streams, with the first stream populating the first pharyngeal arch (Trainor et al., 2003) and yet no guidance cue responsible for the migration of any individual stream has been discovered. We show that loss of Pdgf signaling disrupts the migration of a subpopulation of first stream crest, those destined for the zebrafish palate. As in mouse (Tallquist and Soriano, 2003a), *pdgfra* expression is not limited to crest-derived palatal precursors, as crest in all three streams express *pdgfra*. Rather, the expression of its ligand *pdgfaa* provides a mechanism for Pdgf signaling to specifically guide palatal precursors. Just prior to cranial

neural crest cell migration, the brain adjacent and anterior to the crest-derived palatal precursors expresses *pdgfaa*. As crest cells migrate, elevation of *pdgfaa* expression in the optic stalk and oral ectoderm predicts the pathway to be taken by palatal precursors. We propose that the restricted expression of *pdgfaa* attracts only palatal precursors since Pdgf signaling acts at short range (Betsholtz et al., 2001) and, therefore, more posterior cranial crest would not be receiving Pdgf signaling. The same tissues that express *pdgfaa* in zebrafish also express *Pdgfa* in amniotes (Ho et al., 1994; Orr-Urtreger et al., 1992; Tallquist et al., 2000), consistent with the possibility that Pdgfa signaling plays similar roles in zebrafish and amniotes. Crest migration defects have not been described in mouse *Pdgfra* or *Pdgfa* mutants (Bostrom et al., 1996; Soriano, 1997b; Tallquist and Soriano, 2003a), this could be due to species-specific developmental differences or to improved visualization of crest in zebrafish. It will be of great interest to determine if palatal precursor migratory defects are evident in mouse *Pdgfra* and *Pdgfa* mutants, although conditional mutation of *Pdgfa* would be necessary to overcome the early death of severely affected *Pdgfa* mutant mice (Bostrom et al., 1996).

Following crest cell migration, our results combined with others demonstrate a signaling hierarchy that patterns neural crest-derived skeletal elements in the first pharyngeal arch, such as the palate. It is known that first arch cranial neural crest cells regulate the timing of oral ectodermal *Shh* expression (Schneider and Helms, 2003), and now we know that the expression of *shh* in the oral ectoderm absolutely requires cranial crest. We have previously shown that regulatory gene expression in the oral ectoderm, including the oral ectodermal expression of *shh* itself, requires Shh signaling from the neural to the oral ectoderm at the end of gastrulation (Eberhart et al., 2006). Due to the early nature of the Shh signal received by the oral ectoderm, it is likely that Shh signaling from the neuroepithelium provides competence of the oral ectoderm to respond to later crest-derived signals. The identity of these crest-derived signals is unknown in zebrafish, but Bmp signaling is necessary to induce *Shh* expression in the oral ectoderm in avians (Foppiano et al., 2007). Ectodermal Shh, in turn, is critical in directing the outgrowth of first arch crest-derived skeletal elements (Hu and Helms, 1999), including the zebrafish

palate (Wada et al., 2005). These results suggest a signaling hierarchy where signals from cranial neural crest cells induce a signaling environment in the oral ectoderm, made competent by early Shh signaling, which then impinges back onto the crest.

Continued exploration of how microRNAs and other factors modulate the early signaling environment underlying palatogenesis will assuredly provide insights into the cause of, and possible treatments for, human craniofacial disease. Due to the powerful genetic and cell biological tools available, zebrafish will continue to provide important insights into the early events underlying palatogenesis.

2.4. Materials and Methods for *Mirn140* Studies

2.4.1. Zebrafish Care and Use

The *b1059* mutant allele was obtained via ENU mutagenesis (Westerfield, 1993) in an AB background and was out-crossed to a WIK background for genetic mapping. PCR-based microsatellite mapping placed the *b1059* allele in a 1.4 cM interval of LG20, between microsatellite markers z14542 (7 cross overs/434 meioses) and z20582 (2 cross overs/434 meioses), which contains *pdgfra*. Sequence analysis of *pdgfra* in wild-type and *b1059* embryos revealed an adenosine-to-thymidine nucleotide change resulting in an Isoleucine 855 to Asparagine missense mutation, thus placing a charged residue in the hydrophobic core of the kinase C-lobe in the second tyrosine kinase domain of the receptor. $pdgfra^{b1059}$ mutants were identified by PCR amplification using dCAPs primers (Neff et al., 1998), forward: 5' TGTCTCCAAAGGAAGCGTG 3' and reverse: 5' ACCGAGAGAGAAGATCTCCCATAACTAG 3', followed by digestion with SpeI, resulting in a wild-type fragment of 263 bp and a *b1059* fragment of 239 bp.

All embryos were raised and cared for using established protocols with IACUC approval (Westerfield, 1993). $Tg(fli1{:}EGFP)^{y1}$ transgenic embryos express GFP in neural crest cells shortly after the onset of migration, and in the vasculature (N and BM, 2002),

while *Tg(-4.9sox10:EGFP)*^{ba2} transgenics express GFP in neural crest prior to the onset of migration (Wada et al., 2005); here they are called *fli1:EGFP* and *sox10:EGFP*, respectively, through the text. We used heterozygous *sox10:EGFP* transgenics for our analyses, because homozygous embryos can have craniofacial defects (Wada et al., 2005). Embryos were treated with 0.5 μM Pdgfr inhibitor V (Calbiochem) from 10 hpf- 4 dpf and Kaede photoconversion was carried out as described previously (Eberhart et al., 2006).

2.4.2. Morpholino and RNA Injection

Gene Tools (Philomath, OR, USA, http://www.gene-tools.com) supplied morpholino oligonucleotides (MOs) with the sequences: Mirn140 MO (mature), 5'-CTACCATAGGGTAAAACCACTG-3'; Mirn140 MO (Dicer inhibitor), 5'-GACGTAACCTACCATAGGGTAAAACCACTGA-3'; *p53* MO, 5'-GCGCCATTGCTTTGCAAGAATTG-3' (Robu et al., 2007) *pdgfaa* I1E2 (splice inhibitor) 5' GGAATTGGTGCTTCCTGTTAAAGA 3' and *pdgfaa* I2E3 (splice inhibitor) 5' CCTCCAGCACTTCATTCTCTGCAAC.

We injected one or two-cell stage zebrafish embryos with approximately 3 nl of morpholinos: 0.4 mM *pdgfaa*, 1.2 mM mature Mirn140, or 0.6 mM Dicer inhibitor Mirn140. Injecting higher concentrations of *pdgfaa* morpholino resulted in embryos with disrupted body axes, consistent with *pdgfaa* playing a role in gastrulation movements(Nagel et al., 2004). To control for the effects of nonspecific cell death, we co-injected either *pdgfaa* morpholino or *mirn140* morpholino (Dicer inhibitor, 1.2 mM) with *p53* morpholino (0.3 mM) (Robu et al., 2007).

Integrated DNA Technology (Coralville, IA, USA, http://www.idtdna.com) supplied RNA oligonucleotides with the sequences: Mirn140, 5'-CAGUGGUUUUACCCUAUGGUAG-3'; Mirn140 mismatch, 5'-CACACCAAGAACCCUAUGGUAG-3'; Mirn140* (the complementary natural strand),

5'- UACCACAGGGUAGAACCACGGAC-3'. To make 50 μM working stocks, 10 μL of 100 μM Mirn140 or Mirn140 mismatch plus 10 μL of 100 μM Mirn140 * were mixed together, boiled briefly to denature, and then cooled to 4°C and stored at -80°C until injection. Embryos were injected with three nl of this 50 μM working stock or a 25 μM dilution of this stock, with identical results. To rescue the cleft palate phenotype in *mirn140* duplex injected embryos (25 uM), we co-injected *mirn140* MO (Dicer inhibitor, 1.2 mM).

2.4.3. Reporter Constructs

The primers pdgfraUTR-F (5'-TCTGCGTCATCTTGTCACTTTTTCTTCAC-3') and pdgfraUTR-R (5'-AACACAGCCATTTTCTTCATTTTAGGAC-3') amplified a 653 nt long fragment from genomic DNA containing the *pdgfra* 3' untranslated region (UTR), which was inserted into the pCR4-TOPO vector (Invitrogen, Carlsbad, CA, USA, http://www.invitrogen.com). To make the construct for synthesizing GFP with the *pdgfra* 3'UTR, we used Not I and Spe I enzymes to liberate the 3'UTR region of *pdgfra* gene, and ligated it to the *GFP* gene isolated from pEGFP-N3 vector (Clontech, Mountain View, CA, USA, www.clontech.com) by Not I and Xho I digestion while inserting into the PCRII-TOPO (Invitrogen) vector between Spe I and Xho I sites. To make mRNA, the vector was linearized with Spe I. Co-injections were accomplished by double injection, first by injecting 0.6 mM Dicer inhibitor Mirn140 MO or 25 μM Mirn140 duplex, and then by injecting 250 ng/μL of the synthetic GFP-*pdgfra* UTR mRNA. *GFP-nog3* UTR construct was made similarly to the *GFP-pdgfra* UTR with the primers: nog3-F (5'-GAAATAAGCTCCGCACTCATCCTCACAT-3') and nog3-R (5'-TCCATTCCCCTTATATTTACAGCACACCA-3'), amplifying a 504 nt fragment containing the *nog3* 3'UTR.

To make the full-length *pdgfra* lacking the Mirn140 binding site (*pdgfra**), we used pdgfra-F (5'-TCATGTTCCCGGTGCTGCC-3') and pdgfra-R (5'-

GGGCTCCATAAGACTGAGGTGAAG-3'). The resulting 3418 nt PCR product was ligated into pCR4-TOPO vector and linearzied with Spe I. To make mRNAs, about 1 μg of purified linear template was transcribed by T7 RNA polymerase using mMessenger mMachine kit (Ambion, Austin, TX, USA, http://ambion.com) at 37 °C for 2 h. mRNAs were purified with RNA clean up kit (Zymo Research, Orange County, CA, http://www.zymoresearch.com) and diluted to 15 μL with nuclease-free water.

2.4.4. Cloning and *in situ* Hybridization

Primers for generating PCR products containing the full open reading frame of Pdgf family members and mirn140 are: *pdgfra* (Ensembl Gene ID ENSDARG00000030379) forward 5' TCATGTTCCCGGTGCTGCC 3' and reverse 5' GGGCTCCATAAGACTGAGGTGAAG, *pdgfaa* (Ensembl Gene ID ENSDARG00000030379) forward 5' TGGGACACTTTTGGACCACAGG 3' and reverse 5' TCGTTTTTCAGGCTGTCGTTG 3', *pdgfab* (Ensembl Gene ID ENSDARG00000058424) forward 5' TGACATTGGAAGGAGATGAGAACC 3' and reverse 5' TTATTGAATATCCTTGTTGATCAGTGC 3' and *pdgfc* (Genbank accession XM 683962.2) forward 5' CCAAATGATTCCGTTGCTTCTG 3' and reverse 5' GCGTCTTCTCTCTGGGACTGATT 3'. A 902 nt fragment of pri-mirn140 was isolated from 24 hpf embryo cDNA library by the primers primiR140-F (5'-GCAAGTCAAACCCTGTAGCATCCCGTT-3') and primiR140-R (5'-GCGAGCCGATAGAGCGATTGTTT-3'). PCR products were cloned in pCR4-TOPO (Invitrogen). ClustalX alignment confirmed our Pdgf orthologue assignments. Capped mRNA was synthesized using the mMessage mMachine kit (Ambion, Austin, TX).

Integrated DNA Technology synthesized Mirn140 LNA (Locked Nucleic Acid) probe (5'-CtACcATaGGgTAaAAcCAcTG-3', lowercase nucleotides represent LNA nts) with 3' end Digoxigenin-labeling. Probe was diluted to 0.5 μM in hybridization buffer (50% formamide, 2XSSC, 0.3% Tween-20, 0.5 mg/mL baker's yeast RNA and 0.05 mg/mL heparin). *In situ* hybridization occurred at 43 °C on whole mounted embryos and frozen

sections following protocols provided by Exiqon (Woburn, MA, USA, http://exiqon.com). Conventional *in situ* hybridization with digoxigenin-labeled RNA probes utilized a protocol similar to that for the LNA probe, but at a hybridization temperature of 68 °C. Cutting circular plasmid with Not I and synthesizing RNA with T3 polymerase generated antisense *pdgfra, pdgfaa,* and *pdgfc* riboprobes, while cutting with SpeI and synthesizing with T7 polymerase produced *pdgfab* and *pri-mirn140* riboprobe. *pitx2* and *shh* riboprobes have been described (Eberhart et al., 2006).

Accession numbers for sequences used in this work: pdgfaa, NM_194426; pdgfab, NM_001076757; pdgfb, ESTs DV584985 and EB884207; pdgfc, XM_683962 and EST EH559317; pdgfd, XM_001333193; pdgfra, NM_131459 ENSDART00000011915; *mirn140 (*dre-mir-140 primary transcript, EU116273) was cloned by RT-PCR and 3' RACE from 24 hpf zebrafish embryo cDNA.

2.4.5. Cartilage Staining

Four day postfertilization zebrafish embryos were stained with Alcian Blue and flat mounted (Walker et al., 2007).

2.4.6. Cell Transplants and Bead Implants

For all transplants, donors were injected with 10,000 MW Alexa 568 dextran, labeling all cells. Shield stage transplants were carried out as described elsewhere (Eberhart et al., 2006).

Affi-gel blue gel (BioRad) was incubated overnight at 4° with 10 µg/ml rat recombinant Pdgfaa (R&D Systems) or BSA (Sigma). Individual Affi-gel beads from the gel were inserted into *pdgfaa* morpholino injected embryos at 12 hpf and implanted embryos were imaged at 20 hpf.

2.4.7. Time-Lapse Analysis, Confocal Microscopy and Figure Processing

Confocal z-stacks were collected on a Zeiss LSM Pascal. Images were processed in Adobe Photoshop CS and Adobe Illustrator. Recordings, 15 min/frame, and confocal analysis of transgenic embryos were performed according to established protocols (Walker et al., 2007). To quantitate GFP levels, pixels of individual layers were selected by setting Fuzziness level to 170. The histogram function was then used to calculate the number and standard deviations of green pixels for each fish.

2.4.8. Western Blotting

Immunoblotting used the Upstate (http://www.upstate.com) protocol with minor modifications. Proteins extracted from thirty 24 hpf fish were separated by SDS polyacrylamide gel electrophoresis and transferred to a nitrocellulose membrane using 3% blocking solution. The blot was probed with anti-human PDGFRA antibody (catalog# 07-276, Upstate) and anti-mouse ACTIN antibody (product# A4700, Sigma, St. Louis, MO, USA, http://www.sigmaaldrich.com) using as secondary antibody, anti-rabbit (catalog # AP132P) (Chemicon, Temecula, CA, USA, http://www.chemicon.com) and anti-mouse (AP124P) (Chemicon). Protein blots were visualized by ECL Western Blotting Detection System (Catalog # RPN2132, Amersham, Piscataway, NJ, USA. http://www.amersham.com).

2.5. The Relationship of Chapter II with the Rest of the Dissertation

This chapter summarizes the study of microRNA *mirn140* (*mir140*, miR-140) in zebrafish palatogenesis. As an important regulator of developing cartilage genes, *mirn140* is strongly expressed in the developing cartilage cells in different vertebrate species, implying the importance of this miRNA for skeletogenesis. This study presented here is an important example showing the involvement of miRNAs in the regulation of

skeletogenesis. Together with the study of microRNA miR-196 in Chapter III as another example, and the review discussion in Chapter IV, my studies of miRNAs in skeletogenesis showed the involvement and importance of miRNA regulation of skeletal system during early embryonic development.

CHAPTER III

MIR196 REGULATES ZEBRAFISH SKELETAL DEVELOPMENT

This chapter includes unpublished co-authored material to be published in the journal of *Development* and was written in the style of journal of *Development*. I designed the project and performed the experiments with the help from Yi-Lin Yan, Johann Eberhart, Amaury Herpin, Toni Wagner, Jesse Buss, Jiin Park. Profs. Manfred Schartl, Judith Eisen, Charles Kimmel, William Cresko and Andrew Berglund helped with consulting on experimental design and trouble-shooting. Prof. John Postlethwait was the principal investigator for the research project and helped with manuscript writing. This project is the second major research project for my Ph.D. dissertation.

3.1. *Mir196* and Zebrafish Skeletal Patterning

As discussed in Chapter I, *hox*-cluster genes control animal body patterning. MicroRNA *mir196* is conserved among vertebrates between *hox9* and *hox10*. MiR-196 targets *Hoxb8* mRNA by accelerating its cleavage. This interaction has been hypothesized to be important for hindlimb initiation. Knockdown of miR-196 in chicken induced homoeotic transformation of a cervical vertebra to thoracic identity. Here I show that precise levels of expression of *mir196* are required to initiate zebrafish pectoral fins, to develop the correct number of pharyngeal arches, and to specify correct number and identity of rostral vertebrae and ribs. I show that miR-196 fine-tunes pectoral fin initation by altering retinoic acid signaling via modulating the expression of the retinoic acid receptor gene Rarab.

3.2. Results

3.2.1. *Mir196* Genomics

The human genome has three copies of *MIR196* located between paralogy groups 9 and 10 (Yekta et al., 2008), but due to the teleost genome duplication (Amores et al., 1998; Jugessur et al., 2003; Postlethwait et al., 1998b), zebrafish has five *mir196* genes. The teleost whole genome duplication would have initially produced six *mir196* genes, but one of the two *hoxbb mir196* duplicates was lost and duplicates of only the *hoxa* and *hoxc* cluster genes were maintained. The five zebrafish *mir196* paralogs encode four different mature miR-196 sequences with a central nucleotide trio containing (C/G/T) (A) (A/T). The duplicate *hoxa* and *hoxc* clusters have *mir196* paralogs that differ by one nucleotide (CAT/TAT and CAT/GAT), respectively (**Fig. 3.1A**). Because miRNAs often bind their targets with some mismatch (He and Hannon, 2004; Yekta et al., 2004), all four miR-196 sequences probably regulate the same targets.

3.3.2. *Mir196* Expression Patterns

mir196 genes share spatial expression patterns in the central nervous system (CNS) and pectoral fin bud with nearby *hox* genes (Wienholds et al., 2005; Woltering and Durston, 2006; Yekta et al., 2008) (**Fig. 3.1C-J**), suggesting that *hox*-cluster miRNAs may share regulatory mechanisms with nearby *hox* genes. To investigate temporal aspects of *mir196* expression, we used gene-specific primers for *mir196* primary transcripts and RT-PCR to discover that *mir196a1(hoxca)* transcript had begun to accumulate at 24 hours post fertilization (hpf), but *mir196a2(hoxaa)* transcript, which encodes the same mature miRNA sequence as *mir196a1*(*hoxca*), was maternally expressed (**Fig. 3.1B**). Transcripts from *mir196b*(*hoxba*) and *mir196c*(*hoxcb*) genes first appeared at bud stage, and transcript from *mir196d*(*hoxab*) first accumulated at 5 hpf (**Fig. 3.1B**) when gastrulation initiates. This gene-specific timing suggests that different *mir196* genes experience different regulation and may play different roles in development. In addition,

whole mount *in situ* hybridization experiments showed that *mir196* genes are expressed in a pattern similar to but different from each other at 24 hpf (**Fig. 3.1C-J**).

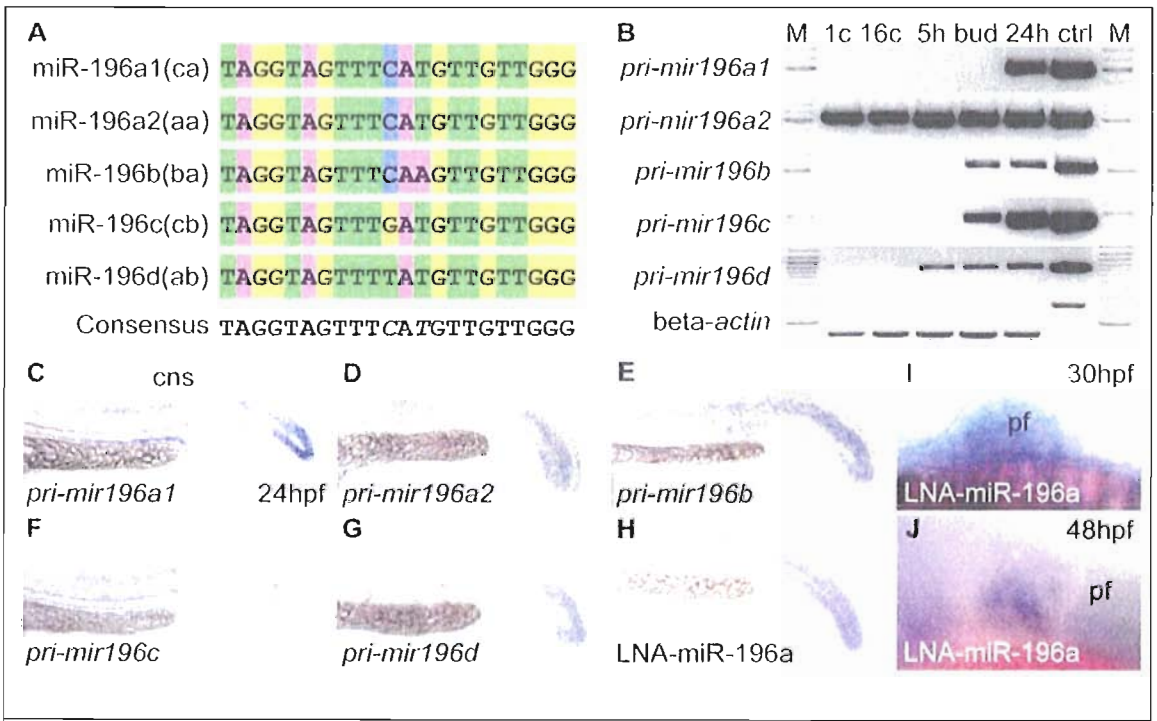

Fig. 3.1. Sequence and Expression of *Mir196* Genes. (A) Alignment of mature miR-196 encoded by five *mir196* genes. (B) Expression of *mir196* paralogs studied by RT-PCR. Beta-*actin* (*bactin1)* was used as control for contaminating genomic DNA (ctrl lane). M, size marker; 1c, 1 cell stage; 16c, 16 cell stage; 5h, 5 hpf (hours post-fertilization); bud, bud stage, about 10 hpf; 24h, 24 hpf; ctrl, genomic DNA control. (C-H) Whole mount *in situ* hybridization for *mir196* primary transcripts showed expression in the neural tube. (H) Linked nucleic acid (LNA) probe for miR-196a showed an expression pattern similar to the primary transcript. (I, J) LNA probes for miR-196a in the pectoral fin bud at 30 and 48 hpf. cns, central nerve system; pf, pectoral fin.

3.3.3. *Mir196* and *Hox* Targets

Sequence comparisons revealed that the 3' UTRs of several zebrafish *hox*-cluster genes surrounding *mir196* contain predicted miR-196 targets (He et al., 2009b; Yekta et

al., 2008). The *mir196* genes lie between posterior *hox* paralogy groups 9 and 10, and ten *hox* cluster genes ranging from group 5 to 13 contain predicted miR-196 binding sites. Conversely, *mir10* genes lie between anterior paralogy groups 4 and 5 and predicted targets are in anterior *hox* paralogy groups 1 to 4 and in *hoxd10a*. This conserved non-random organization of *hox*-cluster miRNA genes and their predicted targets suggests a conserved functional role between *hox*-cluster genes and their neighboring miRNA genes (Yekta et al., 2008).

To test whether miR-196 regulates transcript levels of predicted *hox* cluster targets, we over-expressed miR-196 duplex or knocked down *mir196* expression with morpholino antisense oligonucleotide (Mo) designed to inhibit miR-196 maturation and then examined transcript levels by *in situ* hybridization in 24 hpf embryos using the hindbrain marker *egr2a* as internal control. Results showed that *hox* genes that had mismatch target sites, including *hoxb5a, hoxb5b, hoxb6b and hoxc6a,* mostly retained their native expression level, but with a weakened anterior boundary after overexpression of *mir196* (Data not shown). We conclude that *hoxb5a, hoxb5b, hoxb6b,* and *hoxc6a* might be fine-tuned in their anterior border either as direct targets of miR-196 or are downstream of a miR-196 target.

Zebrafish *hoxb8a* mRNA has a perfect target site for miR-196a like its orthologous *HoxB8* gene in human and mouse (Yekta et al., 2008), and the level of transcript was knocked down after over-expression of *mir196*. This result can be explained if *hoxb8a* transcript, like other transcripts with perfect matches of miRNA to target site, is degraded after miRNA binding (Hornstein et al., 2005; Kawasaki and Taira, 2004; McGlinn et al., 2009a; Yekta et al., 2004). To confirm the inhibition of miR-196 on *hoxb8a*, we made a reporter gene construct by attaching the 3'UTR of *hoxb8a* to the coding region of GFP. Results showed that fluorescence signal was inhibited after the co-injection of mRNA transcribed from this reporter gene with either miR-196a or miR-196b duplex; as expected, fluorescence increased after knockdown of endogenous *mir196* (data not

shown). This result showed that miR-196 inhibits *hoxb8a* expression by degrading *hoxb8a* mRNA in zebrafish as in mammals (Yekta et al., 2004).

3.3.4. *Mir196* Blocks Zebrafish Pectoral Fin Initiation

To learn the roles of miR-196 in embryonic development, we injected miR-196 duplex into early cleavage embryos and inhibited miR-196 processing and binding with morpholinos. Resulting animals survived to adulthood but showed highly specific phenotypes in the pectoral appendage, pharyngeal arches, and rostral vertebrae and ribs.

After miR-196 duplex injection, at least one pectoral fin was absent in 161 of 183 injected animals (**Fig. 3.2A-G**), and fin loss persisted into adulthood (**Fig. 3.2H-J**). At 5 dpf (days post fertilization), the pectoral apparatus from 234 animals over-expressing miR-196 either lacked endochondral discs and scapulo corocoid (42.3%, **Fig. 3.2L**), lacked endochondral discs only (6.0%, **Fig. 3.2M**) or had normal fin buds (51.7%, **Fig. 3.2N**). The cleithrum, a dermal bone that does not form in fin mesenchyme (Mercader, 2007), was always present (**Fig. 3.2K-N**). We conclude that miR-196 blocks an early stage in pectoral fin development.

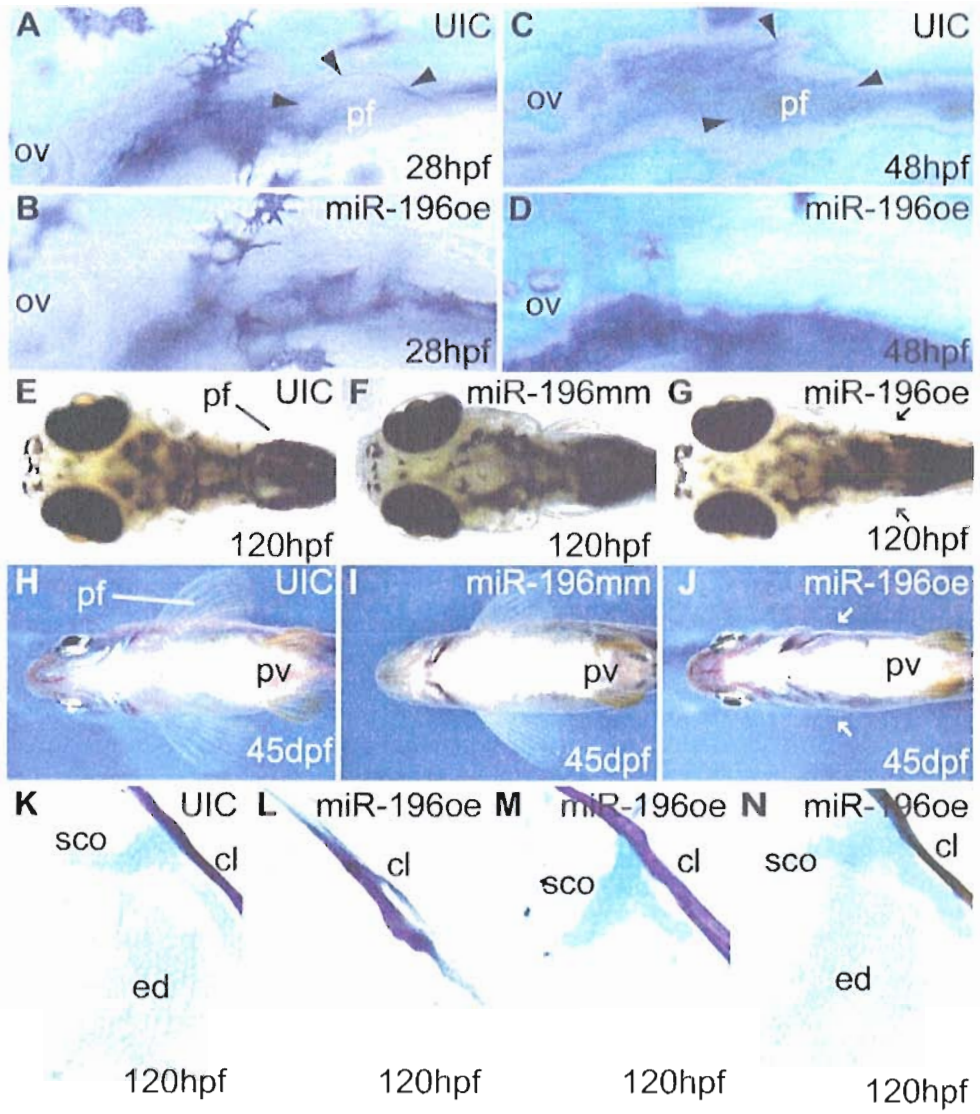

Fig. 3.2. *Mir196* Over-expression Inhibits Pectoral Fin Initiation. (A, C) Pectoral fin buds are detectable at 28 hpf and 48 hpf in control animals, but not in embryos over-expressing miR-196 (B, D). (E, F, H, I) Uninjected controls or miR-196 mismatch injected controls showed normal pectoral fins by 5 and 45 days post fertilization (dpf), but larvae over-expressing miR-196 had not recovered pectoral fins by 5 dpf and became paraplegic adults (G, J). Pelvic fins were normal in fish with pectoral fin defects. (K-N). Pectoral fins stained with Alcian blue and Alizarin red showed defects ranging from absence of the endochondral disc and scapulocoracoid (42.3%) to normal (51.7%, n=234); the remaining 6% had no pectoral fin disc, but did have the pectoral girdle (soc) (**Fig. 3.2M**). Abbreviations: cl, cleithrum; ed, endochondral disc; ov, otic vesicle; pf, pectoral fin or bud; pv, pelvic fin; sco, scapulocoracoid.

To learn how miR-196 acts to block pectoral fin formation, we interrogated steps in appendage development. In pectoral fin development (**Fig. 3.3A**), somite-derived retinoic acid (RA) acts on intermediate mesoderm to induce *wnt2ba*, which, along with RA acting via the retinoic acid receptor Rarab (Linville et al., 2009), causes lateral plate mesoderm (LPM) to express *tbx5a* (Garrity et al., 2002), which turns on *fgf24* leading to expression of *fgf10a*, which activates the apical epidermal fold (AEF), thereby promoting fin bud outgrowth followed by the development of *lbx1b*-expressing fin muscle (Mercader, 2007; Wotton et al., 2008). Genes like *prdm1a* that are necessary for pectoral fin bud initiation are downstream of RA (Mercader et al., 2005). To discover the miR-196-sensitive process, we examined pectoral fin gene expression after *mir196* manipulation. miR-196-injected embryos lost expression of *lbx1b*, showing that miR-196 acts before fin muscle induction (**Fig. 3.3B, C**). Working backward through development, miR-196 injection blocked expression of *fgf10a, fgf24,* and *tbx5a*, the earliest expressed pectoral-fin specific gene (**Fig. 3.3D-I**). *wnt2ba* is weakly expressed even in wild types (Koudijs et al., 2008; Mercader et al., 2006), thus, it is hard to predict the the weakened expression of *wnt2ba* in the fin field region after miR-196 over-expression in some animals (data not shown). The expression of the gene *prdm1a* in the pectoral fin bud is downstream of RA signaling (Linville et al., 2009; Mercader et al., 2006; Mercader et al., 2005). We found that miR-196 injection blocked the expression of *prdm1a* in the pectoral fin field without affecting the expression in the CNS or pharyngeal arches, implying that the action of miR-196 is upstream of *prdm1a* activity in pectoral fin (**Fig. 3.3J, K**). RA induces *Hoxc6* expression in the mesenchyme of chick wing bud (Oliver et al., 1990) and we found that miR-196 injection blocked the expression of *hoxc6a* in the pectoral fin field (**Fig. 3.3L, M**). This result is consistent either with the direct action of miR-196 on *hoxc6a* activity or on indirect action via retinoic acid signaling. miR-196 knockdown disrupted neither the expression of *fgf24* and *tbx5a* in the pectoral fin field (data not shown) nor the development of pectoral fins.

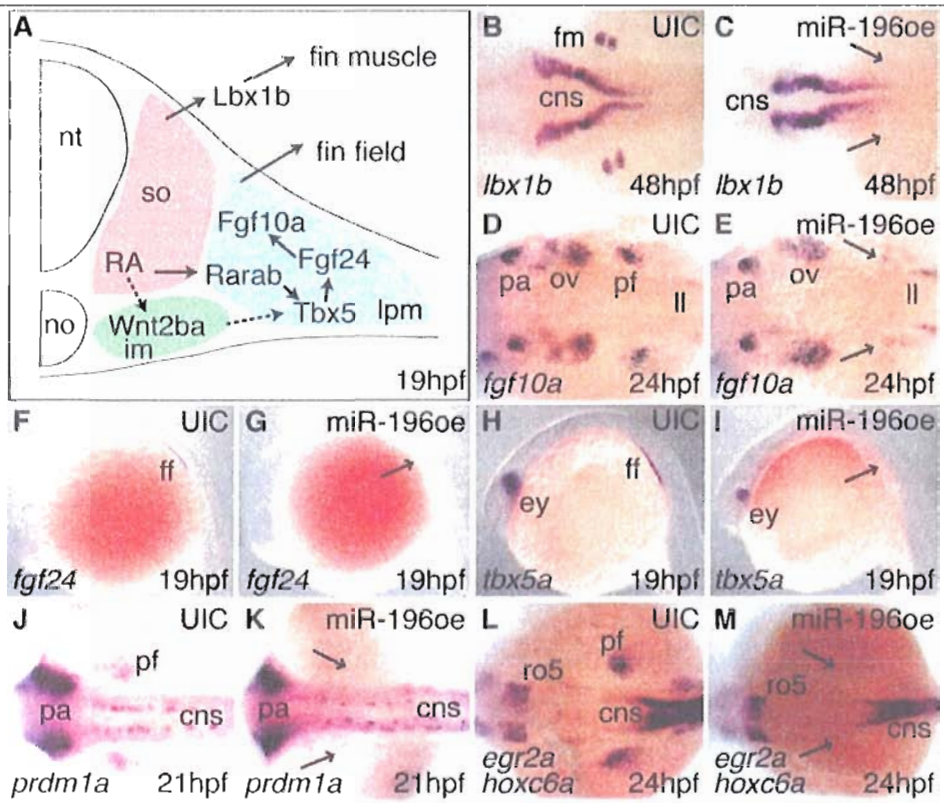

Fig. 3.3. MiR-196 Duplex Injection Inhibits Expression of Zebrafish Fin Development Genes. (A) Model of the pectoral fin developmental pathway. *In situ* hybridization for *lbx1b* (B, C), *fgf10a* (D, E), *fgf24* (F, G), *tbx5a* (H, I), *wnt2ba* (J, K), *prdm1a* (L, M), on controls (B, D, F, H, J, L) and miR-196 over-expression (oe) animals (C, E, G, I, K, M) at ages indicated in the lower right of each panel. Arrowheads show the presumptive pectoral fin region in miR-196 duplex-injected animals. Abbreviations: cns, central neural system; ff, fin field; fm, pectoral fin muscle; im, intermediate mesoderm; ll, lateral line primordium; no, notochord; nt, neural tube; ov, otic vesicle; pa, pharyngeal arch; pf, pectoral fin bud.

3.3.5. *Mir196*, Fin Buds, and Retinoic Acid Signaling

To learn if *mir196* overexpression disrupts RA signaling, we examined control, miR-196 morpholino-injected, and miR-196 duplex-injected transgenic animals in which RA signaling activates a retinoic acid response element leading to expression of Yellow

Fluorescent Protein (YFP) in the CNS by 43 hpf (**Fig. 3.4A-D**, left embryo). Embryos over-expressing miR-196 displayed less fluorescence, signifying reduced RA signaling (**Fig. 3.4A, B**, right embryo). Conversely, *mir196* knockdown gave elevated fluorescence and hence enhanced RA signaling (**Fig. 3.4C, D**, right embryo). These results demonstrate that miR-196 can inhibit RA signaling in the CNS, and, coupled with the fact that mutation of an RA-synthesizing enzyme can delete the fin bud (Begemann et al., 2001), suggest the hypothesis that the pectoral fin phenotype of miR-196 over-expression results from decreased RA signaling.

The hypothesis that miR-196 negatively regulates RA signaling in fin bud initiation predicts that the inhibition of RA signaling by other methods should lead to the same phenotype. To test this prediction, we used DEAB, a reversible inhibitor of RA-synthesizing enzymes (Perz-Edwards et al., 2001). RA inhibition, like miR-196 over-expression (**Fig. 3.2**), caused a loss of pectoral fin outgrowth that persisted to adulthood (data not shown) and inhibited expression of *fgf24, tbx5a, fgf10a,* and *lbx1b* (data not shown). These results are as expected if miR-196 blocks fin bud development by inhibiting RA signaling.

If miR-196 inhibits RA signaling, then excess RA should rescue the fin phenotype of miR-196 over-expression and miR-196 knockdown should rescue diminished RA signaling. We increased RA signaling either by exposing 12 hpf embryos to synthetic RA (10^{-7} M) for two hours or by the use of mutants in *cyp26a1*, which encodes an RA catabolic enzyme (Emoto et al., 2005). At 120 hpf, both treatments resulted in short or absent pectoral fins (Grandel et al., 2002) (data not shown). In homozygous *cyp26a1*^{rw716} mutants, the endochondral disc was more sensitive than the scapulocoracoid. While 89% (n=63) of animals over-expressing miR-196 (5 nL) had no pectoral fin (**Fig. 3.4E**), only 48% of animals co-injected with miR-196 and treated with 10^{-7}M RA lacked pectoral fins (n=81). Reciprocally, the knockdown of endogenous miR-196 partially rescued defective fins resulting from DEAB-inhibited RA signaling (**Fig. 3.4F**). We interpret this rescue to mean that with less miR-196 there is more Rarab, which can overcome diminished RA

signal caused by DEAB. These results show that endogenous miR-196 inhibits pectoral fin bud initiation by interfering with RA signaling.

3.3.6. A Target for MiR-196 in Fin Bud Development

To identify a molecular target related to RA signaling, we looked for potential miR-196 binding sites in the 3'UTRs of genes that are in RA signaling pathway or related to RA signaling, as well as genes involved in pectoral fin initiation. Checking miRbase database and use of MicroInspector (Rusinov et al., 2005) binding site prediction software showed that transcripts encoding Cyp26a1 and the retinoic acid receptor Rarab have predicted miR-196 target sites, but other RA-pathway genes, including *aldh1a2,* all other *rar* genes, *prdm1a, fibin, tbx5a, wnt2b* and *fgf* pathway genes lacked such sites. If miR-196 exerted its effect on pectoral fin bud initiation by inhibiting *cyp26a1*, then the phenotypes of the two should be identical. In contrast, however, the pectoral fin bud in zebrafish *cyp26a1* mutants initiates and forms the scapulocorocoid [data not shown, and (Emoto et al., 2005)], which does not usually happen in *mir196* over-expression (**Fig. 3.2K-N**). In addition, the expression domain of *tbx5a* is shifted anteriorly in *cyp26a1* mutants (Emoto et al., 2005) rather than being deleted completely as in *mir196* over-expression (**Fig. 3.3H, I**). Furthermore, inhibition of an RA degrading enzyme should augment RA signaling rather than reduce RA signaling as we observed after *mir196* over-expression. These data rule out *cyp26a1* as the major miR-196 target relevant for the fin bud phenotype.

The hypothesis that *rarab* is the miR-196 target for the fin bud predicts that the knockdown of *rarab* activity should mimic the over-expression of miR-196. To test this prediction, we knocked down and over-expressed *rarab*. Like miR-196 over-expression, *rarab* knockdown blocked pectoral fin initiation (**Fig. 3.4G-N** and (Linville et al., 2009)) and inhibited the expression of genes in the pectoral fin developmental pathway, including *tbx5a, fgf24, fgf10a, hoxc6a* and *lbx1b* (**Fig. 3.4O-X**). As with miR-196 over-expression, *rarab* knockdown fish became adults lacking pectoral fins (**Fig. 3.4M, N**).

Analysis showed that after *rarab* knockdown, pectoral fins either lacked the endochondral disc and scapulocoracoid (70%, n=101) or had normal fins. Over-expressing *rarab* by injection of *rarab* mRNA did not give a pectoral fin phenotype (data not shown), mimicking results for *mir196* knockdown. Collectively, these results are consistent with the hypothesis that miR-196 targets *rarab* during fin initiation.

Fig. 3.4. Mir196 Activity Modulates RA Signaling. (A) Brightfield microscopy of an uninjected control transgenic RA-signaling reporter individual and a miR-196 injected 43 hpf RA-reporter embryo oriented back-to-back as in the insert at left of part (A), with the boxed region blown up in A-D. (B) The animals in (A) viewed in fluorescence microscopy. (C) Brightfield and (D) fluorescence views of a control (left) and a miR-196-morpholino injected 43 hpf embryo. (E, F) Rescue experiments. (E) Although injecting cleavage embryos with 5nL of miR-196 duplex (++) and treating with DMSO control caused a greater fraction of animals to develop without pectoral fins (89%, n=63) than injections with 1nL (+) (78%, n=76), both can be rescued by RA treatment (+) (48%, n=81 and 28% n=61 without fin respectively). This experiment was repeated four times (F) Treating embryos with 1x10-5M (++) or 5x10-6M (+) DEAB to decrease RA levels resulted in all (100%, n=31) or most of the animals (87.5%, n=16) lacking pectoral fins respectively, but first injecting cleavage embryos with 1nL of 3mM mir196-Mo (+) to diminish the inhibition of RA signaling before treating embryos with DEAB, partially rescued the fin phenotype by 53% (n=51) and 54% (n=48) respectively. Compared to controls (G, I, K, M), rarab-Mo injection (H, J, L, N) inhibited pectoral fin outgrowth already by 28 hpf (G, H) and this phenotype was maintained through 48 hpf (I, J), 120 hpf (K, L), and into adulthood (M, N). Arrowheads mark the edge of the pectoral fin edge and arrows direct attention to missing pectoral fins and buds. (O-V) rarab-Mo inhibited expression of the pectoral fin genes tbx5a (O, P), fgf24 (Q, R), fgf10a (S, T), and hoxc6a (U, V), as well as the fin muscle marker gene lbx1b (W, X) specifically in the fin field region while leaving other expression domains intact. Arrows: missing pectoral fin buds. cns, central neural system; ey, eye; he, heart; im, intermediate mesoderm; ll, lateral line primordium; ov, otic vesicle; pa, pharyngeal arch; pf, pectoral fin; pv, pelvic fin; ro3, -5, rhombomere3, -5.

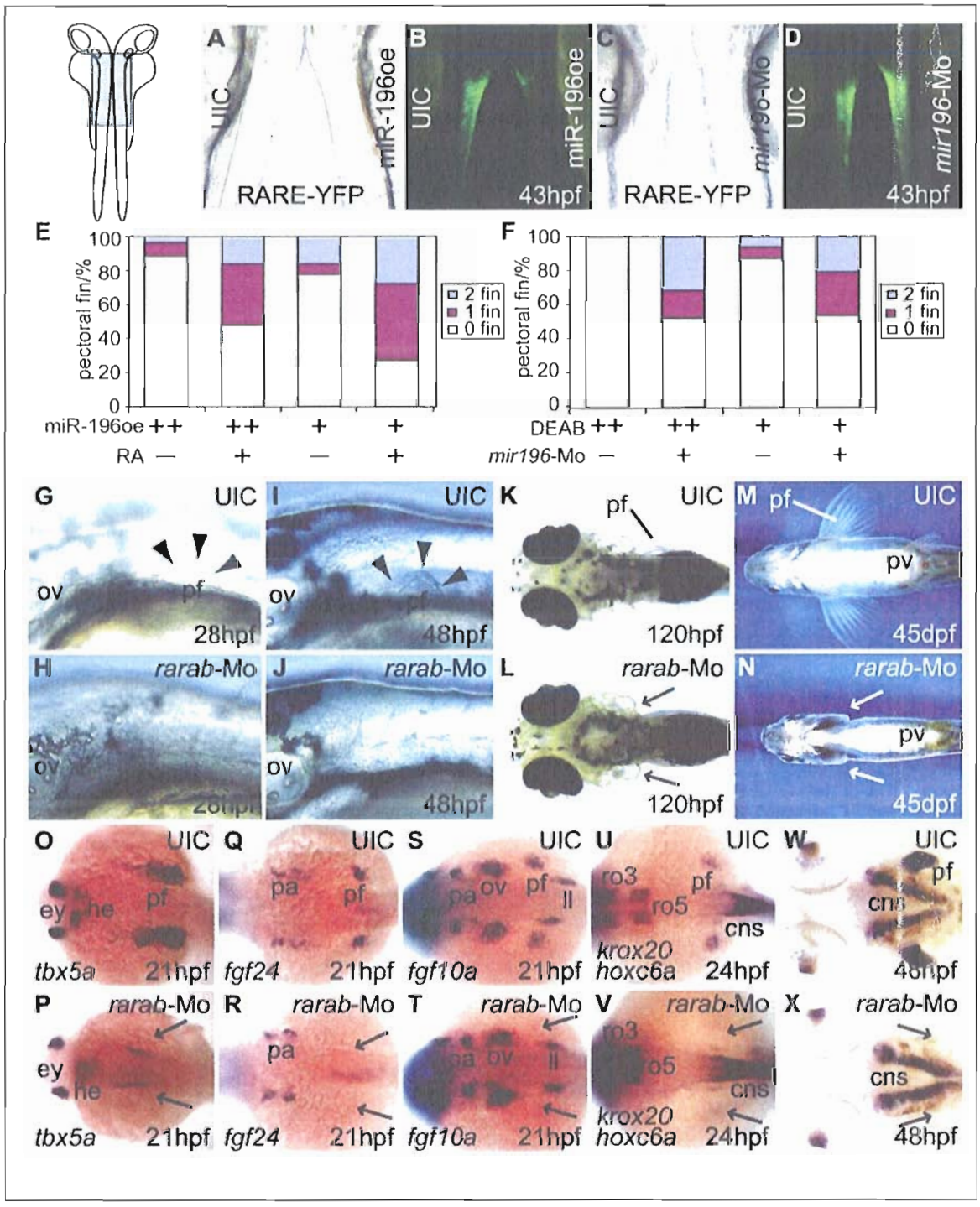
A
UIC
miR-196oe
RARE-YFP
B
UIC
miR-196oe
43hpf
C
UIC
mir196-Mo
RARE-YFP
D
UIC
mir196-Mo
43hpf
E
pectoral fin/%
100
80
60
40
20
0
2 fin
1 fin
0 fin
miR-196oe ++ ++ + +
RA — + — +
F
pectoral fin/%
DEAB ++ ++ + +
mir196-Mo — + — +
G
UIC
ov
pf
28hpf
I
UIC
ov
48hpf
K
pf
UIC
120hpf
M
pf
UIC
pv
45dpf
H
rarab-Mo
ov
J
rarab-Mo
ov
48hpf
L
rarab-Mo
120hpf
N
rarab-Mo
pv
45dpf
O
UIC
ey
he
pf
tbx5a
21hpf
Q
UIC
pa
pf
fgf24
21hpf
S
UIC
pa
ov
pf
II
fgf10a
21hpf
U
UIC
ro3
pf
ro5
cns
krox20
hoxc6a
24hpf
W
UIC
pf
cns
48hpf
P
rarab-Mo
ey
he
tbx5a
21hpf
R
rarab-Mo
pa
fgf24
21hpf
T
rarab-Mo
pa
ov
II
fgf10a
21hpf
V
rarab-Mo
ro3
ro5
cns
krox20
hoxc6a
24hpf
X
rarab-Mo
cns
48hpf

If miR-196 attenuates *rarab*, then both transcripts should be expressed in the same cells. Analysis showed that the expression of *rara* (Hale et al., 2006; Linville et al., 2009) is similar to that of miR-196 in fin bud initiation (**Fig. 3.5A-D**). To see if miR-196 could target the *rarab* 3'UTR, we used a firefly luciferase assay in cultured cells using *Renilla* luciferase as an internal standard. We attached the *rarab* 3'UTR with its three predicted miR-196 binding sites to luciferase coding sequence (**Fig. 3.5E, F**) and co-transfected this construct and miR-196 into human 293T cells. MiR-196 led to reduced luciferase fluorescence from the *rarab* 3'UTR construct compared to the control (**Fig. 3.5G**), showing that miR-196 can act on the *rarab* 3'UTR to inhibit message stability and/or translation. To test this interaction in living embryos, we co-injected a construct containing the GFP coding region followed by the *rarab* 3'UTR (**Fig. 3.5E**) and then over-expressed or knocked down miR-196. Embryos injected with miR-196 had less GFP fluorescence than uninjected controls or controls injected with miR196 mismatch duplex, but embryos experiencing miR-196 knockdown had more fluorescence than controls (**Fig. 3.5H-K**). However, when we mutated the three predicted binding sites for miR-196 in the *rarab* 3'UTR but keep the other portion of the sequence intact, we did not notice significant difference for GFP fluorescence (**Fig. 3.5L-O**). This reporter assay confirmed direct interaction between miR-196 and the *rarab* 3'UTR in living embryos. We conclude that *rarab* is the miR-196 target responsible for the pectoral fin initiation phenotype. Because the amount of *rarab* transcript is not changed after miR-196 over-expression or knockdown (data not shown), miR-196 is likely to act more strongly on *rarab* translation than on message stability.

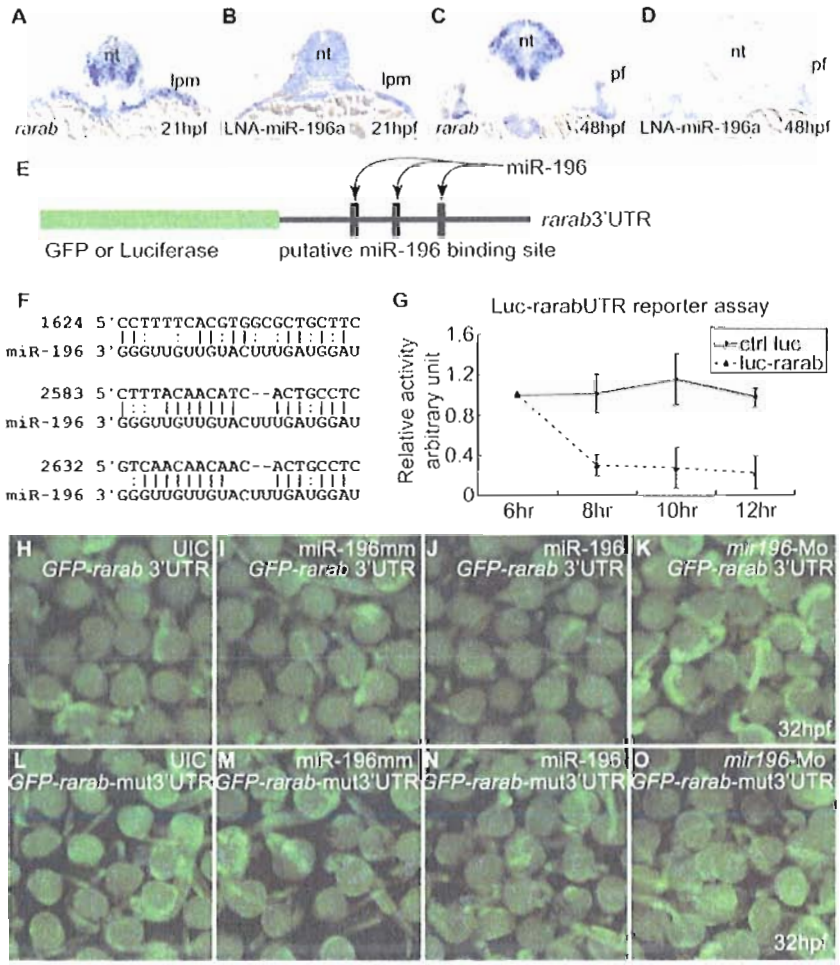

Fig. 3.5. *Rarab* Is a Target of MiR-196. (A-D) *In situ* hybridization for *rarab* (A, C) and miR-196 (B, D) at 21 hpf (A, B) and 48 hpf (C, D). (E) The reporter assay constructs used luciferase in (G) and GFP in (H-K). (F) The 3'UTR of *rarab* has three predicted binding sites for miR-196 (nucleotide position according to NM_131399). (G) miR-196 interferes with expression of a luciferase reporter bearing the 3'UTR of *rarab*. This experiment was repeated three times. (H-K) GFP-*rarab* 3'UTR mRNA was injected either by itself (H) or co-injected with miR-196 mismatch (I), with miR-196 duplex (J), or with *mir196*-Mo (K). MiR-196 depressed fluorescence but *mir196* knockdown enhanced fluorescence. This experiment was repeated four times. (L-O) the three predicted binding sites were removed from the GFP-*rarab 3'*UTR construct to make a GFP-*rarab*-mut3'UTR. GFP-*rarab* mut3'UTR mRNA was injected into early cleavage stage embryos either by itself (L) or co-injected with miR-196 mismatch (M), with miR-196 duplex (N), or with *mir196*-Mo (O). MiR-196 did not depress fluorescence (N) and *mir196* knockdown did not enhance fluorescence (O) from this mutant construct. This experiment was repeated three times. lpm; lateral plate mesoderm; pf, pectoral fin bud.

3.3.7. *Mir196* Inhibits Branchial Arch Segmentation

Animals over-expressing *mir196* lacked not only pectoral fins, but also one pharyngeal arch (PA). Zebrafish have seven PAs, including mandibular (PA1), hyoid (PA2), and five branchial (gill) arches (PA3-7). After miR-196 over-expression, PA1 and PA2, as well as the tooth-bearing PA7, were normal. In 84% (n=254) miR-196 duplex injected animals, however, one or both sides of the animal had four rather than five gill arches (**Fig. 3.6A, B**). Although individual gill arches were generally normal in morphology, occasionally a short arch was fused to PA7 after miR-196 over-expression (**Fig. 3.6B**, insert), suggesting that the missing arch was PA6. This result shows that high or ectopic *mir196* is sufficient to reduce the number of branchial arch segments. We infer that miR-196 inhibits a process necessary to add branchial arches, probably PA6.

To test whether endogenous miR-196 regulates branchial arch formation, we knocked down miR-196. Results showed that 33% of injected animals (n=140) had six rather than the normal five branchial arches (**Fig. 3.6C**). Some animals with five branchial arches had an additional skeletal element fused to PA7, suggesting that miR-196 normally inhibits the arch just anterior to PA7. This result shows that normal levels of miR-196 are necessary to prevent the addition of supernumerary branchial arches. Because the miR-196 knockdown phenotype is opposite to that of miR-196 over-expression, we conclude that precisely adjusted levels of miR-196 are required for proper branchial arch segmentation.

Cartilage-forming cells in pharyngeal arches arise from post-migratory neural crest that is divided into several streams by endodermal pouches [**Fig. 3.6D** and ref. (Crump et al., 2004)]. To determine whether miR-196 acts primarily on the endodermal pouches or only on the neural crest, we used transgenic *fli*-GFP fish in which the skeletogenic crest fluoresces green (Lawson and Weinstein, 2002) and stained animals with the antibody zn-8 as a marker for pharyngeal endoderm (Trevarrow et al., 1990). In contrast to normal 36 hpf embryos with seven pharyngeal arches (**Fig. 3.6D**), *mir196* over-expression embryos lacked one endodermal pouch (**Fig. 3.6E**). Conversely, *mir196* knockdown

embryos had an extra endodermal pouch that resulted in an extra pharyngeal arch precursor (**Fig. 3.6F**). These results in embryos correspond to the cartilage phenotype of miR-196 manipulated larvae and support the hypothesis that miR-196 derived defects in pharyngeal arch patterning arise from initial affects in the patterning of pharyngeal pouch endoderm. Together, these results lead to the conclusion that *mir196* acts in pharyngeal arch endoderm to suppress the formation of a posterior pharyngeal pouch.

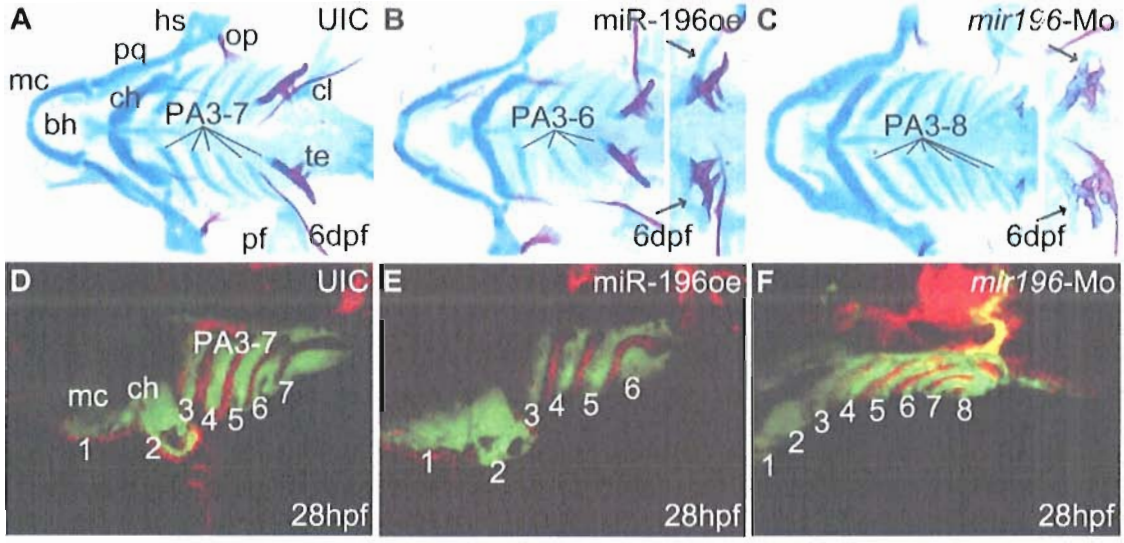

Fig. 3.6. *Mir196* Regulates Pharyngeal Arch Segmentation via Pharyngeal Endoderm. (A-C) Zebrafish embryos injected with miR-196 duplex or *mir196*-Mo were raised to 6 dpf and stained with Alcian blue for cartilage and Alizarin red for bone. A. Control larvae had seven pharyngeal arches, including Meckels and ceratohyal cartilages (PA1 and PA2) and five branchial arches (PA3-7). B. Animals over-expressing miR-196 lacked one branchial arch. Some animals with four branchial arches (insert) possessed a skeletal element attached to the last arch (arrows), suggesting that the missing arch was the one anterior to the tooth-bearing branchial arch-5. C. Injection of *mir196*-Mo resulted in animals with extra branchial arches. Some animals with seven pharyngeal arches (insert) displayed extra skeletal elements attached to branchial arch-5 (arrows), suggesting that the extra arch was the one just anterior to branchial arch-5. (D-F) Transgenic animals expressing GFP in the neural crest (green) that were either over-expressing (E) or knocked down (F) for miR-196 showed defective segmentation of endodermal pouches stained with zn-8 antibody (red) and pharyngeal arches (green) consistent with observed alterations in arch numbers. Abbreviations: bh, basihyal; ch, ceratohyal; cl, cleithrum; hs, hyosymplectic; mc, Meckels cartilage; op, opercle; pa, pharyngeal arch; pf, pectoral fin; pq, palatoquadrate; te, teeth.

3.3.8. Normal *Mir196* Levels are Essential to Pattern the Axial Skeleton

Proper levels of miR-196 are important not only for proper segmentation of branchial arches but also for normal segmentation of the rostral axial skeleton. The anterior four vertebrae of zebrafish and other Otophysi form the Weberian apparatus, bones that transmit sound from the swim bladder to the inner ear (Grande and Young, 2005). The Weberian apparatus is followed by about ten rib-bearing precaudal vertebrae (**Fig. 3.7A, D** and ref. (Bird and Mabee, 2003)). Adult fish developing from embryos injected with miR-196 duplex showed disrupted rostral axial skeletons, including axial shifts in the patterning of the Weberian apparatus and fewer precaudal vertebrae and ribs (**Fig. 3.7B, D, E-L**). Adult fish developing from embryos injected with *mir196* Mo did not show defects in the Weberian apparatus, however, they had more ribs and rib bearing precaudal vertebrae than normal (**Fig.3.7C, D**). Statistically, miR-196 injected animals had on average 0.7 fewer segments in the Weberian apparatus than wild types (73.2%, n=56 injected animals), and 2.5 fewer ribs (81.8%), and 2.1 fewer rib-bearing vertebrae than normal (36.2%) (**Fig. 3.8D**).

In wild-type fish, the Weberian apparatus has four highly modified vertebrae, each with bone and cartilage morphologies that specify their identity (**Fig. 3.7E, F, I, J**). The lateral process-1 (lp1), the lateral process-2 (lp2), the intercalarium (in), the tripus bones (tr), the neural arch-3 (na3) and neural arch-4 (na4), the highly modified rib-4 (r4), os suspensorium, supranueral-3 (sn3) and supranueral-4 (sn4) are attached to one of the four vertebra in the Weberian apparatus. These different skeletal structures facilitated identification of each of the vertebrae in the Weberian apparatus.

Animals over-expressing miR-196 showed fate transformations in the Weberian apparatus. For example, in the animal in Figure 8G, the second segment (segment #2) had the joint for the intercalarium, which is appropriate for a normal vertebra-2, but it possessed a dorsal projection that appeared similar to, but not as broad as, neural arch-3 (asterisk in **Fig. 3.7G**). The morphology of this animal's segment #3 was similar to the normal v4 with a neural arch-4 and rib-4 like rib (arrow in **Fig. 3.7G**). Segment #4 had a

rib appropriate for v5 (arrowhead in **Fig. 3.7G**). We conclude that in this fish, the identity of segments #2-4 were partially transformed into more posterior fates, an apparent homeotic transformation. Alternatively, v2 or v3 was deleted and segment #2 assumed an identity intermediate between v2 and v3. The animal in Fig. 3.7H had a normal v1 with a normal lateral process-1, but segment #2 had an abnormally short lateral process-2; segment #3 had a ventral projection intermediate in character between the tripus (**Fig. 3.7E, F**) and anteriorly projecting, forked rib-4 (r4) which is more appropriate for the next segment more posterior (arrow in **Fig. 3.7H**), and a neural arch more similar to neural arch-4 than neural arch-3; in addition, segment #4 had a rib with the morphology of rib-5 rather than rib-4 (arrowhead in **Fig. 3.7H**). Figure 7K is a ventral view of the Weberian apparatus of an animal over-expressing miR-196 with relatively normal v1 and v2, but v3 showed partial posterior transformation on the right side with a forked tripus anteriorly oriented like rib-4, although the left side was relatively normal; segment #4 had a rib on the left side that was appropriate for rib-4, but on the right side, the rib pointed backwards and was not forked, which are characteristics of the more posterior rib-5. The Weberian apparatus of the animal in Figure 7L had a segment #2 with a normal tripus on the right side (rather than on the normal v3) and a malformed tripus on the left side; segment #3 of this animal had an rib-4-like structure on the right side and a nearly normal tripus on the left side (arrows in **Fig. 3.7L**); segment #4 on both sides had ribs appropriate for rib-5 (arrowheads in **Fig. 3.7L**). This phenotype occurred repeatedly in affected animals. In summary, analysis of miR-196 over-expression animals suggests that the identities of rostral vertebrae are transformed into structures appropriate for more posterior elements.

In contrast to the over-expression results, as discussed above, knockdown of miR-196 resulted in fish that had a morphologically normal Weberian apparatus but tended to have extra ribs and extra rib-bearing precaudal vertebrae (**Fig. 3.7C, D**). This result shows that native miR-196 expression levels are important for axial segment morphology. With regard to rib and precaudal vertebrae number, the results from miR-196 knockdown (segment gain) were opposite that of miR-196 over-expression (segment loss). In

summary, the manipulation of miR-196 levels resulted in altered numbers and homeotic-like fate transformations and segmentation abnormalities along the axial skeletal system.

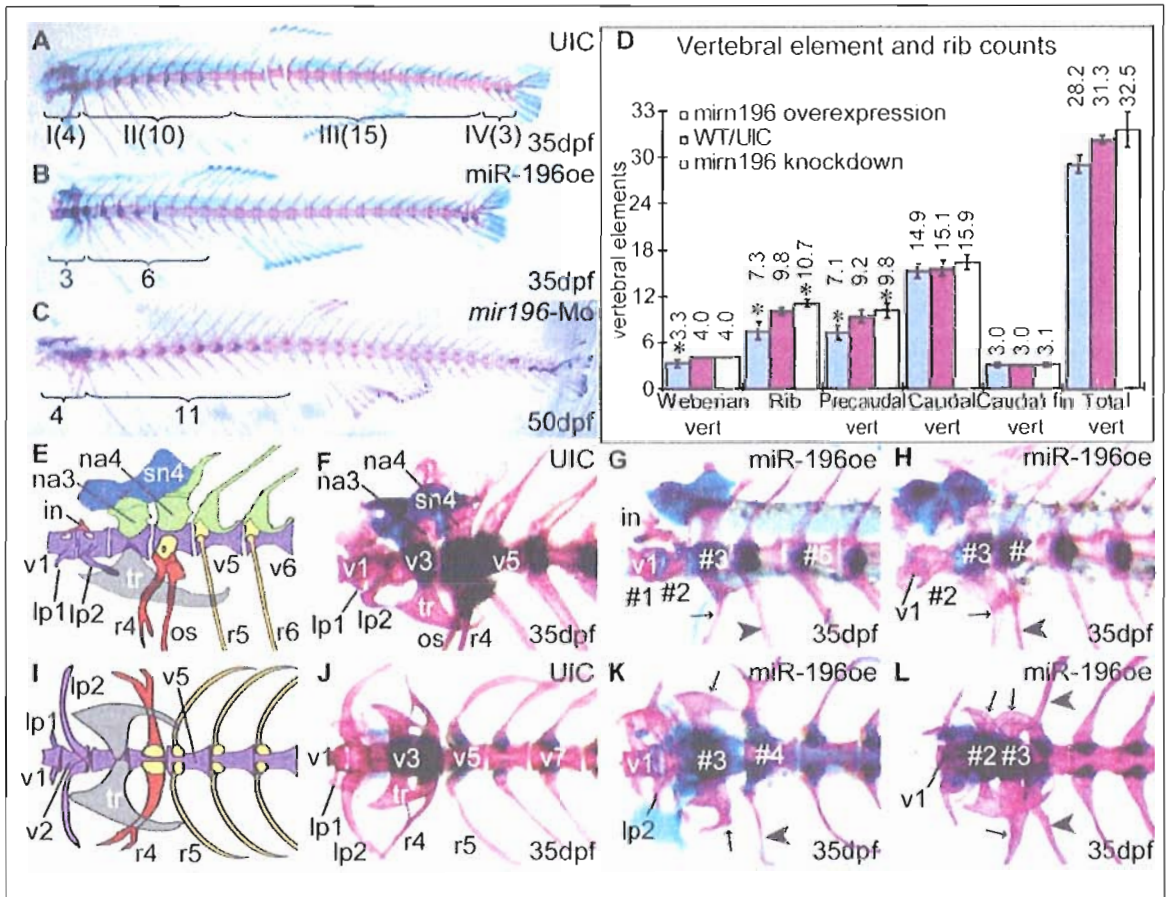

Fig. 3.7. Misexpression of MiR-196 Disrupts Patterning of the Axial Skeleton. (A) Normal axial skeleton stained for cartilage (Alcian blue) and bone (Alizarin red) showing 4, 10, 15 and 3 vertebrae in the Weberian apparatus (region I), rib-bearing precaudal vertebra (region II), caudal vertebra (region III) and caudal fin vertebra (region IV), respectively. (B, D) Over-expression of *mir196* showing deletion of one Weberian vertebra and four ribs with their precaudal vertebrae. (C, D) Knockdown of miR-196 resulted in extra ribs and extra precaudal vertebrae. (D) Skeletal element counts showing reciprocal effects. Asterisks indicate statistical significance (Student T-test, $p < 0.001$). UIC, n=79; miR-196oe, n=56; *mir196*-Mo, n=122. (E, F, I, J) Weberian apparatus sketch and skeleton staining (after (Grande and Young, 2005)). (G, H, K, L) Over-expression of miR-196, lateral (G, H) and ventral (K, L) views of the Weberian apparatus from different individuals. Abbreviations: #1, #2, #3, vertebrae numbers from anterior without regard to identity; in, intercalarium; lp1, lp2, lateral processes; na3, na4, neural arches; os, os suspensorium; r4, r5, ribs; tr, tripus; v1, v2, v3, v4, v5, v7 vertebrae with identities.

To understand how miR-196 regulates the segmentation of axial skeleton, we scored somite numbers after either miR-196 overexperssion or knockdown. Four-day old wild type zebrafish embryos fully develop about 30 or 31 somites (78.4%, n=74). We found that overexpression of miR196 reduces total somite number (81.1%, somite number less than 30, n=53), while knockdown of *mir196* induces extra somites than control fish (62.1%, somite number bigger than 31, n=66). This result is consistent with our prediction that somitogenesis is regulated by miR-196.

3.4. *Mir196* Controls Zebrafish Skeletal Patterning

Over-expressing the *hox*-cluster microRNA miR-196 caused three highly specific phenotypes – failure of pectoral appendage initiation, aberrant development of pharyngeal arches, and pattern transformations of vertebrae.

3.4.1. The Interaction of *Hox*-Cluster Genes and *Mir196* Genes

The similar expression patterns of miR-196 and the *hox*-cluster protein-coding genes nearby would be expected if miR-196 shares regulatory information with neighboring *hox*-cluster protein-coding genes. The expression of *hox*-cluster protein-coding genes is maintained partially by retinoic acid signaling. Thus we predict that miR-196 expression is also maintained, at least partially, by retinoic acid signaling.

Zebrafish *hox* cluster protein-coding genes are rich in miR-196 targets like that in mammals (Yekta et al., 2008). Functional experiments, however, are needed to verify this prediction. Except for *hoxb8a* (*HoxB8* orthologs in mammals), the predicted *hox* target genes for miR-196 have partial complementary matches with miR-196, indicating that these *hox*-cluster protein-coding genes are regulated by miR-196 in the way by inhibiting their translation instead of inducing the degradation of their messenger RNAs. Thus, to test the prediction that these predicted *hox*-cluster protein-coding genes are really

regulated by miR-196, the protein production instead of mRNA abundance should be affected after miR-196 alteration. However, our selective expression study showed that *hoxb5a, hoxb5b, hoxb6b* and *hoxc6a* have weakened anterior expression borders. This result indicated that there is/are other genes regulated by miR-196 but upstream of these *hox*-cluster protein-coding genes. Since retinoic acid signal is one of the confirmed regulators that control the expression of groups of *hox*-cluster protein-coding genes. Mutation of retinoic acid signaling components (such as mutation in *raldh1a2* and *cyp26a1* in zebrafish) induces shifting of the anterior border of *hox* cluster protein-coding genes. The similar effect on multiple *hox* genes by mutation of retinoic acid signal pathway genes and alteration of miR-196 implies that miR-196 is regulating some genes like retinoic acid pathway genes. In addition, the phenotypic differences between the mutations of retinoic acid signal component and alteration of miR-196 maybe explained that the regulation of miR-196 imposed on that master gene is subtle, the similar result we have seen that miR-196 fine-tunes the expression of *rarab.* This result showed that the regulation of *hox*-cluster protein coding genes by miR-196 is both direct and indirect.

For *hoxb8a*, like its mammalian orthologs *HoxB8* in human and mice, it has perfect complementary binding site predicted for miR-196 and its expression is inhibited after miR-196 over-expression, implying that *hoxb8a* messenger stability is regulated by miR-196. In conclusion, the regulation of hox cluster protein coding genes by miR-196 might be realized at different levels, both direct and indirect regulation are involved in this complex regulatory network.

3.4.2. *Mir196* Inhibits Pectoral Fin Induction by Inhibiting *Rarab*

Animals injected with miR-196 duplex lacked pectoral fins and showed diminished expression of early fin bud markers. We conclude that miR-196 over-expression inhibits the initiation, rather than patterning or elongation, of pectoral fin buds. No conclusions can be drawn with respect to the effect of miR-196 on pelvic fin bud because it develops more than two weeks after fertilization (Grandel et al., 2002), which is long after the

injected miRNA would have an effect. Retinoic acid signaling acts upstream of pectoral appendage initiation (Gibert et al., 2006; Grandel et al., 2002; Linville et al., 2009; Mercader et al., 2006). Because miR-196 knockdown partially rescued diminished RA-signaling, endogenous miR-196 must play a role in normally developing zebrafish. Transcript from *rarab* appears in both the CNS and lateral plate mesoderm (Hale et al., 2006; Linville et al., 2009) and contains three predicted binding sites for miR-196, suggesting the hypothesis that miR-196 attenuates RA signaling by lowering levels of Rarab protein production. Furthermore, *rarab* knockdown blocks pectoral appendage initiation (Linville et al., 2009), which would be expected if miR-196 inhibits pectoral fin initiation by limiting *rarab* function. Likewise, miR-196 over-expression diminished RA signaling in the CNS as detected in an RARE-YFP transgenic line as also happened in the same line after knockdown of *rarab* activity (Linville et al., 2009). Finally, a luciferase assay in tissue culture cells and a GFP assay in living embryos both showed that miR-196 functions via the 3'UTR of *rarab*. Because miR-196 over-expression does not inhibit the accumulation of significant quantities of *rarab* transcript - but similar experiments showed a substantial decrease of transcript levels for *hoxb8a*, a positive control - miR-196 must act more on translation than on message stability to modulate expression of *rarab*. We conclude that miR-196 over-expression blocks fin bud initiation, at least partially, by binding the *rarab* 3'UTR in lateral plate mesoderm to inhibit its translation, thereby diminishing the ability of lateral plate cells to detect somite-derived RA, which leads to lack of *tbx5a* induction, without which the fin bud cannot initiate. Although miR-196 morpholino knockdown did not give a pectoral fin bud phenotype in otherwise normal development, evidence that endogenous miR-196 is involved in pectoral fin bud initiation comes from the demonstration that miR-196 knockdown rescued diminished RA signaling. Thus, we conclude that *rarab* is a target of miR-196 for pectoral fin bud initiation, but other targets may also exist.

Tetrapods have three *Rar* genes (*Rara, Rarb, Rarg*), and zebrafish has duplicate copies of *Rara* and *Rarg* but no *Rarb* gene (Hale et al., 2006), the functions of which appear to have partitioned between zebrafish *raraa, rarab, rarga* and *rargb* genes

(Linville et al., 2009). As in zebrafish, pectoral appendage initiation in mouse requires RA signaling (Niederreither et al., 1999), and double knockout of *Rara* and *Rarg* in mouse causes hypoplastic pectoral limb buds (Wendling et al., 2001). Thus, the mechanism of pectoral appendage initiation is generally conserved between zebrafish and tetrapods, but because none of the *Rar* or *Rxr* genes in mouse, human, or chicken have predicted miR-196 targets, the role of miR-196 may differ in zebrafish and tetrapods.

Although several *hox* genes that are expressed in pectoral fins have predicted miR-196 binding sites, they are unlikely to be responsible for the fin bud phenotype because most are expressed downstream of RA signaling and their temporal-spatial expression patterns exclude them from functioning during pectoral fin induction. For example, although *hoxb5b* is an RA-responsive gene expressed in the forelimb field, its function is dispensable for forelimb formation (Waxman et al., 2008), and, although miR-196 causes a decrease in *hoxb8a* message levels in zebrafish as in tetrapods (Kawasaki and Taira, 2004; McGlinn et al., 2009a; Yekta et al., 2004), *hoxb8a* is unlikely to be the gene responsible for miR-196 regulation of fin bud initiation because it is expressed in zebrafish pectoral fin buds well after initiation, because *hoxb8a* knockdown in zebrafish does not affect pectoral fin development (data not shown), and because *hoxb8a* mutants in medaka do initiate fin buds but do not maintain their outgrowth (Sakaguchi et al., 2006). In addition, we knocked down the expression of *hoxb5a, hoxb5b, hoxb6b, hoxc6a* and none of them showed pectoral fin defects. Thus none of the 5 *hox* genes we checked are required for pectoral fin initiation.

3.4.3. *Mir196* and Pharyngeal Arch Patterning

Our over-expression and knockdown experiments both showed that miR-196 inhibits the formation of a posterior arch, probably PA6. In principle, miR-196 could perform this role by modulating signaling by *hox* genes, RA, or FGF. In mouse, *Hox2* paralogs help control PA2 and PA1 identity (Minoux et al., 2009) and *Hox3* paralogs help specify PA3 and PA4 (Minoux et al., 2009). Mechanisms that control identity of PA4 to PA7,

however, are as yet unclear. In zebrafish, *hoxb5a* is expressed strongly and *hoxb5b* weakly in PA3-7 (Bruce et al., 2001; Jarinova et al., 2008), suggesting that *Hox5* paralogs could help pattern posterior arches. Although *hoxb5a* and *hoxb5b* are predicted miR-196 *hox* gene targets expressed in PAs, and our experiments showed that they are sensitive to miR-196, the knockdown of *hoxb5a* and *hoxb5b* in zebrafish and *Hoxb5* in mouse gives no reported arch phenotype (McIntyre et al., 2007; Waxman et al., 2008), making it unlikely that *hoxb5* genes are the miR-196 targets responsible for the arch phenotype.

Because retinoic acid is a posteriorizing factor in pharyngeal endoderm (Bayha et al., 2009) and suppression of RA signaling deletes branchial arches (Begemann et al., 2001; Birkholz et al., 2009), it is possible that miR-196 inhibits RA signaling in pharyngeal endoderm. Inhibiting RA signaling progressively between 16 and 30 hpf results in fewer deleted PAs (Kopinke et al., 2006), suggesting that, if miR-196 acts through RA signaling to suppress PA6, it must act at or after 30 hpf. Double knockout of *Rara* and *Rarb* alters development of posterior PAs in mouse (Dupe et al., 1999) in ways that mimic miR-196 over-expression in zebrafish. These considerations suggest that pharyngeal phenotypes of miR-196 manipulated zebrafish might, like the fin phenotype, be mediated by *rarab*. Although *rarab* is expressed in PAs (Hale et al., 2006; Linville et al., 2009), *rarab* morpholino knockdown had no effect on branchial arch phenotype (Linville et al., 2009). In contrast, knockdown of *rarga*, which lacks predicted miR-196 binding sites, did alter gill arch formation (Linville et al., 2009). Thus, either *rarab* inhibition does not explain the gill arch phenotype of miR-196 manipulation, or the knockdown of *rarab* activity by miR-196 over-expression is more profound than morpholino knockdowns. The endoderm of the pharyngeal arches expresses *cyp26a1*, but PA3-7 are normal in *cyp26a1* mutants (Emoto et al., 2005). Thus, miR-196-regulated arch development seems likely to act either on a component of the pharyngeal segmentation mechanism or on an as yet unknown gene essential for the specification of PA6.

Mesoderm- and CNS-derived Fgf3 and Fgf8 help direct the segmentation of pharyngeal pouches (Crump et al., 2004), suggesting that miR-196 may alter Fgf signaling. Our finding that manipulating miR-196 levels alters RA signaling in the hindbrain could lead to alterations in Fgf signaling that promote the loss or gain of PA6. Again, however, the great specificity of the miR-196 phenotype contrasts to the broader perturbation of PA3-7 development caused by Fgf manipulations, and suggests that, if miR-196 acts on Fgf signaling, it must be through a tissue-specific downstream target of Fgf because none of the zebrafish *fgf, fgfr* and other Fgf pathway genes have predicted miR-196 binding sites.

These considerations lead us to propose that in normal development, miR-196 attenuates action of a gene essential to direct the formation of pharyngeal pouches between PA5 and PA7. The identity of this target is as yet unknown.

3.4.4. *Mir196* and Axial Skeleton Patterning

Manipulating miR-196 levels provoked patterning anomalies specifically in regions of the axial skeleton that express *hox* genes that have predicted miR-196 targets. The predicted miR-196 target *hoxb5a* is expressed in somites-2 and -3 but the target *hoxb5b* is not expressed in the somites (Bruce et al., 2001; Jarinova et al., 2008). Somites-1 and -2 and the anterior of somite-3 do not contribute to vertebrae in zebrafish or tetrapods, but in tetrapods at least, they contribute to the caudal part of the skull (Huang et al., 2000; Morin-Kensicki et al., 2002), which was morphologically normal in zebrafish we caused to over- or under-express miR-196. Furthermore, altered patterning of the zebrafish axial skeleton has not been reported after knockdown of *hoxb5a* or *hoxb5b* [(Waxman et al., 2008) and our unpublished experiments]. In mouse, *Hoxb5* mutants show an anteriorizing homoeotic transformation of the caudal cervical and first thoracic (rib bearing) vertebrae (Rancourt et al., 1995); while, conversely, we observed a posteriorizing effect in the homologous vertebrae after miR-196 over-expression.

Five predicted miR-196 targets (*hoxb6b, hoxc6a, hoxb8a, hoxb8b* and *hoxc8a*) are expressed with anterior borders in somites-3 to -7, which form the Weberian apparatus (Amores et al., 1998; Bruce et al., 2001; Morin-Kensicki et al., 2002). Morpholino knockdown of these genes, however, did not result in changes in the Weberian apparatus (data not shown). Correspondingly, we found that miR-196 injection led to posteriorizing homeotic transformations or vertebral segment deletion in Weberian vertebrae, which are homologous to vertebrae surrounding the cervical-to-thoracic transition in tetrapods (Burke et al., 1995; Morin-Kensicki et al., 2002). If miR-196 inhibits expression of these *hox* genes, then miR-196-injected animals should show *hox* loss-of-function phenotypes and miR-196 knockdown animals should show *hox* gain-of-function phenotypes, as observed in chick after miR-196 knockdown (McGlinn et al., 2009a). In contrast, loss of function mutations for mouse orthologs of *hoxb6b, hoxc6a, hoxb8a* and *hoxb8b* give rise to anteriorizing, not posteriorizing, homeotic transformations at the cervical/thoracic transition (Garcia-Gasca and Spyropoulos, 2000; Rancourt et al., 1995; van den Akker et al., 2001), and *Hoxc8* mutations cause anteriorizations of the caudal thoracic vertebrae (van den Akker et al., 2001). How can we understand this discrepancy?

In contrast to most *Hox* genes, *Hoxa5* and *Hoxa6* mutants show a posterior homoeotic transformation in the rostral mouse vertebral column (Drin et al., 1994; Jeannotte et al., 1993). Mouse *Hoxa5* is expressed with an anterior border in the third cervical vertebra and continuing expression into thoracic vertebrae (Jeannotte et al., 1993); this region is homologous to the zebrafish Weberian vertebrae. Zebrafish has no *hoxa6* gene and has a single *hoxa5* gene (Amores et al., 1998), which is not a predicted miR-196 target and is not expressed in somites (Thisse, 2005); the final *hox5* paralogy group gene, *hoxc5a*, is also not expressed in somites (Ericson et al., 1993). In addition, genes of the *hoxb* cluster (*hoxb1a* and *hoxb1b*) have newly assumed, or have maintained, functions equivalent to the same paralogy group but different cluster in mouse (*Hoxa1*), a process called 'function shuffling' (McClintock et al., 2002). The *hox1* findings suggest the analogous hypothesis that function shuffling occurred for the zebrafish *hoxb5* duplicates and the mouse *Hoxa5* gene. According to this interpretation, the posterior transformations at the

cervical/thoracic transition found after *Hoxa5* knockout in mouse, which are similar to the posterior transformations of the homologous region in zebrafish after miR-196 action, are caused by the miR-196-induced inhibition of zebrafish *hoxb5a*, which is expressed in a pattern homologous to that of mouse paralog *Hoxa5* and which we showed to respond to miR-196, at least in the CNS, by changed transcript patterns.

An alternative explanation for miR-196 induced re-patterning is that a Weberian vertebra is missing rather than showing a homeotic transformation. Loss of *Hoxa3* and *Hoxd3* function deletes a cervical vertebra in mouse (Horan et al., 1995), and deletion of a zebrafish homolog of a cervical vertebra could mimic the observed posteriorization, causing, for example, the third segment to have the morphology of the fourth.

Besides pattern changes among Weberian vertebrae, increased and decreased miR-196 levels produced animals with fewer and more ribs than normal, respectively. Morpholino knockdown of *hoxb5a, hoxb5b, hoxb6b* and *hoxc6a* did not cause changes in rib and vertebral number, while knockdown of *hoxb8a* resulted in one extra rib (data not shown), contradicting the prediction that knockdown of *Hox* gene targets for *mir196* should result in missing ribs and vertebrae. The predicted miR-196 target *hoxa10b* is expressed in somites that give rise to rib-bearing (pre-caudal) vertebrae with the same anterior border as the non-targets *hoxb10a* and *hoxd10a* (Morin-Kensicki et al., 2002). In mouse, knockdown of the miR-196 predicted target *Hoxa10* gives rise to posterior transformations of caudal thoracic vertebrae (Rijli et al., 1995). Over-expression of miR-196 should knockdown *hoxa10b* function, and an accompanying posterior transformation as in mouse could change pre-caudal, rib-bearing vertebrae into caudal, non-rib-bearing vertebrae, thereby decreasing rib number. Conversely, knockdown of miR-196 could cause over-expression or ectopic expression of *hoxa10b,* which could transform caudal vertebrae to pre-caudal, rib-bearing vertebrae, thereby increasing the number of vertebrae, as we observed.

Our results showed that the total number of vertebrae decreased after miR-196 over-expression and increased after miR-196 knockdown, so a simple one-to-one fate

transformation model does not provide a full explanation for our results. In normal zebrafish, length variation arises mostly from variation in caudal vertebrae (Morin-Kensicki et al., 2002), whereas length variation in miR-196-manipulated fish involved mostly Weberian and precaudal vertebrae, indicating a difference between the mechanism of miR-196 action and the origin of naturally occurring variation. This suggests that miR-196 may interfere with the segmentation clock, the mechanism that dictates the rhythm of somitogenesis from pre-segmental mesoderm (Gehring et al., 2009). Our somites analysis found that miR-196 inhibits normal somite segmentation. Overexpression of miR-196 results in fish with up to 7 less somites, while *mir196* knockdown induces up to 4 more somites than control fish, although players in the zebrafish segmentation clock (*her1, her4, her7, notch1a, notch1b, notch5, notch6, deltaC, deltaD, Mespa/b, ephA4, ephrinA11* and *ephrin-B2*) (Lewis et al., 2009) do not appear to have predicted miR-196 binding sites. Involvement of miR-196 in the segmentation clock seems unlikely because altering the number of cycles should add somites in the caudal region, not in the rostral region of the axis, as we observed.

3.5. Conclusions of *Mir196* Study

These experiments revealed three exquisitely specific viable phenotypes caused by manipulating miR-196 levels in zebrafish embryos. Analysis showed that the miR-196-induced failure of fin bud initiation arises from the suppression of retinoic acid signaling in lateral plate mesoderm by fine-tuning expression of the retinoic acid receptor *rarab* that is essential for fin bud outgrowth. The miR-196-induced loss or gain of a pharyngeal arch between PA5 and PA7 may not arise from the inhibition of any of the predicted *hox* targets but from inhibiting segmentation of pharyngeal pouches, about which we currently know little. The posteriorizing effect of miR-196 on vertebrae that correspond to the cervical-to-thoracic transition are best understood by the differential sorting out of ancestral functions common to *Hoxa* and *Hoxb* genes in zebrafish and tetrapod lineages.

These experiments shown remarkable parallels between the patterning functions of the protein-coding genes of the *Hox* clusters and a microRNA gene embedded between them.

3.6. Methods for *Mir196* Study

3.6.1. Animals

Wild-type fish were ABC/TU hybrids and the *Tg(fli1:EGFP)*^{y1} line (alias *fli-GFP*) (Lawson and Weinstein, 2002) provided animals with labeled cranial crest. The *Tg(RARE-gata2:NTD-eYFP)ld1* line (Perz-Edwards et al., 2001) provided RA signaling reporters. The *cyp26a1*^{rw716} mutant fish was kindly provided by Lei Feng (C. Moens laboratory). Skeleton preparations were as described (Walker and Kimmel, 2007). Experiments involving animals used protocols approved by the IACUC.

3.6.2. Injections

Morpholino oligonucleotides (Mos, Gene Tools) sequences were: *mir196a*-MO: AATCCCAACAACATGAAACTACCTAA, *mir196b* mutiple blocking (MB)-MO: ACGTCCAGCCCAACAACTTGAAACTACCTAA. We injected one-cell stage zebrafish embryos with approximately 3 nL of these two MOs at a final concentration of 1.5 mM *mir196a*MO and 0.5 mM *mir196b*MB-MO. RNA oligonucleotide (Integrated DNA Technology) sequences were: miR-196a: UAGGUAGUUUCAUGUUGUUGGG; miR-196a*: CGACAACAAGAAACUGCCUUGA; miR-196b UAGGUAGUUUCAAGUUGUUGGG; miR-196b*: CAGGAACCUGAAACUGCCUGAA; miR-196bmm (mismatch control): UUCCGUCAAUCAAGUUGUUGGG. Because 3 nL of 12.5 μM stock of miR-196a or miR-196b duplexes yielded identical phenotypese, we used miR-196b duplex for most reported experiments.

3.6.3. Reporter Constructs

From genomic DNA, we amplified a 1349 nt fragment (primers: rarab+314: GTAGACTTTGACCCGGACTGAACA and rarab-1639: AGAAGGCTTTTGGGTGAACTATCC) containing all three predicted miR-196 binding sites and inserted it into pCR4-TOPO (Invitrogen). To fuse *GFP* with the *rarab* 3' UTR, we used NotI and SpeI to liberate the *rarab* 3'UTR from pCR4-TOPO and used NotI and XhoI to extract *GFP* from pEGFP-N3 (Clontech). To make the *GFP-rarab3'*UTR construct, we ligated fragments into PCRII-TOPO (Invitrogen) between SpeI and XhoI sites. To make the luciferase reporter, ptkLuc+ vector digested with NgoMIV and KpnI was ligated to the *rarab* 3'UTR cloned from genomic DNA by the above primers containing NgoMIV and KpnI sites (primers: rarab+314NgoMIV: gggccggcGTAGACTTTGACCCGGACTGAACA and rarab-1639KpnI: ggggtaccAGAAGGCTTTTGGGTGAACTATCC). To make GFP-*rarab*3'UTR mRNA, the construct PCRII-GFP-rarab3'UTR was linearized with SpeI and transcribed *in vitro* using mMESSAGE mMACHINE T7 kit (Ambion). GFP-*rarab*3'UTR mRNA was purified with an RNA clean-up kit (Zymo Research) and diluted to 15 μL with nuclease-free water to store in -80°C. For coinjections, we injected first 200 ng/μL of the synthetic *GFP-rarab* 3'UTR mRNA and then *mir196* morpholino mix or 12.5 μM miR-196 duplex or miR-196bmm control.

To make GFP-*rarab*-mut3'UTR construct, the following primers were used to skip the predictted binding sites for miR-196 in the 3'UTR of *rarab*. rarab+314NotI: gggcggccgcTAGACTTTGACCCGGACTGAACA; rarabUTR-430XhoI: ggctcgagGCTCTTGTAGTCGCTGAATC; rarabUTR+468XhoI: ggctcgagCTTCACAGAGATGACAGAACA; rarabUTR-1393sacII: ttggccgcggTAAAGTACAGAAGAAGAGGAA; rarabUTR+1479sacII: ttccgcggTGTGACAATCACTTCAAGTAA; rarabUTR-1639SpeI: ggactagtAGAAGGCTTTTGGGTGAACTATCC. PCR products were digested by restriction enzymes identified in the primer names and were sequentially ligated to insert

into GFP downstream of the same vector for GFP-*rarab*3'UTR. mRNA was synthesized and injected and scored as for GFP-*rarab*3'UTR.

3.6.4. Reporter Assay

One cell embryos were injected with 3μL of a 200 ng/μL solution of GFP-*rarab*3'UTR mRNA and was coinjected with 1μL of a solution of 12.5 μM miR-196 duplex or 2 mM *mir196*-MO. Embryos raised at 28.5 °C to 28 hpf were imaged in 3 % methyl cellulose. To quantify GFP intensity, we used Photoshop, selected fuzziness to 40 and used the "select" and "color range" function to set a threshold, then used the histogram function to calculate the numbers and standard deviation of the green pixels. For the luciferase assay in 293T cells, we used the original ptkLuc+ vector for which luciferase expression is driven by a thymidine kinase promoter with luciferase flanked by either rarab 3'UTR or SV40 polyadenylation signal as a control. For the assay, either 50 ng of ptkLuc+ control plasmid or ptKLuc-*rarab* 3'UTR with 10 ng of CMV-*Renilla* plasmid and 200 ng miR-196 duplex were cotransfected. Cells were harvested at 2-hour intervals from 4 to 12 hours after transfection. Firefly and *Renilla* (sea pansy) luciferase activities were both directly quantified within each sample directly after cell lysis (Dual-*Luciferase* Reporter Assay System, Promega) and the firefly luciferase activity was calculated relative to the *Renilla* luciferase control. In addition, the relative luciferase activity of ptkLuc-*rarab* 3'UTR construct was normalized to the ptkLuc+ control.

3.6.5. Cloning and *in situ* Hybridization

To generate PCR products containing partial *mir196* primary transcript, we used 1 dpf zebrafish whole embryo cDNA reverse transcribed with oligo-dT primer. Cloning of *mir196* primary transcripts used the primers: mir196a1+523 ATTAAATGAACGCTAGCGGCTGTATGATG, mir196a1-1014 TTTTGCTAGCGCTTTGTCTTTGTAACCA; mir196a2+1349 GCAGACAGGAGAGCGGCAAGAA, mir196a2-1891

AGCAGGCAAGGCAAGATTATGGTA; mir196b+756
GTATCTCTTTGCCCCGCTGTGG, mir196b-1292
TGGAAAAACGATGGGAAAGTATTG; mir196c+1016
ATTGCTTTAGATTATGCGCGGGTATTT, mir196c-1339
CAAGCTATGTCAAGGCGTGTCTGTCT; mir196d+467
TATGCTACCTGGTGCCGTGAAG, mir196d-1325
CCGCTGATAATGGAAGACAACC. Other probes were cloned with primers: tbx5+305
TCAACAGGGAATGGAGGGAATCAAA, tbx5-1213
AGAGTAGCTTAGGGGCCGGTAGTAGTGGT; fgf10a+11
ATGCCCCTCGTCGCCTCTTATTCTG, fgf10a-1458
TTCCCTGGTGCCAATAACTTAAACAA; wnt2b+344
GGTGGTACATTGGTGCGTTAGGAG, wnt2b-1304
GCCAGTCGGGTTTCTTGTGTAGTT; prdm1+2208
GAGGGCATGGTGGAGAAGCAGATA, prdm1-3391
AAAGGCCGAGGTGACGTGAAGAGT; *lbx1b* was from Dr. Haruki Ochi (nt 67 to 810 of NM_001025532) and *fgf24* probe was as described (Draper et al., 2003). PCR products were cloned into pCR4-TOPO (Invitrogen) vector and *in situ* hybridization was as described (Hale et al., 2006). Antisense LNA (locked nucleic acid) probe for miR-196a with the sequence, 5'Dig/CCCAACAACATGAAACTACCTA/3'Dig, was ordered from Exiqon (http://Exiqon.com) and *in situ* hybridization was according to the manufacturer.

3.7. The Relationship of Chapter III with the Rest of the Dissertation

In this chapter, I discussed the study of microRNA miR-196 in zebrafish skeletal development. I discovered that miR-196, which is found between homologous *hox9* and *hox10* of different vertebrate species, is regulating axial skeletal segmentation and is involved in the initiation of paired pectoral fins in zebrafish. Since miR-196 is widely found in the genomes of vertebrates, the function of miR-196 might be conserved between zebrafish and other species too. The study of miR-196 indicates that miRNAs,

by fine-tuning specific target gene expression, can control highly complex developmental events like skeletogenesis. Together with another example from the study of miR-140 in Chapter II, the study of miR-196 provides another good example that miRNAs are extensively involved in the regulation of the skeletal development processes.

CHAPTER IV

MICROMANAGING THE SKELETON IN DISEASE, DEVELOPMENT, AND EVOLUTION

This chapter includes previously published co-authored material. This work was published in volume 13 of the journal *Journal of Cellular and Molecular Medicine* in April 2009 as an invited review paper. I performed the experiments and wrote the manuscript draft; Dr. Johann Eberhart and Prof. John Postlethwait helped to rewrite, polish and format the paper; Prof. John Postlethwait was the principal investigator for this work.

4.1. MicroRNAs and Skeletal Diseases

Decades of genetic analyses have shown that the proper development of an organ system, such as the vertebrate skeleton, requires the precise execution of various genetic pathways. Small RNAs have recently been recognized to function as important modulators of gene regulation. MicroRNAs (miRNAs) function in post-transcriptional modulation of genetic pathways that regulate various developmental and physiological processes. In vertebrates, microRNAs often act as subtle negative regulators of gene translation by recognizing and binding to complementary sites in the 3' untranslated regions (UTRs) of target genes [reviewed in (He and Hannon, 2004)]. The developing skeletal system expresses several different miRNAs, often with precise temporal and cell-type specificity, and therefore it is likely that miRNAs play a significant role in sculpting skeletal form. A central question is the role miRNAs play in the evolution of new skeletal

forms and in the origin of skeletal diseases, including osteopenia that almost universally accompanies the ageing process.

Osteopenia is a reduction in bone mineral density (BMD). About 34 million American women and 12 million American men have osteopenia. Osteopenia often leads to osteoporosis, a disease characterized by low bone mass, bone deterioration, bone fragility, increased susceptibility to fracture, and slow healing of bone fracture (NIH, 2001). Osteoporosis is a threat to the health of about 44 million Americans. Of Americans over 50 years old, 55% already have osteoporosis (National_Osteoporosis_Foundation, 2007). Osteoporosis increases the lifetime risk of fractures to about 50% in women and about 20% in men. As the population ages, the number of hip fractures worldwide is predicted to increase from 1.7 million in 1990 to 6.3 million in 2050 (Dennison et al., 2006). After hip fracture due to bone loss, half of all patients fail to recover their previous mobility and independence, and in the first year after the fall, more than 25% die (Gruntmanis, 2007). A better understanding of the biological mechanisms of osteopenia and osteoporosis should help lead to improved therapies for the prevention and treatment of bone loss diseases. We review here the evidence that miRNAs are involved in skeletal development and raise the question whether the change in miRNA action over developmental time may be involved in the loss of bone density that accompanies ageing.

Osteoporosis has a major genetic component, but is also affected by the environment (Pelat et al., 2007). For example, obesity, diet, and weight-bearing exercise have major effects on bone mineral density, but family and twin studies reveal high heritability for osteopenia and osteoporosis (Deng et al., 2000). Thus, susceptibility to osteoporosis, like many other common human diseases, has both genetic and environmental risk factors. We suggest the possibility that environmental factors may act to alter bone density via a miRNA-mediated process.

The skeletons of various vertebrate species are variations on a theme and even populations within a species often have subtle differences in bone shapes – compare, for

example, limb proportions of Athabascans inhabiting the frigid Alaskan tundra to the Masai living in the hot Serengetti Plain of Kenya (Walensky, 1965). Likewise, a rich diversity of craniofacial forms equip various species of cichlid fish in the Great Rift Lakes of Africa to a diet of hard-shelled benthic mollusks, or plankton in the water column, or scales on exclusively the left side of other fish (Albertson et al., 2003). Different but closely related species of teleost fish (Mabee et al., 2000; Parichy and Johnson, 2001) have subtle differences in the craniofacial skeleton (**Fig. 4.1**). How do such differences arise during development? What evolutionary forces promote the fixation of these genetic differences over many generations? And might the same mechanisms that differ between species to effect different skeletal features also differ between individuals or change during a person's life time to contribute to skeletal disease?

Arguments concerning the genetic mechanisms that lead to the evolution of morphological differences like those shown in Figure 4.1 or to skeletal differences among individuals are currently contentious – is evolution primarily due to genetic change in protein coding regions or in non-coding regulatory regions [see, e.g., (Hoekstra and Coyne, 2007; Wray, 2007)]. An additional hypothesis is that the subtle kinds of morphological changes that result in ecologically important variation in skeletal structure can also occur by variation at regulatory sites embedded in noncoding regions of transcripts, for example in miRNA binding sites in messenger RNAs.

This review poses the following questions: (1) What roles do miRNAs play in skeletal development? (2) To what degree are miRNAs involved in the fine-tuning of skeletal structure that occurs in adaptive evolution? (3) What might be the roles of miRNAs in skeletal diseases of ageing? To approach these questions, we first briefly overview skeletal development and our current understanding of miRNA biology, then focus on new discoveries of miRNA action in skeletal system development, and finally discuss the hypothesis that variation in miRNA biology may contribute to the evolution of skeletal system diversity and human skeletal disease.

4.2. An Overview of Skeletal Development

The vertebrate skeletal system is composed of cartilage and bone. Cartilage is composed of cartilage cells surrounded by extracellular matrix rich in proteoglycans and staining positive for Alcian Blue, while bone is an acellular calcium matrix staining positive for Alizarin Red (**Fig. 4.1A**). Cartilage and bone both develop from mesenchyme derived from neural crest, paraxial mesoderm, or lateral plate mesoderm. During embryogenesis, some bones form by endochondral ossification and others by intramembranous ossification (Huysseune and Sire, 1992; Javidan and Schilling, 2004; Lefebvre and Smits, 2005) (**Fig. 4.2A**). In the endochondral skeleton, bone forms on a cartilage model, as in bones of limbs in tetrapods and paired fins in fish. Mesenchymal cells differentiate into chondrocytes that form a condensation with the shape of the future cartilage element. Chondrocytes differentiate, become hypertrophic, and deposit extracellular matrix. Hypertrophic chondrocytes terminally differentiate and undergo apoptosis. At the periphery of the condensation, osteoblasts develop from the perichondrium surrounding the cartilage (**Fig. 4.2B**) and secrete bone, which merges with the cartilage matrix. As the matrix thickens and calcifies, osteoblasts trapped by the extracellular matrix (ECM) differentiate into osteocytes, which maintain the bone. In contrast, in intramembranous ossification, mesenchymal cells bypass the cartilage model and differentiate directly into osteoblasts, which secrete extracellular matrix that becomes mineralized, thus forming bone.

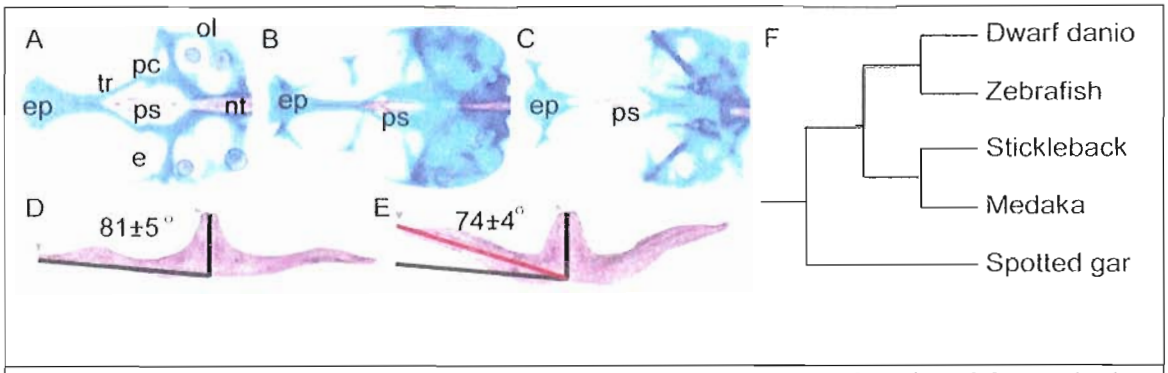

Fig. 4.1. Closely Related Species and Populations Within a Species Often Display Subtle Morphological Differences in Skeletal Systems. Such morphological variation probably results from slight differences in the timing or location or intensity of the action of specific genes. (A-C) Skeletal variation in the palate and neurocrania of three species of teleost fish. (A) *Danio rerio* (zebrafish), (B) *Gasterosteus aculeatus* (stickleback) and (C) *Oryzias latipes* (medaka). Note species-specific differences in the shapes of the palate, consisting of ethmoid plate and parasphenoid. (D-E) Anterior view of the premaxilla bone showing variation in shape between *D. rerio* (zebrafish) (D) and *D. nigrofasciatus* (dwarf danio) (E). The angle of zebrafish premaxilla bone is 81±5° (n=44) for *D. rerio* while the angle of *D. nigrofasciatus* is 74±4° (n=35). (F) Evolutionary relationships of some fish discussed in this review, including the basally diverging non-teleost *Lepisosteus oculatus* (spotted gar). Abbreviations: e, eye; ep, ethmoid plate; nt, notochord; ol, otolith; pa, palate; pc, parachordal; ps, parasphenoid, tr, trabeculum.

Several genetic pathways help regulate the developmental programs that specify the type, size and shape of each skeletal element. For instance, Sox9 and Runx2 transcription factors together regulate differentiation of cartilage and bone (Depew et al., 2005; Kawakami et al., 2006; Komori, 2003; Okazaki and Sandell, 2004; Samee et al., 2007). The Bmp, Hh and Fgf signaling pathways sculpt skeletal morphogenesis (Chen and Deng, 2005; Day and Yang, 2008; Ehlen et al., 2006; Kronenberg, 2006; Ornitz, 2005; Wu et al., 2007) and extracellular matrix components like collagens, Sparc, and glycosaminoglycans influence cell signaling and cell shape (Blair et al., 2002; Cancedda et al., 2000; Goldring et al., 2006; Holmbeck, 2005; Velleman, 2000). Modulation of the Edn1 pathway causes alterations in bone morphologies (Kimmel et al., 2003; Miller et

al., 2000; Miller et al., 2003; Walker et al., 2006; Walker et al., 2007). In principle, any or all of these genetic pathways are potentially subject to miRNA modulation and, thus provide numerous genetic inroads to understand the roles of miRNAs in skeletal development, morphological evolution, and skeletal disease.

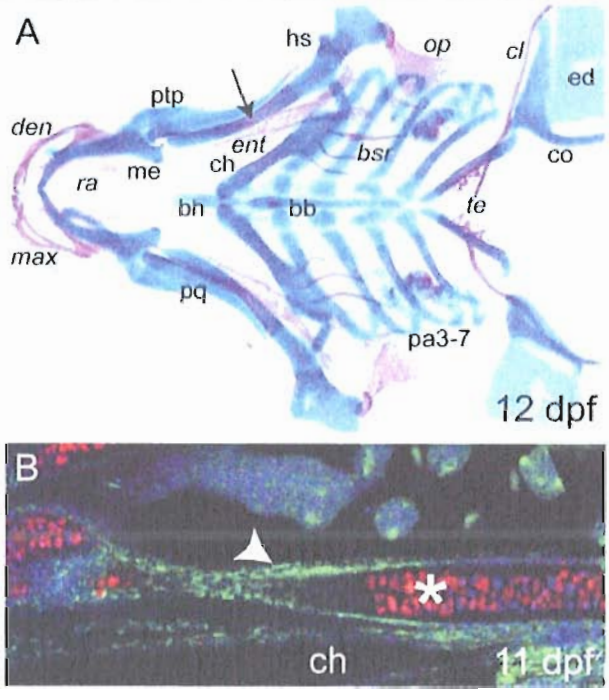

Fig. 4.2. Endochondral Ossification and Intramembranous Ossification. A. 12 day old G. aculeatus pharyngeal skeleton stained with Alcian Blue for cartilage and Alizarin Red for bone shows intramembranous and endochondral ossification. Italic bold font labels intramembranous ossification and roman font indicates endochondral ossification. The arrow indicates the endochondral ossification center of the ceratohyal cartilage. B. Endochondral ossification of ceratohyal of 11 day old spotted gar. Green, Col II staining includes the perichondrium, which surrounds the cartilage core; red, Col X staining in chondrocytes of the ceratohyal; blue, nuclear stain. Abbreviations: bb, basibranchial; bh, basihyal; bsr, branchiostegal ray; cc, chondrocytes; ch, ceratohyal; cl, cleithrum; co, scapulocoracoid; den, dentary; ed, endoskeletal disc; ent, entopterygoid; hs, hyosymplectic; mx, maxilla; me, Meckel's cartilage; op, opercle; pa, pharyngeal arch; pc, perichondrium, pmx, premaxillary; pq, palatoquadrate; ptp, pterygoid process; ra, retroarticular; te, teeth.

4.3. The Biogenesis of MiRNAs

MiRNAs are a group of small regulatory RNAs that attenuate gene function by inhibiting the production of proteins and they were first discovered in the nematode *Caenorhabditis elegans* (Lee et al., 1993; Reinhart et al., 2000; Wightman et al., 1993). MiRNAs are involved in many developmental signaling pathways and in housekeeping regulation for organ physiology (Lee et al., 1993; Reinhart et al., 2000; Wightman et al., 1993). Consistent with their broad involvement in regulation, thousands of miRNAs have been recognized across the genomes of viruses, plants, fungi and animals (Aboobaker et al., 2005; Clarke and Sanseau, 2006; Jiang et al., 2006; Kidner and Martienssen, 2005; Nair and Zavolan, 2006; O'Driscoll, 2006), with at least 542 human miRNAs deposited in the miRNAMap database (Hsu et al., 2008). Genes encoding miRNAs are scattered across genomes in intergenic or intragenic regions, in untranslated regions (UTRs) or in translated sequences of protein-coding genes, and they can be oriented either in sense or in antisense orientation with respect to their primary transcript and host gene [see (Gregory et al., 2004)]. Previous studies revealed that most miRNA genes are transcribed by RNA polymerase II, with 5' caps and 3' polyA tails, like most protein coding genes (Lee et al., 2004).

The pathway of miRNA biosynthesis has been well explored. In the canonical pathway, an mRNA-like primary transcript (pri-miRNA) forms a stem-loop secondary structure in the nucleus. The Drosha-DGCR8 complex, an RNase III machine, digests the pri-miRNA into a free hairpin structure called a pre-miRNA (Denli et al., 2004; Lee et al., 2003). Some miRNA genes, called mirtrons, are embedded in introns and are spliced out directly from their host gene transcript into a pre-miRNA, thus avoiding the Drosha processing step (Lund et al., 2004). Exportin5, a nuclear envelope protein, transports free pre-miRNA hairpins into the cytoplasm (Jaskiewicz and Filipowicz, 2008). Dicer, a cytoplasmic RNase III enzyme, then processes the pre-miRNA by cutting off the loop region and releasing mature miRNA duplexes, which can diffuse in the cytoplasm and

bind to mRNA targets (Berezikov et al., 2007; Ruby et al., 2007). Special nomenclature rules help keep these various parts of the system straight (**Table 4.1**).

Table 4.1. MicroRNA Nomenclature

Nomenclature Conventions [1]	Human (*Homo sapiens*)	Mouse (*Mus musculus*)	Zebrafish (*Danio rerio*)
MicroRNA (guide strand)	Has-miR-140	mmu-miR-140	dre-miR-140
Precursor hairpin	Has-mir-140	mmu-mir-140	dre-mir-140
'Passenger' strand in hairpin [3]	Has-mir-140*	mmu-mir-140*	dre-mir-140*
MicroRNA gene [2]	*MIRN140*	*Mirn140*	*mirn140*

[1] Nomenclature conventions are important for distinguishing between genes and gene products, for conveying information about orthologies, and for avoiding confusing synonyms. According to miRBase (http://microrna.sanger.ac.uk/), miRNAs are named using an abbreviation of three or four letters to designate the species followed by an officially assigned number (Griffiths-Jones et al., 2006). [2] MicroRNAs are encoded by genes that are given names in the 'Gene' database at NCBI (http://www.ncbi.nlm.nih.gov/sites/entrez?db=gene). [3] Passenger strands of duplexes that occur at less than 15% of the amount of the guide strand are called the 'star' miRNAs, miR-xxx*. When the passenger and guide strands are about equal in quantity, they are called miR-xxx-3p and miR-xxx-5p based on their location in the miRNA duplex.

Mature cytoplasmic miRNA duplexes are the ultimate regulatory components of the system, and they carry both a stable passenger miRNA strand and an unstable guide miRNA strand (Matranga et al., 2005; Rand et al., 2005). In the cytoplasm, the miRNA duplex interacts with a group of proteins to form an RNA-protein complex called miRNA Induced Silencing Complex (miRISC) (Tomari et al., 2004). In the miRISC, the miRNA guide strand recognizes its binding site in the 3'UTR of target mRNAs. MiRNA target

sites do not need to be perfectly complementary to the miRNA for binding and target regulation. Perfect binding of miRNAs, however, usually leads to target degradation, while incomplete complementarity often inhibits target translation either by interfering with 5'cap recognition or by causing message deadenylation or by blocking translation elongation (Mathonnet et al., 2007; Nottrott et al., 2006; Petersen et al., 2006). Because of their short sequence and ability to act as regulators even without a perfect match, miRNAs can have many predicted targets (see prediction tools in **Table 2**). It is easy to understand how miRNAs could have a profound influence on evolution because each one of the hundreds of miRNAs can potentially regulate hundreds of target genes.

4.4. MiRNAs and Genome Evolution

Support is emerging for the notion that miRNAs are closely associated with evolutionary novelty and some hypothesize this link to be causative. For example, one burst of new miRNAs occurred at about the time of the origin of vertebrate characters and another increase occurred as placental mammals evolved (Heimberg et al., 2008; Hertel et al., 2006). Once new miRNAs have integrated into genetic regulatory networks, their primary sequences tend to remain highly conserved and miRNAs are rarely lost secondarily (Mathonnet et al., 2007; Nottrott et al., 2006; Petersen et al., 2006). This conservation over time suggests that substantial selective pressure preserves miRNAs. Because the evolution of a mineralized endoskeleton is one of the novel features that characterize vertebrates, we hypothesize that miRNAs participated in the origin of the skeletal system and today contribute to its development as well as to its evolving morphological diversity. Supporting this notion, miR-140, miR-199, and mir-214, three miRNAs expressed strongly and specifically in developing skeletal systems, all appeared at the base of the vertebrate radiation (Hertel et al., 2006).

4.5. MiRNAs and the Micromanagement of Development

The development of morphologies, the evolution of morphological diversity, and the prevention of bone deterioration diseases all require the precise regulation of protein levels during crucial processes such as cell fate specification, cell differentiation, cell proliferation, cell migration, and stem cell maintenance. Although miRNAs are likely to provide a widely-used post-transcriptional developmental control mechanism, and recent reports estimate that the hundreds of miRNAs in the human genome may together regulate about 30% of human genes (Lewis et al., 2005), the functional significance of miRNA utilization remains largely under-explored.

To understand the aggregate roles of miRNAs in development, researchers constructed knockout situations for the miRNA-processing enzyme Dicer in mice and fish. Because the maturation of all miRNAs requires Dicer, embryos lacking this enzyme should be deficient in all miRNAs at once and thus, Dicer knockdown should reveal the functions of at least early-acting miRNAs. The knockout of zygotic (but not maternal) *Dicer* in mouse caused homozygous mutant embryos to die before the establishment of the body plan during gastrulation. This result suggests that Dicer function is necessary for the maturation of miRNAs essential for normal embryonic patterning, morphogenesis, and maintenance of embryonic stem cells in mouse embryos (Bernstein et al., 2003; Harfe et al., 2005).

Zebrafish mutants lacking both the maternal and the zygotic function of *dicer* have relatively normal axis formation and can differentiate multiple cell types, but mutants showed abnormal morphogenesis during gastrulation and irregularities in the development of the brain, somites, and heart (Giraldez et al., 2005). Collectively, the mouse and zebrafish studies reveal first, that miRNAs as a group play important developmental roles, and second, that different vertebrate species vary in their apparent reliance on miRNAs as developmental regulators.

While it is useful to learn the phenotype that results from the knockdown of all miRNAs in all embryonic cells, this sledgehammer approach results in embryonic defects

at the earliest embryonic stage that requires any miRNA; thus, the functions of miRNAs that act later in development, such as those acting during skeletogenesis, are likely to remain undetected by this procedure.

4.6. Micromanaging Skeletal System Development

The first *in vivo* evidence that miRNAs regulate skeletal development came from the knockout of Dicer specifically in cartilage cells expressing the collagen gene *Col2a1* (Kobayashi et al., 2008). Skeletal cells defective in Dicer function showed a progressive reduction in proliferating chondrocytes that resulted in severe skeletal defects and premature death. The defect in Dicer-deficient skeletal cells was due to decreased chondrocyte proliferation and precocious differentiation of chondrocytes to the hypertrophic stage. The acceleration of chondrocyte differentiation in mutant cells suggested that one or more miRNAs inhibit action of a gene that normally slows chondrocyte maturation. Analysis of miRNA abundance showed that the level of many miRNAs in Dicer-deficient chondrocytes was retained at 30 to 40% of control levels, suggesting that residual miRNA function may have obscured a true null effect in these studies and a complete null effect might result in substantially more severe phenotypes. Analysis of over 4000 predicted miRNA targets in microarray expression profiling failed to show significant reduction of messenger RNA levels in Dicer-deficient chondrocytes, consistent with the expectation that miRNAs act primarily post-transcriptionally (Behm-Ansmant et al., 2006a; Behm-Ansmant et al., 2006b; Jing et al., 2005; Kobayashi et al., 2008). These experiments imply that miRNAs are important for embryonic skeletal development. Further investigation suggested that skeletal miRNAs may act by a pathway independent of Pthrp and Ihh, two signaling molecules that regulate skeletal maturation (Kobayashi et al., 2008; Kronenberg, 2006), and thus, the experiments may suggest a new, miRNA-based mechanism for chondrocyte maturation.

miRNAs have also been knocked out in aggregate specifically in the developing limb and its skeleton. Removal of *Dicer* function specifically from limb-forming mesodermal

cells that contribute to the limb skeleton, results in embryos with twisted long bones of the forelimb and hindlimb and delayed differentiation of endochondral bones (Harfe et al., 2005). Results showed that although all skeletal elements were generally present, forelimbs had fewer digits than normal and some digits were fused together. Driving *Dicer* loss only in cells of the limb's ZPA (zone of polarizing activity, a signaling center that controls anterior-posterior patterning of the limb) showed that digit abnormalities arise from decreased cell numbers in the developing handplate rather than from a defect in limb bud patterning. Differences in cell number such as this are important for the diversification of animal form: for example, variation in chondrocyte number rather than differences in primary patterning is what makes a bat's wing with its very long digits different from a mouse's forelimb (Sears et al., 2006). So although many possible mechanisms could affect the number of cells in the limb skeleton, variation in miRNA quantity or variation in miRNA affinity for target binding sites in messenger RNAs that regulate chondrocyte number could provide a hypothetical mechanism for generating skeletal variation over evolutionary time and perhaps skeletal robustness over a person's lifetime.

Tissue specific *Dicer* knockout gives insight into the importance of miRNAs in development, but this technique also has limitations. The method does not identify which miRNA(s) regulate skeletal morphogenesis nor the identity of the miRNA targets. Aggregate loss of miRNAs could also mask the influences of pairs of miRNAs that have antagonistic effects. For these reasons, it is imperative to identify and analyze the functions of individual candidate miRNAs during skeletal development.

4.7. Candidate MiRNAs Controlling Skeletal Development

Because miRNAs act only on messenger RNA targets transcribed in the cells in which the miRNA is expressed, miRNAs that are expressed in the skeleton are candidates for playing a role in skeletal development. Unlike messenger RNAs, however, mature miRNAs are too short for conventional *in situ* hybridization experiments. Therefore, the

systematic investigation of miRNA expression patterns undertaken in zebrafish and chicken (Antin et al., 2007; Wienholds et al., 2005) has relied heavily on the use of locked nucleic acid (LNA) oligonucleotide probes. In LNAs, a methylene bridge between the 2'-O atom and 4'-C atom 'locks' the ribose ring, thereby dramatically increasing the affinity of probe for the target and increasing the melting temperature of the probe-target duplex even for probes less than 30 nucleotides in length (Nielsen et al., 2004). LNA probes, however, have the disadvantage that they are expensive. Conventional *in situ* hybridization costs less than LNAs and can detect expression patterns of the primary transcripts and pre-miRs, which are much longer than the mature forms (Eberhart et al., 2008).

Wienholds and their colleagues (Wienholds et al., 2005) investigated the expression patterns of 115 miRNAs in zebrafish development. This sweeping survey identified several miRNAs that are specifically expressed in the developing skeleto-muscular system. Zebrafish skeletal muscles express *mirn1, mirn133a, mirn206,* and *mirn216*, while the pharyngeal skeleton specifically expresses *mirn140, mirn199, mirn214,* and *mirn27b* (Wienholds et al., 2005). *Mirn140* is expressed in the pharyngeal arches, head skeleton, and fin skeleton in the chondrocytes but not the perichondrium (**Fig. 4.3A**). In contrast, both *mirn199* and *mirn214* are expressed in the eye capsule, the endochondral disc of the pectoral fin, and the pharyngeal arch skeleton, but in the perichondrium and surrounding mesenchyme instead of the chondrocytes like *mirn140* (**Fig. 4.3B** and **C**). The observed specific expression patterns suggest that these miRNAs may play a role in the embryonic development of specific parts of the zebrafish craniofacial and appendicular skeleton.

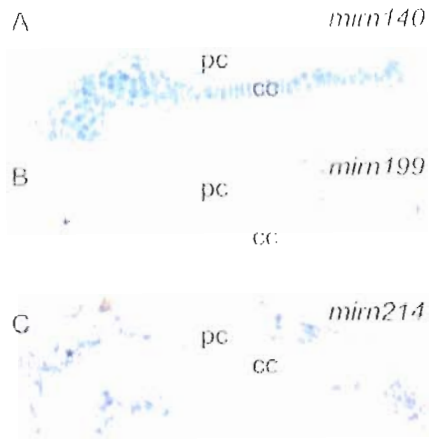

Fig. 4.3. Skeletal MiRNAs Are Expressed in Discrete Patterns. Conventional *in situ* hybridization to pre-miRNAs in 3dpf zebrafish larvae shows that *mirn140, mirn199* and *mirn214* are expressed in the ceratohyal cartilage, confirming results with LNAs. In both skeletal elements, *mirn140* is expressed in the chondrocytes while *mirn199* and *mirn214* are expressed in the perichondrium and surrounding mesenchyme cells. Abbreviations: cc, chondrocytes; mc, mesenchyme; pc, perichondrium.

Based on expression analyses, miRNAs are likely to also regulate skeletal development in embryos of amniotes. The expression patterns of 117 miRNAs are available for chick embryos at the Geisha expression database (see **Table 4.2** and reference (Antin et al., 2007)). At least *mirn106*, *mirn128*, *mirn135*, *mirn140*, *mirn200*, *mirn216*, *mirn217*, *mirn218*, and *mirn223* appear to be expressed in developing pharyngeal and/or limb cartilage in chick embryos. Comparisons of the expression patterns of orthologous miRNAs in chicken and zebrafish showed similarities and differences that will be discussed in detail below. Expression patterns such as these can provide the first step in a mechanistic analysis of miRNA function because miRNAs must be co-expressed with their targets.

Table 4.2. Selected Online Resources for MicroRNAs

Resource	URL	Description
Zebrafish miRNA expression gallery	http://www.exiqon.com/SEEEMS/4519.asp	Database containing ~1000 images of zebrafish microRNA expression patterns
GIESHA: Gallus expression *in situ* hybridization analysis	http://geisha.arizona.edu/geisha/index.jsp	Online repository for chicken *in situ* hybridization information.
miRBase: microRNA Registry	http://microrna.sanger.ac.uk/	Database for miRNA sequences, their genomic locations, predicted miRNA target genes, and for assigning official names to newly discovered miRNAs
miRNAMap	http://mirnamap.mbc.nctu.edu.tw	Genomic maps of mammalian microRNA genes and their target genes
TarBase	http://diana.cslab.ece.ntua.gr/tarbase/	Database for searching experimentally supported miRNA targets in 8 species
TargetScan	http://www.targetscan.org	Identifies predicted miRNA targets.
microInspector	http://mirna.imbb.forth.gr/microinspector	A web server for detecting miRNA binding sites
miRanda	http://www.microrna.org/microrna/home.do	miRNA target prediction for human, drosophila and zebrafish

4.8. The Function of *Mirn140* in Skeletal Development: A Case Study

Skeletogenic cells, including precursors of the palate (defined as the skeletal elements situated in the roof of the mouth), express *mirn140 (miR-140)* in fish, chicken, and mouse

(Ason et al., 2006; Darnell et al., 2007; Tuddenham et al., 2006; Wienholds et al., 2005). This result suggests that *mirn140* may modulate signaling during palatogenesis across vertebrate species. But how does miR-140 act?

Over-expression analysis showed that miR-140 causes a cleft lip and cleft palate phenotype in zebrafish (Eberhart et al., 2008). If miR-140 acts by diminishing the expression of a target gene, then a mutation in the miR-140 target should also have cleft lip and cleft palate. In mouse (Duchek et al., 2001; Soriano, 1997b; Tallquist and Soriano, 2003a) and in zebrafish (Eberhart et al., 2008), knockout of components of the PDGF (platelet derived growth factor) signaling pathway can cause cleft lip and cleft palate. Sequence comparisons showed that among PDGF ligands and receptors, only the receptor *Pdgfra* had miR-140 binding sites in the 3' UTR that were conserved across vertebrate phylogeny. In all species analyzed, neural crest cells express Pdgfra, hence both expression analysis and mutant phenotypes are consistent with the hypothesis that miR-140 modulates Pdgfra levels. Transcripts containing the 3' UTR of *pdgfra* fused to the coding sequence for *EGFP* were translated less effectively than normal in miR-140-injected embryos and more efficiently than normal in miR-140 antisense-treated embryos (Eberhart et al., 2008). This result shows that the 3' UTR of *pdgfra* is a target of miR-140 and suggests a mechanism for the disrupted palate phenotypes in miR-140 injected zebrafish.

Time-lapse video-microscopy of GFP-expressing transgenic cranial neural crest cells revealed that neural crest cells normally migrate over and in front of the eyes and past the optic stalk to occupy the location of the future palate on the oral ectoderm. Few neural crest cells, however, reach the oral ectoderm in either miR-140 injected embryos or in *pdgfra* mutants. Collectively, these results demonstrate that miR-140 exerts its effects on palatogenesis through Pdgfra. Loss-of-function analyses, however, were necessary to determine the normal role of miR-140 in palatogenesis.

Loss of miR-140 function elevates Pdgfra protein levels in embryos and alters palatal shape. The injection of embryos expressing EGFP in neural crest with antisense

morpholino directed against miR-140 results in neural crest cells accumulating around the optic stalk, a source of the attractant ligand Pdgfaa, with few crest cells migrating further to the oral ectoderm. Likewise, the injection of embryos with *pdgfra* mRNA that lacks the miR-140 binding site result in Pdgfra production that cannot be regulated by miR-140, and again results in the accumulation of neural crest cells around the optic stalk. These results suggest that miR-140 functions to attenuate Pdgf signaling at the optic stalk, allowing crest cells to migrate onward to the oral ectoderm. These findings suggest an acient conserved regulatory interaction of miR-140 and Pdgfra in the development of the palatal skeleton (Eberhart et al., 2008).

Tissue culture experiments suggest an additional role of miR-140 in skeletogenesis (Tuddenham et al., 2006). Prehypertrophic chondrocytes express *histone deacetylase-4* (*Hdac4*), which inhibits differentiation to hypertrophic chondrocytes, perhaps by regulating the osteogenic gene *Runx2* (Vega et al., 2004). When introduced into mouse 3T3 cells growing *in vitro*, a miR-140 mimicking siRNA down-regulated a co-transfected target construct bearing the *Hdac4* 3' UTR (Tuddenham et al., 2006). The down-regulation of an inhibitor of chondrocyte differentiation would be expected to accelerate the formation of hypertrophic chondrocytes, but in Dicer-deficient mice, chondrocyte hypertrophy was stimulated rather than inhibited, suggesting that down-regulation of *Hdac4* is not likely to be the mechanism for the observed aberrant skeletal development, with the caveat that Dicer knockdown might inhibit several antagonistic pathways. Furthermore, the zebrafish *hdac4* gene does not have a good candidate target site for miR-140, suggesting that for zebrafish at least, *hdac4* is unlikely to be an *in vivo* target for miR-140. Thus, it is unclear if *Hdac4* is a significant *in vivo* target of miR-140 in embryos of any species (Chen et al., 2006).

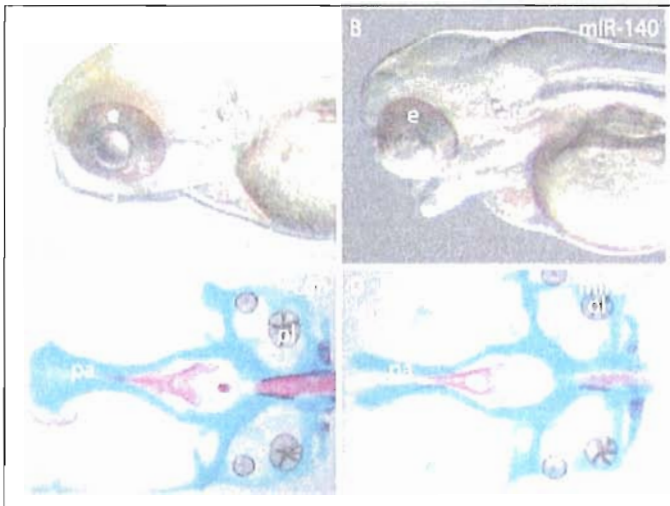

Fig. 4.4. Over Expression of *Mirn140* Causes Cleft Palate. A. Whole mount of 3 dpf control zebrafish larva. B. Whole mount of 3 dpf larva over-expressing miR-140. Note protruding lower jaw. C. Palate (neurocranium) of control larva. D. Cleft palate of larva over-expressing miR-140. Abbreviations: con, control; e, eye; j, jaw; miR-140, over-expression construct for miR-140; ol, otolith; ov, otic vesicle; pa, palate; y, yolk.

4.9. MiRNAs and *Hox* Gene Patterning of the Axial Skeleton

MiRNAs are not only implicated in skeletal morphogenesis, but are also likely to be involved in skeletal patterning. Several miRNA genes are located within *Hox*-clusters (**Fig. 4.5**) and share the expression patterns of nearby *Hox* genes (Pearson et al., 2005). Furthermore, these miRNAs have predicted target sites in *Hox* gene 3' UTRs (Pearson et al., 2005). This is significant because *Hox*-cluster genes help establish axial patterning of animal bodies, and loss-of-function mutations of *Hox*-cluster genes in flies and mice can result in the transformation of body regions to fates appropriate for more posterior regions (Deschamps and van Nes, 2005; Iimura and Pourquie, 2007; Turner and Mahowald, 1979; Wellik, 2007). In mouse, posterior transformations of vertebral segments in the axial skeleton and abnormalities in the appendicular skeleton of the limbs are among the most obvious mutant phenotypes in *Hox* gene mutants [reviewed by (Deschamps and van Nes, 2005)]. Three major families of miRNA genes, *Mirn10, Mirn196*, and *Mirn615,* are located in conserved sites within the *Hox* clusters of animal genomes (Tanzer et al., 2005).

Hox-embedded miRNAs are highly conserved across species, suggesting that they could function in the evolution of the axial skeleton. *Mirn615* lies in the intron of *Hox5* and is likely limited to mammals (Griffiths-Jones et al., 2008); its functions have not yet been investigated, although it is expressed in at least two human colon adenocarcinoma cell lines and a human kidney epithelial line (Cummins et al., 2006; Landgraf et al., 2007). *Mirn10* was originally identified between *Dfd* (*Hox4*) and *Scr* (*Hox5*) in a fruitfly, a mosquito, and a flour beetle (Lagos-Quintana et al., 2001). It occupies orthologous genomic locations in sea urchin, amphioxus, fish, and mammals (Tanzer et al., 2005). When the *Hox* clusters duplicated from one to four in the genome duplication events that occurred at about the time of the vertebrate radiation (R1 and R2) (Dehal and Boore, 2005; Gibson and Spring, 2000; Spring, 1997) and once again just before the teleost radiation (R3) (Amores et al., 1998; Jaillon et al., 2004; Postlethwait et al., 2002; Postlethwait et al., 1998a; Taylor et al., 2003), these *mirn* genes were duplicated with them, although some paralogs have become secondarily lost (Tanzer et al., 2005). We had shown that the zebrafish possesses duplicates of three of the four tetrapod *Hox* clusters, but has a single *Hoxd* cluster (Amores et al., 1998). Despite the loss of all protein-coding genes in the *hoxdb* cluster, the zebrafish lineage surprisingly retained a copy of *mirn10* in the expected genomic location of the *hoxdb* cluster (Woltering and Durston, 2006). This finding suggests that the selective pressure was greater for maintaining the duplicated *mirn10* gene than for retaining duplicates of the *hoxd* protein coding genes. Interestingly, the pufferfish lineage lost all of the protein-coding genes in its *hoxcb* cluster, but even the *miRNAs* of the *hoxcb* cluster have disappeared in pufferfish, in contrast to the *hoxdb* cluster in zebrafish, (Tanzer et al., 2005; Tanzer and Stadler, 2006; Woltering and Durston, 2006). As a result, both pufferfish and zebrafish have five *mirn10* genes, but by different genomic mechanisms. These curious results emphasize the evolutionary importance of miRNAs. It is possible that the zebrafish and pufferfish lineages both retained five copies of *mirn10* after the teleost genome duplication compared to the two copies present in mammals for stoichiometric reasons.

We know that *mirn10* acts in axial patterning because miR-10 represses *hoxb1a* and *hoxb3a* in the spinal cord working cooperatively with *hoxb4.*

Moving along the *Hox* clusters, *Mirn196* lies 5' of *Hox9* paralogs in tetrapods and teleosts (Tanzer et al., 2005), and in the sea lamprey, a basally diverging vertebrate, there are at least two paralogs of *mirn196* (Heimberg et al., 2008; Tanzer et al., 2005). *Mirn196* regulates the expression of *Hoxb8* in mesoderm that is fated to form the forelimb skeleton of chicken and potentially mouse by facilitating cleavage of *Hoxb8* mRNA, although the functional role of this interaction during skeletal morphogenesis remains unclear (Hornstein et al., 2005; Yekta et al., 2004).

The similarity of the expression patterns of *Hox*-cluster *Mirn* genes to *Hox* genes with their predicted targets and the tantalizing results so far available suggests that mis-regulation of *Mirn10* and *Mirn196* might result in skeletal defects similar to those induced by mutations in *Hox* genes. Because *Hox*-cluster miRNAs have multiple *Hox* genes as predicted targets, however, much work will be required to test any of these predictions. A solution to the problem will require more experiments conducted in developing embryos.

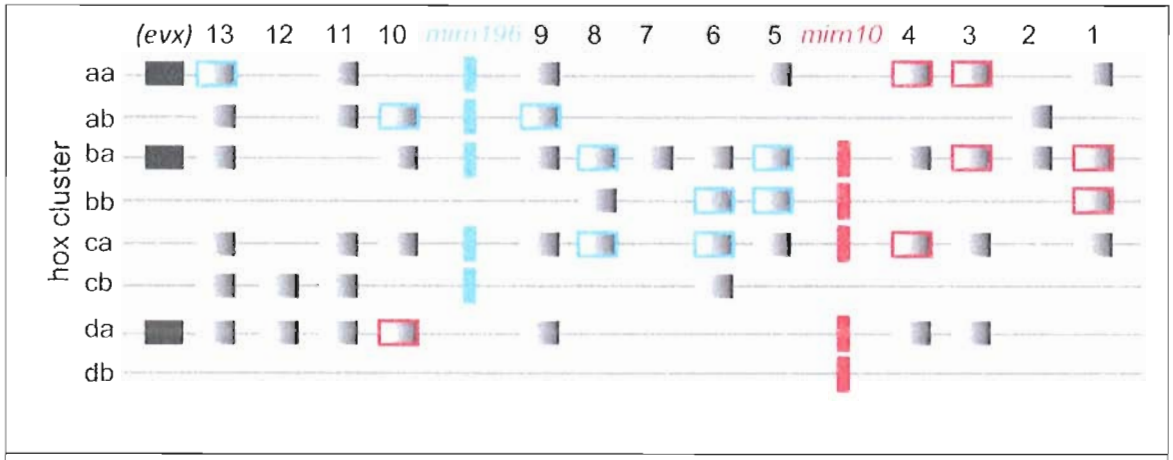

Fig. 4.5. *Hox* Genes Are Predicted Targets for *Mirn10* and *Mirn196*. Due to genome duplication and subsequent gene loss, zebrafish retains seven clusters of *hox* genes (gradient grey boxes) that include five copies of *mirn196* (blue boxes) and five copies of *mirn10* (red boxes). Although protein coding genes of the zebrafish *hoxdb* cluster were lost, this cluster retained a copy of *mirn10*. The *mirn10* (gradient grey boxes with red surroundings) and *mirn196* (gradient grey boxes with blue surroundings) genes both have multiple *hox* genes as computationally predicted targets.

4.10. MicroRNAs and Microevolution: A Hypothesis

MiRNAs are highly conserved in sequence and regulate spatial and temporal expression of other genes during development. The evolution of new miRNA families across species diversity (macroevolution) has accompanied explosions of evolutionary innovation, such as the origin of vertebrates (Heimberg et al., 2008; Hertel et al., 2006). Evidence is sparse, however, about the functional roles of newly evolved *Mirn*s in establishing morphological differences between individuals or populations within a species or between closely related species (microevolution).

Not only do the families of miRNAs found in different lineages differ, but the expression patterns for orthologous *Mirn*s can differ in different species. A comparison of the expression patterns of about 100 miRNAs in medaka fish and chicken with existing

data for zebrafish and mouse showed that the timing and location of miRNA expression varies much more than miRNA structure (Ason et al., 2006). Differences in expression can be associated with changes in miRNA copy number, genomic context, or both between species. For the skeletal system, seven of nine *mirn*s exhibited delayed or different expression patterns in mouse and zebrafish (*mirn27a, mirn27b, mirn140, mirn140*, mirn199a, mirn199a**, and *mirn214*), while two that were expressed strongly in zebrafish showed weak expression or no expression in medaka fish, (*mirn145* and *mirn146*). The degree to which these variations in expression pattern might account for developmental or morphological differences between species has not yet been investigated.

Besides variation between species of vertebrates, variation also exists among individuals within populations. Tourette's syndrome (TS), for example, is a neuropsychiatric disease with a strong genetic component, and 2 of 174 TS patients, but 0 of 3600 control chromosomes, had sequence polymorphisms in the binding site for human miR-189 in the 3' UTR of the mRNA for *SLITRK1*, which encodes a single-pass transmembrane protein (Abelson et al., 2005). Brain regions implicated in Tourette's syndrome co-express *MIRN189* and *SLITRK1*, consistent with the hypothesis that the miRNA regulates expression of the *SLITRK1* gene. These results suggest that miRNAs may play a role in psychiatric disease. In another example, a DNA sequence in the serotonin receptor 1B (HTR1B) mRNA confers repression by miR-96, but a common human polymorphism changes a nucleotide critical for miR-96 binding. Loss of *HTR18* function causes an aggressive phenotype in mice (Jensen et al., 2008), and people with the miR-96 binding site on the *HTR18* message reported more disorderly behavior than individuals with the alternative allele. These studies show that variations in miRNA binding sites exist among individuals within populations and further suggest that these polymorphisms are linked to phenotypes that could be selected upon during evolution.

Because the nuanced differences in skeletal morphology that differentiate related populations are likely to be caused by subtle changes in intensity or duration or spatial

distribution of gene expression patterns, and because miRNAs provide that sort of variation in activity, we suspect that miRNAs may play an important role in microevolution of new morphologies (Plasterk, 2006). We advance the specific hypothesis that diverging lineages can accumulate polymorphisms in *Mirn* expression patterns or in sequence variation in miR binding sites of skeletal development genes that alters the strength or quantity of miRNA binding to their targets, and hence changes the activity of target genes, thereby modifying cell proliferation, cell migration, cell differentiation, or cell function in ways that cause sister lineages to diverge in phenotypes in ways that adapt them to their environments. Experiments to test this hypothesis require well-understood developmental mechanisms of miRNA action coupled to studies investigating the variation of miRNA binding sites within target genes and mechanistic investigations of the consequences of such changes. Resolution of the problem, however, awaits these exciting prospects.

4.11. Skeletal MiRNAs and Skeletal Diseases of Aging

Skeletons generally become less robust as people age, culminating in osteopenias and osteoporosis, or grow inappropriately, resulting in osteoarthritis. In addition, miRNAs are involved in the aging process, at least in the nematode *Caenorhabditis elegans*, where reducing lin-4 activity shortens life span and over-expressing lin-4 extends life span (Boehm and Slack, 2005). Skeletal tissue can arise from mesenchymal stem cells (MSC), which can produce not only osteocytes and chondrocytes for bone and cartilage development, but also adipocytes for maintaining fat tissue(Wagner et al., 2008). As mammalian MSCs age in culture, they experience a reduction in the spectrum of derivatives they can form (Bonab et al., 2006). Correlated with this age-related diminution of differentiative capacity, at least four miRNAs are significantly up-regulated in senescent relative to young MSC (hsa-mir-371, hsamir-369-5P, hsa-mir-29c, and hsa-mir-499) (Wagner et al., 2008). Whether these or other miRNAs are up-regulated in aging skeletal systems in older people is as yet unknown. These results, however,

suggest the hypothesis that osteopenias, osteoarthritis, or other skeletal conditions in older people may result at least in part by an inappropriate changes in the differentiation potential of mesenchymal stem cells arising from, or associated with, changes in the levels of specific miRNAs (**Fig. 4.6**). The targets of miRNAs that are up-regulated in senescing MSCs remain a mystery, but these targets may play a causative role in skeletal aging. MiRNA-based therapies provide a promise for the future, for example the use of antisense to specific miRNAs to prevent them from associating with their endogenous targets or the use of synthetic miRNAs to lower the expression levels of pathogenic targets. Thus, the identification of miRNAs involved in skeletal diseases and their targets might lead to novel miRNA-based therapies for osteopenias, osteoporosis, osteoarthritis, and other skeletal diseases that accompany old age.

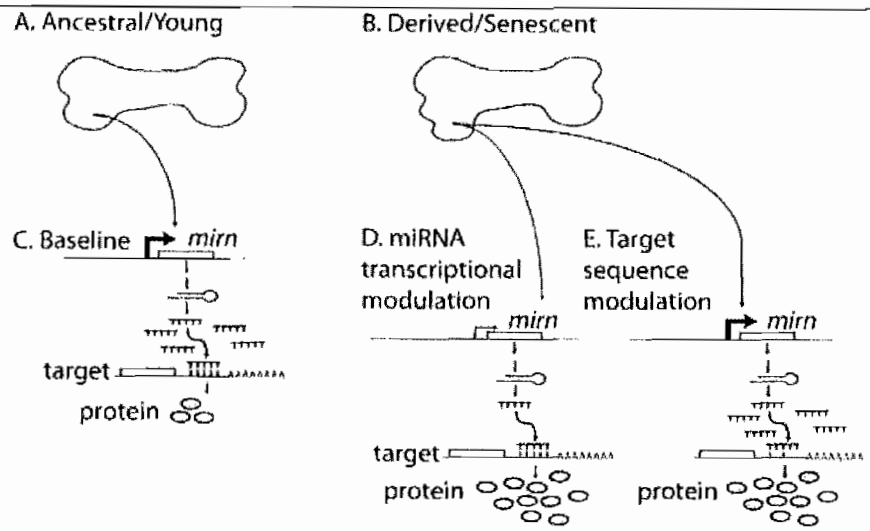

Fig. 4.6. A Model for the Roles of MiRNAs in Evolution and Disease. A. A representation of a skeletal element in an evolutionarily ancestral state, or a young or healthy condition. B. A representation of a skeletal element in an evolutionarily derived state, or a senescent or diseased condition. C. In the baseline condition, the *mirn* gene produces a given level of miR molecules, which bind to their target site with a certain affinity to allow a specific level of translation. D. In the evolutionarily derived state, cis-acting enhancer mutations may decrease or increase (not shown) transcription of the *mirn* gene, which would lead to decreased (or increased, not shown) inhibition of the target mRNA and hence increased (or decreased, not shown) amounts of target protein, which could alter skeletal shape or function. Similar diminution of *mirn* expression could occur by stage specific changes in *mirn* transcription or epigenetic modifications. E. Mutations accumulated during evolution could alter the miRNA recognition site on target mRNAs to increase or decrease binding, which could alter the amount of target protein produced compared to baseline. Altered protein levels could alter the morphologies or the relative rates of skeletal build-up or degradation by osteoblasts and osteoclasts.

CHAPTER V

CONCLUSION

5.1. MicroRNAs and Development

MicroRNAs (miRNAs) are small non-coding RNAs that are about 22 nucleotides (nts) long. There are hundreds of miRNA genes in each metazoan genome. MiRNAs either induce cleavage of target messenger RNAs (mRNAs) or inhibit target mRNA translation to regulate target gene expression.

MiRNAs can regulate a large portion of the transcriptome *in vivo*. It is predicted that at least 60% of genes in human genome are subject to the regulation by miRNAs. Previous studies from over-expression and/or knockdown of individual miRNAs confirmed that miRNAs are widely involved in development and homeostasis. Thus, miRNAs impose an addition layer of gene regulation at the post-transcriptional level.

In zebrafish, at least 352 miRNAs have been identified and most of these miRNAs are conserved across vertebrates [miRBase, http://www.miRBase.org, release 15, April 2010 (Griffiths-Jones et al., 2006; Griffiths-Jones et al., 2008)]. Previous expression study (Wienholds et al., 2005) showed that most of zebrafish miRNAs are expressed in a tissue- and time-specific manner. My study results provided in this manuscript showed that two of these miRNAs, miR-140 (*mir140*) and miR-196 (*mir196*), specifically regulate zebrafish skeletogenesis in two different aspects. MiR-140 specifically regulates zebrafish palate formation by regulating neural crest migration; while miR-196 regulates axial and appendage skeletal development by tuning the body pattern formation. Thus, my studies on these two miRNAs provide good examples by showing that miRNAs are

extensively involved in the regulation of various aspects of zebrafish skeletal development.

5.2. MicroRNA *Mir140* and *Mir196*

5.2.1. MicroRNA *Mir140* Regulates Palatogenesis

Studies in zebrafish, medaka and chicken showed that microRNA miR-140 is strongly and specifically expressed in the developing cartilage tissues (Antin et al., 2007; Ason et al., 2006; Eberhart et al., 2008; Hicks et al., 2008; Wienholds et al., 2005). Chapter II of this manuscript showed that miR-140 is involved in the regulation of palatogenesis in zebrafish by regulating the *platelet derived growth factor alpha* (*pdgfra*) gene expression. Mis-regulation of miR-140 as well as mutation of *pdgfra* gene induced cleft lip and palate in zebrafish (Eberhart et al., 2008). Mutation of *pdgfra* gene in either mice or human can result in cleft lip and palate disease (Ding et al., 2004; Soriano, 1997b; Tallquist and Soriano, 2003a). Thus, the functional role of *pdgfra* as well as miR-140 is likely conserved among fish and other vertebrates.

The zebrafish palate is composed by post-migratory neural crest. Failure in the migration or differentiation of neural crest cells result in defective palate formation (Wada et al., 2005; Yan et al., 2002; Yan et al., 2005). The regulation of zebrafish palatogenesis by miR-140 is through the modulation of neural crest cell migration too (Eberhart et al., 2008). Thus, not only the function of *pdgfra* is conserved between zebrafish and other vertebrates, the manner of action of *pdgfra* gene is also conserved.

The genomic location of miR-140 gene is conserved in the intron of the E3 ubiquitin protein ligase gene *wwp2* between fish and human (Eberhart et al., 2008). It was reported that miR-140 is regulating HDAC4 in cultured cells (Tuddenham et al. 2006). It was also found that miR-140 is also related to tumor malignant progression (Malzkorn et al. 2009). Thus, miR-140 is not only involved in the early skeletogenesis, but is also important for homeostasis after development. Asahara and colleagues revealed that miR-140 is

expressed in articular cartilages (Miyaki et al., 2009). Its expression is significantly reduced in osteoarthritis (OA). They also found that miR-140 down-regulates ADAMTS5 expression, which is linked to the progress of OA(Miyaki et al., 2009). The same group also found that miR-140 plays a critical role in the pathogenesis of OA by partially regulating ADAMTS5. Knockout of miR-140 in mice induced age-related OA while overexpression of miR-140 in chondrocytes protects the animal from OA (Miyaki et al., 2009; Miyaki et al., 2010). These result showed that miR-140 is also involved in later stages of skeletogenesis.

Thus, my zebrafish miR-140 study provides a good example to gain insight into the understanding of the role of microRNAs in development of skeletal systems and implies the possibility of understand microRNA function in disease model study. However, to fully understand the function of a specific miRNA, both early stages during animal development and the late stage to maintain the homeostasis should be studied.

5.2.2. MicroRNA *Mir196* Controls Zebrafish Skeletal Patterning

The zebrafish genome contains five copies of miR-196 (*mir196*) genes that were derived from whole genome duplication events (He et al., 2009a). Similar to their genomic neighbor *Hox*-cluster protein coding genes, the *hox9* and *hox10* homologs, miR-196 genes are expressed in the central nerve system and the pectoral fins of the developing zebrafish. Other studies on mice and chicken have confirmed that miR-196 can regulate multiple *Hox*-cluster protein coding genes including *hoxA7, hoxB7, hoxB8, hoxD8,* and members of *hox9* and *hox10,* indicating the complexity of miR-196 regulation and its function (Hornstein et al., 2005; McGlinn et al., 2009b; Yekta et al., 2004). MiR-196 binds to a *HoxB8* mRNA 3'UTR which carries a perfect binding site for miR-196, thereby accelerating its cleavage, and this interaction has been hypothesized to be important for the outgrowth of hindlimb buds (Hornstein et al., 2005). Knockdown of miR-196 in chicken embryos leads to a homoeotic transformation of a cervical vertebra to thoracic identity (McGlinn et al., 2009b). However, since miR-196 is more broadly

expressed, it is still unknown the function of miR-196 in other tissues at other developmental stages. Thus, we do not yet fully understand the roles of miR-196 in development or the mechanisms by which it acts. In my study, overexpression and knockdown of miR-196 in zebrafish at the early embryonic stage showed that miR-196 controls zebrafish pharyngeal arch segmentation, controls anterior axial skeletal segmentation. MiR-196 overexpression inhibits pectoral fin initiation by reducing *retinoic acid receptor alpha-b* (*rarab*) expression through which miR-196 interacts with RA signaling. These findings indicated that miR-196 is acting as an embryonic patterning gene during the early developmental stage.

In vertebrates, *Hox*-cluster protein coding genes control the anterior-posterior body axis, including the identity of vertebrae and pharyngeal arches and the axes of body appendages. My study still did not identify the target gene(s) that governs the segmentation of pharyngeal arches and axial skeleton in zebrafish. Since *hox* genes are extensively involved in the regulation of the pharyngeal arch segmentation, I expected that one or multiple *hox* genes are involved in this process. To test this hypothesis, I have tried to knockdown the expression of *hox5, hox6* and *hox8* homologs in zebrafish, but unfortunately, I did not see pharyngeal arch segmentation defects. Previous studies showed that RA treatment or depletion of RA by treating with DEAB can result in disrupted pharyngeal arch segmentation. However, treatment of either RA or DEAB usually induce missing of multiple pharyngeal arches, which contradicts with the phenotype I observed, overexpression or knockdown of miR-196 induced deletion or insertion of one, and only one, specific pharyngeal arch. Thus, it is still unclear how miR-196 controls pharyngeal arch segmentation.

My study also did not identify the target gene for miR-196 to control the segmentation of vertebrae in zebrafish. The segmentation phenotype resulted from miR-196 mis-regulation is likely due to defects during the early somitogenesis stage since miR-196 overexpression can induce a shortened body length compared to wild-type fish. *Hox* gene mutations can delete vertebrae or transform vertebral identities and remove or

reduce limb skeletal elements. Knocking down of the predicted miR-196 targets, *hox5, hox6* and *hox8* homologs, however, did not cause segmentation defects I observed in miR-196 mis-regulation. However, some *Hox* genes are themselves directly regulated by RA signal. Thus, it is still possible that miR-196 exerts its controlling function over axial skeletal segmentation, together with pectoral fin initiation, through RA signal.

5.3. Conclusions of MicroRNA Studies in Skeletogenesis

In conclusion, I found that miR-140 regulates palatogenesis by modulating the expression of *pdgfra* gene. The regulatory mechanism is likely to be conserved among vertebrate species. I also showed that the precise levels of miR-196 are required to initiate development of the pectoral appendage, to develop the correct number of pharyngeal arches, and to specify the number and identity of rostral vertebrae and ribs. I have shown that miR-196 acts on pectoral appendage development by altering retinoic acid signaling via fine-tuning the expression of retinoic acid receptor Rarab, a previously unknown mechanism for appendage patterning.

REFERENCES

Abelson, J. F., Kwan, K. Y., O'Roak, B. J., Baek, D. Y., Stillman, A. A., Morgan, T. M., Mathews, C. A., Pauls, D. L., Rasin, M. R., Gunel, M. et al. (2005). Sequence variants in SLITRK1 are associated with Tourette's syndrome. *Science* 310, 317-20.

Aboobaker, A. A., Tomancak, P., Patel, N., Rubin, G. M. and Lai, E. C. (2005). Drosophila microRNAs exhibit diverse spatial expression patterns during embryonic development. *Proc Natl Acad Sci U S A* 102, 18017-22.

Adams, J. Adler, C. Aggarwal, M. M. Ahammed, Z. Amonett, J. Anderson, B. D. Anderson, M. Arkhipkin, D. Averichev, G. S. Badyal, S. K. et al. (2003). Pion-Kaon correlations in central Au+Au collisions at square root [sNN] = 130 GeV. *Phys Rev Lett* 91, 262302.

Albertson, R. C., Streelman, J. T. and Kocher, T. D. (2003). Genetic basis of adaptive shape differences in the cichlid head. *J Hered* 94, 291-301.

Amores, A., Force, A., Yan, Y. L., Joly, L., Amemiya, C., Fritz, A., Ho, R. K., Langeland, J., Prince, V., Wang, Y. L. et al. (1998). Zebrafish hox clusters and vertebrate genome evolution. *Science* 282, 1711-4.

Antin, P. B., Kaur, S., Stanislaw, S., Davey, S., Konieczka, J. H., Yatskievych, T. A. and Darnell, D. K. (2007). Gallus expression in situ hybridization analysis: a chicken embryo gene expression database. *Poult Sci* 86, 1472-7.

Antonchuk, J., Sauvageau, G. and Humphries, R. K. (2001). HOXB4 overexpression mediates very rapid stem cell regeneration and competitive hematopoietic repopulation. *Exp Hematol* 29, 1125-34.

Ason, B., Darnell, D. K., Wittbrodt, B., Berezikov, E., Kloosterman, W. P., Wittbrodt, J., Antin, P. B. and Plasterk, R. H. (2006). Differences in vertebrate microRNA expression. *Proc Natl Acad Sci U S A* 103, 14385-9.

Bachler, M. and Neubuser, A. (2001). Expression of members of the Fgf family and their receptors during midfacial development. *Mech Dev* 100, 313-6.

Bayha, E., Jorgensen, M. C., Serup, P. and Grapin-Botton, A. (2009). Retinoic acid signaling organizes endodermal organ specification along the entire antero-posterior axis. *PLoS ONE* 4, e5845.

Begemann, G., Schilling, T. F., Rauch, G. J., Geisler, R. and Ingham, P. W. (2001). The zebrafish neckless mutation reveals a requirement for raldh2 in mesodermal signals that pattern the hindbrain. *Development* 128, 3081-94.

Behm-Ansmant, I., Rehwinkel, J., Doerks, T., Stark, A., Bork, P. and Izaurralde, E. (2006a). mRNA degradation by miRNAs and GW182 requires both CCR4:NOT deadenylase and DCP1:DCP2 decapping complexes. *Genes Dev* 20, 1885-98.

Behm-Ansmant, I., Rehwinkel, J. and Izaurralde, E. (2006b). MicroRNAs silence gene expression by repressing protein expression and/or by promoting mRNA decay. *Cold Spring Harb Symp Quant Biol* 71, 523-30.

Berezikov, E., Chung, W. J., Willis, J., Cuppen, E. and Lai, E. C. (2007). Mammalian mirtron genes. *Mol Cell* 28, 328-36.

Bernstein, E., Kim, S. Y., Carmell, M. A., Murchison, E. P., Alcorn, H., Li, M. Z., Mills, A. A., Elledge, S. J., Anderson, K. V. and Hannon, G. J. (2003). Dicer is essential for mouse development. *Nat Genet* 35, 215-7.

Betsholtz, C., Karlsson, L. and Lindahl, P. (2001). Developmental roles of platelet-derived growth factors. *Bioessays* 23, 494-507.

Bird, N. C. and Mabee, P. M. (2003). Developmental morphology of the axial skeleton of the zebrafish, Danio rerio (Ostariophysi: Cyprinidae). *Dev Dyn* 228, 337-57.

Birkholz, D. A., Olesnicky Killian, E. C., George, K. M. and Artinger, K. B. (2009). Prdm1a is necessary for posterior pharyngeal arch development in zebrafish. *Dev Dyn* 238, 2575-87.

Blair, H. C., Zaidi, M. and Schlesinger, P. H. (2002). Mechanisms balancing skeletal matrix synthesis and degradation. *Biochem J* 364, 329-41.

Boehm, M. and Slack, F. (2005). A developmental timing microRNA and its target regulate life span in C. elegans. *Science* 310, 1954-7.

Bonab, M. M., Alimoghaddam, K., Talebian, F., Ghaffari, S. H., Ghavamzadeh, A. and Nikbin, B. (2006). Aging of mesenchymal stem cell in vitro. *BMC Cell Biol* 7, 14.

Bostrom, H., Willetts, K., Pekny, M., Leveen, P., Lindahl, P., Hedstrand, H., Pekna, M., Hellstrom, M., Gebre-Medhin, S., Schalling, M. et al. (1996). PDGF-A signaling is a critical event in lung alveolar myofibroblast development and alveogenesis. *Cell* 85, 863-73.

Bruce, A. E., Oates, A. C., Prince, V. E. and Ho, R. K. (2001). Additional hox clusters in the zebrafish: divergent expression patterns belie equivalent activities of duplicate hoxB5 genes. *Evol Dev* 3, 127-44.

Brugmann, S. A., Goodnough, L. H., Gregorieff, A., Leucht, P., ten Berge, D., Fuerer, C., Clevers, H., Nusse, R. and Helms, J. A. (2007). Wnt signaling mediates regional specification in the vertebrate face. *Development* 134, 3283-95.

Burke, A. C., Nelson, C. E., Morgan, B. A. and Tabin, C. (1995). Hox genes and the evolution of vertebrate axial morphology. *Development* 121, 333-46.

Cancedda, R., Castagnola, P., Cancedda, F. D., Dozin, B. and Quarto, R. (2000). Developmental control of chondrogenesis and osteogenesis. *Int J Dev Biol* 44, 707-14.

Chen, F. and Capecchi, M. R. (1997). Targeted mutations in hoxa-9 and hoxb-9 reveal synergistic interactions. *Dev Biol* 181, 186-96.

Chen, J. F., Mandel, E. M., Thomson, J. M., Wu, Q., Callis, T. E., Hammond, S. M., Conlon, F. L. and Wang, D. Z. (2006). The role of microRNA-1 and microRNA-133 in skeletal muscle proliferation and differentiation. *Nat Genet* 38, 228-33.

Chen, L. and Deng, C. X. (2005). Roles of FGF signaling in skeletal development and human genetic diseases. *Front Biosci* 10, 1961-76.

Clarke, N. J. and Sanseau, P. (2006). MicroRNA : biology, function, and expression. Eagleville, PA: DNA Press.

Crump, J. G., Maves, L., Lawson, N. D., Weinstein, B. M. and Kimmel, C. B. (2004). An essential role for Fgfs in endodermal pouch formation influences later craniofacial skeletal patterning. *Development* 131, 5703-16.

Cummins, J. M., He, Y., Leary, R. J., Pagliarini, R., Diaz, L. A., Jr., Sjoblom, T., Barad, O., Bentwich, Z., Szafranska, A. E., Labourier, E. et al. (2006). The colorectal microRNAome. *Proc Natl Acad Sci U S A* 103, 3687-92.

Darnell, D. K., Kaur, S., Stanislaw, S., Konieczka, J. H., Yatskievych, T. A. and Antin, P. B. (2007). MicroRNA expression during chick embryo development. *Dev Dyn* 236, 333.

Darnell, D. K., Kaur, S., Stanislaw, S., Konieczka, J. K., Yatskievych, T. A. and Antin, P. B. (2006). MicroRNA expression during chick embryo development. *Dev Dyn* 235, 3156-65.

Davis, A. P., Witte, D. P., Hsieh-Li, H. M., Potter, S. S. and Capecchi, M. R. (1995). Absence of radius and ulna in mice lacking hoxa-11 and hoxd-11. *Nature* 375, 791-5.

Day, T. F. and Yang, Y. (2008). Wnt and hedgehog signaling pathways in bone development. *J Bone Joint Surg Am* 90 Suppl 1, 19-24.

Dehal, P. and Boore, J. L. (2005). Two rounds of whole genome duplication in the ancestral vertebrate. *PLoS Biol* 3, e314.

Deng, H. W., Chen, W. M., Recker, S., Stegman, M. R., Li, J. L., Davies, K. M., Zhou, Y., Deng, H., Heaney, R. and Recker, R. R. (2000). Genetic determination of Colles' fracture and differential bone mass in women with and without Colles' fracture. *J Bone Miner Res* 15, 1243-52.

Denli, A. M., Tops, B. B., Plasterk, R. H., Ketting, R. F. and Hannon, G. J. (2004). Processing of primary microRNAs by the Microprocessor complex. *Nature* 432, 231-5.

Dennison, E., Mohamed, M. A. and Cooper, C. (2006). Epidemiology of osteoporosis. *Rheum Dis Clin North Am* 32, 617-29.

Depew, M. J., Simpson, C. A., Morasso, M. and Rubenstein, J. L. (2005). Reassessing the Dlx code: the genetic regulation of branchial arch skeletal pattern and development. *J Anat* 207, 501-61.

Deschamps, J. and van Nes, J. (2005). Developmental regulation of the Hox genes during axial morphogenesis in the mouse. *Development* 132, 2931-42.

Ding, H., Wu, X., Bostrom, H., Kim, I., Wong, N., Tsoi, B., O'Rourke, M., Koh, G. Y., Soriano, P., Betsholtz, C. et al. (2004). A specific requirement for PDGF-C in palate formation and PDGFR-alpha signaling. *Nat Genet* 36, 1111-6.

Draper, B. W., Stock, D. W. and Kimmel, C. B. (2003). Zebrafish fgf24 functions with fgf8 to promote posterior mesodermal development. *Development* 130, 4639-54.

Drin, I., Schoket, B., Kostic, S. and Vincze, I. (1994). Smoking-related increase in O6-alkylguanine-DNA alkyltransferase activity in human lung tissue. *Carcinogenesis* 15, 1535-9.

Duboule, D. and Morata, G. (1994). Colinearity and functional hierarchy among genes of the homeotic complexes. *Trends Genet* 10, 358-64.

Duchek, P., Somogyi, K., Jekely, G., Beccari, S. and Rorth, P. (2001). Guidance of cell migration by the Drosophila PDGF/VEGF receptor. *Cell* 107, 17-26.

Dupe, V., Ghyselinck, N. B., Thomazy, V., Nagy, L., Davies, P. J., Chambon, P. and Mark, M. (1999). Essential roles of retinoic acid signaling in interdigital apoptosis and control of BMP-7 expression in mouse autopods. *Dev Biol* 208, 30-43.

Eberhart, J. K., He, X., Swartz, M. E., Yan, Y. L., Song, H., Boling, T. C., Kunerth, A. K., Walker, M. B., Kimmel, C. B. and Postlethwait, J. H. (2008). MicroRNA Mirn140 modulates Pdgf signaling during palatogenesis. *Nat Genet* 40, 290-8.

Eberhart, J. K., Swartz, M. E., Crump, J. G. and Kimmel, C. B. (2006). Early Hedgehog signaling from neural to oral epithelium organizes anterior craniofacial development. *Development* 133, 1069-77.

Ehlen, H. W., Buelens, L. A. and Vortkamp, A. (2006). Hedgehog signaling in skeletal development. *Birth Defects Res C Embryo Today* 78, 267-79.

Emoto, Y., Wada, H., Okamoto, H., Kudo, A. and Imai, Y. (2005). Retinoic acid-metabolizing enzyme Cyp26a1 is essential for determining territories of hindbrain and spinal cord in zebrafish. *Dev Biol* 278, 415-27.

Ericson, J. U., Krauss, S. and Fjose, A. (1993). Genomic sequence and embryonic expression of the zebrafish homeobox gene hox-3.4. *Int J Dev Biol* 37, 263-72.

Finnerty, J. R., Pang, K., Burton, P., Paulson, D. and Martindale, M. Q. (2004). Origins of bilateral symmetry: Hox and dpp expression in a sea anemone. *Science* 304, 1335-7.

Fisher, S. and Halpern, M. E. (1999). Patterning the zebrafish axial skeleton requires early chordin function. *Nat Genet* 23, 442-6.

Foppiano, S., Hu, D. and Marcucio, R. S. (2007). Signaling by bone morphogenetic proteins directs formation of an ectodermal signaling center that regulates craniofacial development. *Dev Biol* 312, 103-14.

Friedman, R. C., Farh, K. K., Burge, C. B. and Bartel, D. P. (2009). Most mammalian mRNAs are conserved targets of microRNAs. *Genome Res* 19, 92-105.

Gammill, L. S., Gonzalez, C. and Bronner-Fraser, M. (2007). Neuropilin 2/semaphorin 3F signaling is essential for cranial neural crest migration and trigeminal ganglion condensation. *Dev Neurobiol* 67, 47-56.

Garcia-Gasca, A. and Spyropoulos, D. D. (2000). Differential mammary morphogenesis along the anteroposterior axis in Hoxc6 gene targeted mice. *Dev Dyn* 219, 261-76.

Garrity, D. M., Childs, S. and Fishman, M. C. (2002). The heartstrings mutation in zebrafish causes heart/fin Tbx5 deficiency syndrome. *Development* 129, 4635-45.

Gehring, W. J., Kloter, U. and Suga, H. (2009). Evolution of the Hox gene complex from an evolutionary ground state. *Curr Top Dev Biol* 88, 35-61.

Gibert, Y., Gajewski, A., Meyer, A. and Begemann, G. (2006). Induction and prepatterning of the zebrafish pectoral fin bud requires axial retinoic acid signaling. *Development* 133, 2649-59.

Gibson, T. J. and Spring, J. (2000). Evidence in favour of ancient octaploidy in the vertebrate genome. *Biochem. Soc, Trans.* 28, 259-264.

Giraldez, A. J., Cinalli, R. M., Glasner, M. E., Enright, A. J., Thomson, J. M., Baskerville, S., Hammond, S. M., Bartel, D. P. and Schier, A. F. (2005). MicroRNAs regulate brain morphogenesis in zebrafish. *Science* 308, 833-8.

Giraldez, A. J., Mishima, Y., Rihel, J., Grocock, R. J., Van Dongen, S., Inoue, K., Enright, A. J. and Schier, A. F. (2006). Zebrafish MiR-430 promotes deadenylation and clearance of maternal mRNAs. *Science* 312, 75-9.

Goldring, M. B., Tsuchimochi, K. and Ijiri, K. (2006). The control of chondrogenesis. *J Cell Biochem* 97, 33-44.

Grande, T. and Young, B. (2005). The ontogeny and homology of the Weberian apparatus in the zebrafish Danio rerio (Ostariophysi: Cypriniformes). *Zoological Journal of the Linnean Society* 104, 241-254.

Grandel, H., Lun, K., Rauch, G. J., Rhinn, M., Piotrowski, T., Houart, C., Sordino, P., Kuchler, A. M., Schulte-Merker, S., Geisler, R. et al. (2002). Retinoic acid signalling in the zebrafish embryo is necessary during pre-segmentation stages to pattern the anterior-posterior axis of the CNS and to induce a pectoral fin bud. *Development* 129, 2851-65.

Gregory, R. I., Yan, K. P., Amuthan, G., Chendrimada, T., Doratotaj, B., Cooch, N. and Shiekhattar, R. (2004). The Microprocessor complex mediates the genesis of microRNAs. *Nature* 432, 235-40.

Griffiths-Jones, S., Grocock, R. J., van Dongen, S., Bateman, A. and Enright, A. J. (2006). miRBase: microRNA sequences, targets and gene nomenclature. *Nucleic Acids Res* 34, D140-4.

Griffiths-Jones, S., Saini, H. K., van Dongen, S. and Enright, A. J. (2008). miRBase: tools for microRNA genomics. *Nucleic Acids Res* 36, D154-8.

Gruntmanis, U. (2007). Male osteoporosis: deadly, but ignored. *Am J Med Sci* 333, 85-92.

Hale, L. A., Tallafuss, A., Yan, Y. L., Dudley, L., Eisen, J. S. and Postlethwait, J. H. (2006). Characterization of the retinoic acid receptor genes raraa, rarab and rarg during zebrafish development. *Gene Expr Patterns* 6, 546-55.

Harfe, B. D., McManus, M. T., Mansfield, J. H., Hornstein, E. and Tabin, C. J. (2005). The RNaseIII enzyme Dicer is required for morphogenesis but not patterning of the vertebrate limb. *Proc Natl Acad Sci U S A* 102, 10898-903.

He, L. and Hannon, G. J. (2004). MicroRNAs: small RNAs with a big role in gene regulation. *Nat Rev Genet* 5, 522-31.

He, X., Eberhart, J. K. and Postlethwait, J. H. (2009a). MicroRNAs and micromanaging the skeleton in disease, development and evolution. *J Cell Mol Med* 13, 606-18.

He, X., Eberhart, J. K. and Postlethwait, J. H. (2009b). MicroRNAs and micromanaging the skeleton in disease, development, and evolution. *J Cell Mol Med.*

Heimberg, A. M., Sempere, L. F., Moy, V. N., Donoghue, P. C. and Peterson, K. J. (2008). MicroRNAs and the advent of vertebrate morphological complexity. *Proc Natl Acad Sci U S A* 105, 2946-50.

Hertel, J., Lindemeyer, M., Missal, K., Fried, C., Tanzer, A., Flamm, C., Hofacker, I. L. and Stadler, P. F. (2006). The expansion of the metazoan microRNA repertoire. *BMC Genomics* 7, 25.

Hicks, J. A., Tembhurne, P. and Liu, H. C. (2008). MicroRNA expression in chicken embryos. *Poult Sci* 87, 2335-43.

Hilliard, S. A., Yu, L., Gu, S., Zhang, Z. and Chen, Y. P. (2005). Regional regulation of palatal growth and patterning along the anterior-posterior axis in mice. *J Anat* 207, 655-67.

Ho, L., Symes, K., Yordan, C., Gudas, L. J. and Mercola, M. (1994). Localization of PDGF A and PDGFR alpha mRNA in Xenopus embryos suggests signalling from neural ectoderm and pharyngeal endoderm to neural crest cells. *Mech Dev* 48, 165-74.

Hoekstra, H. E. and Coyne, J. A. (2007). The locus of evolution: evo devo and the genetics of adaptation. *Evolution Int J Org Evolution* 61, 995-1016.

Holmbeck, K. (2005). Collagenase in cranial morphogenesis. *Cells Tissues Organs* 181, 154-65.

Horan, G. S., Kovacs, E. N., Behringer, R. R. and Featherstone, M. S. (1995). Mutations in paralogous Hox genes result in overlapping homeotic transformations of the axial skeleton: evidence for unique and redundant function. *Dev Biol* 169, 359-72.

Hornstein, E., Mansfield, J. H., Yekta, S., Hu, J. K., Harfe, B. D., McManus, M. T., Baskerville, S., Bartel, D. P. and Tabin, C. J. (2005). The microRNA miR-196 acts upstream of Hoxb8 and Shh in limb development. *Nature* 438, 671-4.

Hornstein, E. and Shomron, N. (2006). Canalization of development by microRNAs. *Nat Genet* 38 Suppl, S20-4.

Hou, W., Tian, Q., Zheng, J. and Bonkovsky, H. L. (2009). MicroRNA-196 represses Bach1 protein and HCV gene expression in human hepatoma cells expressing hepatitis C viral proteins. *Hepatology*.

Hsu, S. D., Chu, C. H., Tsou, A. P., Chen, S. J., Chen, H. C., Hsu, P. W., Wong, Y. H., Chen, Y. H., Chen, G. H. and Huang, H. D. (2008). miRNAMap 2.0: genomic maps of microRNAs in metazoan genomes. *Nucleic Acids Res* 36, D165-9.

Hu, D. and Helms, J. A. (1999). The role of sonic hedgehog in normal and abnormal craniofacial morphogenesis. *Development* 126, 4873-84.

Huang, R., Zhi, Q., Patel, K., Wilting, J. and Christ, B. (2000). Contribution of single somites to the skeleton and muscles of the occipital and cervical regions in avian embryos. *Anat Embryol (Berl)* 202, 375-83.

Hunt, P., Clarke, J. D., Buxton, P., Ferretti, P. and Thorogood, P. (1998). Stability and plasticity of neural crest patterning and branchial arch Hox code after extensive cephalic crest rotation. *Dev Biol* 198, 82-104.

Hurria, A., Leung, D., Trainor, K., Borgen, P., Norton, L. and Hudis, C. (2003). Factors influencing treatment patterns of breast cancer patients age 75 and older. *Crit Rev Oncol Hematol* 46, 121-6.

Huysseune, A. and Sire, J. Y. (1992). Development of cartilage and bone tissues of the anterior part of the mandible in cichlid fish: a light and TEM study. *Anat Rec* 233, 357-75.

Iimura, T. and Pourquie, O. (2007). Hox genes in time and space during vertebrate body formation. *Dev Growth Differ* 49, 265-75.

Jaillon, O., Aury, J. M., Brunet, F., Petit, J. L., Stange-Thomann, N., Mauceli, E., Bouneau, L., Fischer, C., Ozouf-Costaz, C., Bernot, A. et al. (2004). Genome duplication in the teleost fish Tetraodon nigroviridis reveals the early vertebrate proto-karyotype. *Nature* 431, 946-57.

Jarinova, O., Hatch, G., Poitras, L., Prudhomme, C., Grzyb, M., Aubin, J., Berube-Simard, F. A., Jeannotte, L. and Ekker, M. (2008). Functional resolution of duplicated hoxb5 genes in teleosts. *Development* 135, 3543-53.

Jaskiewicz, L. and Filipowicz, W. (2008). Role of Dicer in posttranscriptional RNA silencing. *Curr Top Microbiol Immunol* 320, 77-97.

Javidan, Y. and Schilling, T. F. (2004). Development of cartilage and bone. *Methods Cell Biol* 76, 415-36.

Jeannotte, L., Lemieux, M., Charron, J., Poirier, F. and Robertson, E. J. (1993). Specification of axial identity in the mouse: role of the Hoxa-5 (Hox1.3) gene. *Genes Dev* 7, 2085-96.

Jensen, K. P., Covault, J., Conner, T. S., Tennen, H., Kranzler, H. R. and Furneaux, H. M. (2008). A common polymorphism in serotonin receptor 1B mRNA moderates regulation by miR-96 and associates with aggressive human behaviors. *Mol Psychiatry.*

Jiang, J., Lee, E. J. and Schmittgen, T. D. (2006). Increased expression of microRNA-155 in Epstein-Barr virus transformed lymphoblastoid cell lines. *Genes Chromosomes Cancer* 45, 103-6.

Jing, Q., Huang, S., Guth, S., Zarubin, T., Motoyama, A., Chen, J., Di Padova, F., Lin, S. C., Gram, H. and Han, J. (2005). Involvement of microRNA in AU-rich element-mediated mRNA instability. *Cell* 120, 623-34.

Jugessur, A., Lie, R. T., Wilcox, A. J., Murray, J. C., Taylor, J. A., Saugstad, O. D., Vindenes, H. A. and Abyholm, F. (2003). Variants of developmental genes (TGFA, TGFB3, and MSX1) and their associations with orofacial clefts: a case-parent triad analysis. *Genet Epidemiol* 24, 230-9.

Kanellopoulou, C., Muljo, S. A., Kung, A. L., Ganesan, S., Drapkin, R., Jenuwein, T., Livingston, D. M. and Rajewsky, K. (2005). Dicer-deficient mouse embryonic stem cells are defective in differentiation and centromeric silencing. *Genes Dev* 19, 489-501.

Kawakami, Y., Rodriguez-Leon, J. and Belmonte, J. C. (2006). The role of TGFbetas and Sox9 during limb chondrogenesis. *Curr Opin Cell Biol* 18, 723-9.

Kawasaki, H. and Taira, K. (2004). MicroRNA-196 inhibits HOXB8 expression in myeloid differentiation of HL60 cells. *Nucleic Acids Symp Ser (Oxf)*, 211-2.

Kidner, C. A. and Martienssen, R. A. (2005). The developmental role of microRNA in plants. *Curr Opin Plant Biol* 8, 38-44.

Kim, V. N. (2004). MicroRNA precursors in motion: exportin-5 mediates their nuclear export. *Trends Cell Biol* 14, 156-9.

Kimmel, C. B., Ullmann, B., Walker, M., Miller, C. T. and Crump, J. G. (2003). Endothelin 1-mediated regulation of pharyngeal bone development in zebrafish. *Development* 130, 1339-51.

Kobayashi, T., Lu, J., Cobb, B. S., Rodda, S. J., McMahon, A. P., Schipani, E., Merkenschlager, M. and Kronenberg, H. M. (2008). Dicer-dependent pathways regulate chondrocyte proliferation and differentiation. *Proc Natl Acad Sci U S A* 105, 1949-54.

Komori, T. (2003). Requisite roles of Runx2 and Cbfb in skeletal development. *J Bone Miner Metab* 21, 193-7.

Kopinke, D., Sasine, J., Swift, J., Stephens, W. Z. and Piotrowski, T. (2006). Retinoic acid is required for endodermal pouch morphogenesis and not for pharyngeal endoderm specification. *Dev Dyn* 235, 2695-709.

Koudijs, M. J., den Broeder, M. J., Groot, E. and van Eeden, F. J. (2008). Genetic analysis of the two zebrafish patched homologues identifies novel roles for the hedgehog signaling pathway. *BMC Dev Biol* 8, 15.

Kronenberg, H. M. (2006). PTHrP and skeletal development. *Ann N Y Acad Sci* 1068, 1-13.

Lagos-Quintana, M., Rauhut, R., Lendeckel, W. and Tuschl, T. (2001). Identification of novel genes coding for small expressed RNAs. *Science* 294, 853-8.

Landgraf, P., Rusu, M., Sheridan, R., Sewer, A., Iovino, N., Aravin, A., Pfeffer, S., Rice, A., Kamphorst, A. O., Landthaler, M. et al. (2007). A mammalian microRNA expression atlas based on small RNA library sequencing. *Cell* 129, 1401-14.

Lawson, N. D. and Weinstein, B. M. (2002). In vivo imaging of embryonic vascular development using transgenic zebrafish. *Dev Biol* 248, 307-18.

Lee, C. T., Risom, T. and Strauss, W. M. (2006). MicroRNAs in mammalian development. *Birth Defects Res C Embryo Today* 78, 129-39.

Lee, R. C., Feinbaum, R. L. and Ambros, V. (1993). The C. elegans heterochronic gene lin-4 encodes small RNAs with antisense complementarity to lin-14. *Cell* 75, 843-54.

Lee, Y., Ahn, C., Han, J., Choi, H., Kim, J., Yim, J., Lee, J., Provost, P., Radmark, O., Kim, S. et al. (2003). The nuclear RNase III Drosha initiates microRNA processing. *Nature* 425, 415-9.

Lee, Y., Kim, M., Han, J., Yeom, K. H., Lee, S., Baek, S. H. and Kim, V. N. (2004). MicroRNA genes are transcribed by RNA polymerase II. *Embo J* 23, 4051-60.

Lefebvre, V. and Smits, P. (2005). Transcriptional control of chondrocyte fate and differentiation. *Birth Defects Res C Embryo Today* 75, 200-12.

Lewis, B. P., Burge, C. B. and Bartel, D. P. (2005). Conserved seed pairing, often flanked by adenosines, indicates that thousands of human genes are microRNA targets. *Cell* 120, 15-20.

Lewis, J., Hanisch, A. and Holder, M. (2009). Notch signaling, the segmentation clock, and the patterning of vertebrate somites. *J Biol* 8, 44.

Linville, A., Radtke, K., Waxman, J. S., Yelon, D. and Schilling, T. F. (2009). Combinatorial roles for zebrafish retinoic acid receptors in the hindbrain, limbs and pharyngeal arches. *Dev Biol* 325, 60-70.

Liu, L., Chong, S. W., Balasubramaniyan, N. V., Korzh, V. and Ge, R. (2002). Platelet-derived growth factor receptor alpha (pdgfr-alpha) gene in zebrafish embryonic development. *Mech Dev* 116, 227-30.

Lund, A. H. (2009). miR-10 in development and cancer. *Cell Death Differ.*

Lund, E., Guttinger, S., Calado, A., Dahlberg, J. E. and Kutay, U. (2004). Nuclear export of microRNA precursors. *Science* 303, 95-8.

Ma, L., Teruya-Feldstein, J. and Weinberg, R. A. (2007). Tumour invasion and metastasis initiated by microRNA-10b in breast cancer. *Nature* 449, 682-8.

Mabee, P. M., Olmstead, K. L. and Cubbage, C. C. (2000). An experimental study of intraspecific variation, developmental timing, and heterochrony in fishes. *Evolution* 54, 2091-106.

Mathonnet, G., Fabian, M. R., Svitkin, Y. V., Parsyan, A., Huck, L., Murata, T., Biffo, S., Merrick, W. C., Darzynkiewicz, E., Pillai, R. S. et al. (2007). MicroRNA inhibition of translation initiation in vitro by targeting the cap-binding complex eIF4F. *Science* 317, 1764-7.

Matranga, C., Tomari, Y., Shin, C., Bartel, D. P. and Zamore, P. D. (2005). Passenger-strand cleavage facilitates assembly of siRNA into Ago2-containing RNAi enzyme complexes. *Cell* 123, 607-20.

McClintock, J. M., Kheirbek, M. A. and Prince, V. E. (2002). Knockdown of duplicated zebrafish hoxb1 genes reveals distinct roles in hindbrain patterning and a novel mechanism of duplicate gene retention. *Development* 129, 2339-54.

McGlinn, E., Yekta, S., Mansfield, J. H., Soutschek, J., Bartel, D. P. and Tabin, C. J. (2009a). In ovo application of antagomiRs indicates a role for miR-196 in patterning the chick axial skeleton through Hox gene regulation. *Proc Natl Acad Sci U S A.*

McGlinn, E., Yekta, S., Mansfield, J. H., Soutschek, J., Bartel, D. P. and Tabin, C. J. (2009b). In ovo application of antagomiRs indicates a role for miR-196 in patterning the chick axial skeleton through Hox gene regulation. *Proc Natl Acad Sci U S A* 106, 18610-5.

McIntyre, D. C., Rakshit, S., Yallowitz, A. R., Loken, L., Jeannotte, L., Capecchi, M. R. and Wellik, D. M. (2007). Hox patterning of the vertebrate rib cage. *Development* 134, 2981-9.

McLennan, R. and Kulesa, P. M. (2007). In vivo analysis reveals a critical role for neuropilin-1 in cranial neural crest cell migration in chick. *Dev Biol* 301, 227-39.

Mercader, N. (2007). Early steps of paired fin development in zebrafish compared with tetrapod limb development. *Dev Growth Differ* 49, 421-37.

Mercader, N., Fischer, S. and Neumann, C. J. (2006). Prdm1 acts downstream of a sequential RA, Wnt and Fgf signaling cascade during zebrafish forelimb induction. *Development* 133, 2805-15.

Mercader, N., Tanaka, E. M. and Torres, M. (2005). Proximodistal identity during vertebrate limb regeneration is regulated by Meis homeodomain proteins. *Development* 132, 4131-42.

Miller, C. T., Schilling, T. F., Lee, K., Parker, J. and Kimmel, C. B. (2000). sucker encodes a zebrafish Endothelin-1 required for ventral pharyngeal arch development. *Development* 127, 3815-28.

Miller, C. T., Yelon, D., Stainier, D. Y. and Kimmel, C. B. (2003). Two endothelin 1 effectors, hand2 and bapx1, pattern ventral pharyngeal cartilage and the jaw joint. *Development* 130, 1353-65.

Minoux, M., Antonarakis, G. S., Kmita, M., Duboule, D. and Rijli, F. M. (2009). Rostral and caudal pharyngeal arches share a common neural crest ground pattern. *Development* 136, 637-45.

Miyaki, S., Nakasa, T., Otsuki, S., Grogan, S. P., Higashiyama, R., Inoue, A., Kato, Y., Sato, T., Lotz, M. K. and Asahara, H. (2009). MicroRNA-140 is expressed in differentiated human articular chondrocytes and modulates interleukin-1 responses. *Arthritis Rheum* 60, 2723-30.

Miyaki, S., Sato, T., Inoue, A., Otsuki, S., Ito, Y., Yokoyama, S., Kato, Y., Takemoto, F., Nakasa, T., Yamashita, S. et al. (2010). MicroRNA-140 plays dual roles in both cartilage development and homeostasis. *Genes Dev* 24, 1173-85.

Morin-Kensicki, E. M., Melancon, E. and Eisen, J. S. (2002). Segmental relationship between somites and vertebral column in zebrafish. *Development* 129, 3851-60.

N, L. and BM, W. (2002). In vivo imiagining of embryonic vascular development using transgenic zebrafish. *Developmental Biology* 248, 307–318.

Nagel, M., Tahinci, E., Symes, K. and Winklbauer, R. (2004). Guidance of mesoderm cell migration in the Xenopus gastrula requires PDGF signaling. *Development* 131, 2727-36.

Nair, V. and Zavolan, M. (2006). Virus-encoded microRNAs: novel regulators of gene expression. *Trends Microbiol* 14, 169-75.

National_Osteoporosis_Foundation. (2007). About Osteoporosis.

Neff, M. M., Neff, J. D., Chory, J. and Pepper, A. E. (1998). dCAPS, a simple technique for the genetic analysis of single nucleotide polymorphisms: experimental applications in Arabidopsis thaliana genetics. *Plant J* 14, 387-92.

Neuhauss, S. C., Solnica-Krezel, L., Schier, A. F., Zwartkruis, F., Stemple, D. L., Malicki, J., Abdelilah, S., Stainier, D. Y. and Driever, W. (1996). Mutations affecting craniofacial development in zebrafish. *Development* 123, 357-67.

Niederreither, K., Subbarayan, V., Dolle, P. and Chambon, P. (1999). Embryonic retinoic acid synthesis is essential for early mouse post-implantation development. *Nat Genet* 21, 444-8.

Nielsen, K. E., Rasmussen, J., Kumar, R., Wengel, J., Jacobsen, J. P. and Petersen, M. (2004). NMR studies of fully modified locked nucleic acid (LNA) hybrids: solution structure of an LNA:RNA hybrid and characterization of an LNA:DNA hybrid. *Bioconjug Chem* 15, 449-57.

NIH. (2001). Consensus Development Panel on Osteoporosis Prevention.

Nolte, C., Amores, A., Nagy Kovacs, E., Postlethwait, J. and Featherstone, M. (2003). The role of a retinoic acid response element in establishing the anterior neural expression border of Hoxd4 transgenes. *Mech Dev* 120, 325-35.

Nottrott, S., Simard, M. J. and Richter, J. D. (2006). Human let-7a miRNA blocks protein production on actively translating polyribosomes. *Nat Struct Mol Biol* 13, 1108-14.

O'Driscoll, L. (2006). The emerging world of microRNAs. *Anticancer Res* 26, 4271-8.

Okazaki, K. and Sandell, L. J. (2004). Extracellular matrix gene regulation. *Clin Orthop Relat Res*, S123-8.

Oliver, G., De Robertis, E. M., Wolpert, L. and Tickle, C. (1990). Expression of a homeobox gene in the chick wing bud following application of retinoic acid and grafts of polarizing region tissue. *Embo J* 9, 3093-9.

Ornitz, D. M. (2005). FGF signaling in the developing endochondral skeleton. *Cytokine Growth Factor Rev* 16, 205-13.

Orr-Urtreger, A., Bedford, M. T., Do, M. S., Eisenbach, L. and Lonai, P. (1992). Developmental expression of the alpha receptor for platelet-derived growth factor, which is deleted in the embryonic lethal Patch mutation. *Development* 115, 289-303.

Osumi-Yamashita, N., Ninomiya, Y., Doi, H. and Eto, K. (1994). The contribution of both forebrain and midbrain crest cells to the mesenchyme in the frontonasal mass of mouse embryos. *Dev Biol* 164, 409-19.

Parichy, D. M. and Johnson, S. L. (2001). Zebrafish hybrids suggest genetic mechanisms for pigment pattern diversification in *Danio*. *Dev. Genes Evol.* 211, 319-328.

Pearson, J. C., Lemons, D. and McGinnis, W. (2005). Modulating Hox gene functions during animal body patterning. *Nat Rev Genet* 6, 893-904.

Pelat, T., Hust, M., Laffly, E., Condemine, F., Bottex, C., Vidal, D., Lefranc, M. P., Dubel, S. and Thullier, P. (2007). High-affinity, human antibody-like antibody fragment (single-chain variable fragment) neutralizing the lethal factor (LF) of Bacillus anthracis by inhibiting protective antigen-LF complex formation. *Antimicrob Agents Chemother* 51, 2758-64.

Perz-Edwards, A., Hardison, N. L. and Linney, E. (2001). Retinoic acid-mediated gene expression in transgenic reporter zebrafish. *Dev Biol* 229, 89-101.

Petersen, C. P., Bordeleau, M. E., Pelletier, J. and Sharp, P. A. (2006). Short RNAs repress translation after initiation in mammalian cells. *Mol Cell* 21, 533-42.

Plasterk, R. H. (2006). Micro RNAs in animal development. *Cell* 124, 877-81.

Postlethwait, J. H., Amores, A., Yan, G. and Austin, C. A. (2002). Duplication of a portion of human chromosome 20q containing Topoisomerase (Top1) and Snail genes provides evidence on genome expansion and the radiation of teleost fish. In *Aquatic Genomics: Steps Toward a Great Future*, (ed. N. Shimizu T. Aoki I. Hirono and F. Takashima), pp. 20-31. Tokyo: Springer-Verlag.

Postlethwait, J. H. and Schneiderman, H. A. (1969). A clonal analysis of determination in Antennapedia a homoeotic mutant of Drosophila melanogaster. *Proc Natl Acad Sci U S A* 64, 176-83.

Postlethwait, J. H., Yan, Y.-L., Gates, M., Horne, S., Amores, A., Brownlie, A., Donovan, A., Egan, E., Force, A., Gong, Z. et al. (1998a). Vertebrate genome evolution and the zebrafish gene map. *Nat Genet* 18, 345-349.

Postlethwait, J. H., Yan, Y. L., Gates, M. A., Horne, S., Amores, A., Brownlie, A., Donovan, A., Egan, E. S., Force, A., Gong, Z. et al. (1998b). Vertebrate genome evolution and the zebrafish gene map. *Nat Genet* 18, 345-9.

Pruett, N. D., Visconti, R. P., Jacobs, D. F., Scholz, D., McQuinn, T., Sundberg, J. P. and Awgulewitsch, A. (2008). Evidence for Hox-specified positional identities in adult vasculature. *BMC Dev Biol* 8, 93.

Rancourt, D. E., Tsuzuki, T. and Capecchi, M. R. (1995). Genetic interaction between hoxb-5 and hoxb-6 is revealed by nonallelic noncomplementation. *Genes Dev* 9, 108-22.

Rand, T. A., Petersen, S., Du, F. and Wang, X. (2005). Argonaute2 cleaves the anti-guide strand of siRNA during RISC activation. *Cell* 123, 621-9.

Rebagliati, M. R., Toyama, R., Fricke, C., Haffter, P. and Dawid, I. B. (1998). Zebrafish nodal-related genes are implicated in axial patterning and establishing left-right asymmetry. *Dev Biol* 199, 261-72.

Reinhart, B. J., Slack, F. J., Basson, M., Pasquinelli, A. E., Bettinger, J. C., Rougvie, A. E., Horvitz, H. R. and Ruvkun, G. (2000). The 21-nucleotide let-7 RNA regulates developmental timing in Caenorhabditis elegans. *Nature* 403, 901-6.

Rijli, F. M., Matyas, R., Pellegrini, M., Dierich, A., Gruss, P., Dolle, P. and Chambon, P. (1995). Cryptorchidism and homeotic transformations of spinal nerves and vertebrae in Hoxa-10 mutant mice. *Proc Natl Acad Sci U S A* 92, 8185-9.

Riley, B. M., Mansilla, M. A., Ma, J., Daack-Hirsch, S., Maher, B. S., Raffensperger, L. M., Russo, E. T., Vieira, A. R., Dode, C., Mohammadi, M. et al. (2007). Impaired FGF signaling contributes to cleft lip and palate. *Proc Natl Acad Sci U S A* 104, 4512-7.

Robu, M. E., Larson, J. D., Nasevicius, A., Beiraghi, S., Brenner, C., Farber, S. A. and Ekker, S. C. (2007). p53 activation by knockdown technologies. *PLoS Genet* 3, e78.

Roessler, E., Belloni, E., Gaudenz, K., Jay, P., Berta, P., Scherer, S. W., Tsui, L. C. and Muenke, M. (1996). Mutations in the human Sonic Hedgehog gene cause holoprosencephaly. *Nat Genet* 14, 357-60.

Ruby, J. G., Jan, C. H. and Bartel, D. P. (2007). Intronic microRNA precursors that bypass Drosha processing. *Nature* 448, 83-6.

Rusinov, V., Baev, V., Minkov, I. N. and Tabler, M. (2005). MicroInspector: a web tool for detection of miRNA binding sites in an RNA sequence. *Nucleic Acids Res* 33, W696-700.

Sakaguchi, S., Nakatani, Y., Takamatsu, N., Hori, H., Kawakami, A., Inohaya, K. and Kudo, A. (2006). Medaka unextended-fin mutants suggest a role for Hoxb8a in cell migration and osteoblast differentiation during appendage formation. *Dev Biol* 293, 426-38.

Samee, N., de Vernejoul, M. C. and Levi, G. (2007). Role of DLX regulatory proteins in osteogenesis and chondrogenesis. *Crit Rev Eukaryot Gene Expr* 17, 173-86.

Schneider, R. A. and Helms, J. A. (2003). The cellular and molecular origins of beak morphology. *Science* 299, 565-8.

Sears, K. E., Behringer, R. R., Rasweiler, J. J. t. and Niswander, L. A. (2006). Development of bat flight: morphologic and molecular evolution of bat wing digits. *Proc Natl Acad Sci U S A* 103, 6581-6.

Shalgi, R., Lieber, D., Oren, M. and Pilpel, Y. (2007). Global and Local Architecture of the Mammalian microRNA-Transcription Factor Regulatory Network. *PLoS Comput Biol* 3, e131.

Song, L. and Tuan, R. S. (2006). MicroRNAs and cell differentiation in mammalian development. *Birth Defects Res C Embryo Today* 78, 140-9.

Soriano, P. (1997a). The PDGF alpha receptor is required for neural crest cell development and for normal patterning of the somites. *Development* 124, 2691-2700.

Soriano, P. (1997b). The PDGF alpha receptor is required for neural crest cell development and for normal patterning of the somites. *Development* 124, 2691-700.

Spring, J. (1997). Vertebrate evolution by interspecific hybridization — are we polyploid? *Fed. Eur. Biol. Soc. Lett.* 400, 2-8.

Tallquist, M. D. and Soriano, P. (2003a). Cell autonomous requirement for PDGFRalpha in populations of cranial and cardiac neural crest cells. *Development* 130, 507-18.

Tallquist, M. D. and Soriano, P. (2003b). Cell autonomous requirement for PDGFRalpha in populations of cranial and cardiac neural crest cells. *Development* 130, 507-518.

Tallquist, M. D., Weismann, K. E., Hellstrom, M. and Soriano, P. (2000). Early myotome specification regulates PDGFA expression and axial skeleton development. *Development* 127, 5059-70.

Tanzer, A., Amemiya, C. T., Kim, C. B. and Stadler, P. F. (2005). Evolution of microRNAs located within Hox gene clusters. *J Exp Zoolog B Mol Dev Evol* 304, 75-85.

Tanzer, A. and Stadler, P. F. (2006). Evolution of microRNAs. *Methods Mol Biol* 342, 335-50.

Taylor, J., Braasch, I., Frickey, T., Meyer, A. and Van De Peer, Y. (2003). Genome duplication, a trait shared by 22,000 species of ray-finned fish. *Genome Res.* 13, 382-390.

Thisse, C., and Thisse, B. . (2005). High Throughput Expression Analysis of ZF-Models Consortium Clones. *ZFIN Direct Data Submission (http://zfin.org).*

Tomari, Y., Matranga, C., Haley, B., Martinez, N. and Zamore, P. D. (2004). A protein sensor for siRNA asymmetry. *Science* 306, 1377-80.

Trainor, P. (2003). Development. The bills of qucks and duails. *Science* 299, 523-4.

Trainor, P. A. and Krumlauf, R. (2001). Hox genes, neural crest cells and branchial arch patterning. *Curr Opin Cell Biol* 13, 698-705.

Trainor, P. A., Melton, K. R. and Manzanares, M. (2003). Origins and plasticity of neural crest cells and their roles in jaw and craniofacial evolution. *Int J Dev Biol* 47, 541-53.

Trevarrow, B., Marks, D. L. and Kimmel, C. B. (1990). Organization of hindbrain segments in the zebrafish embryo. *Neuron* 4, 669-79.

Tuddenham, L., Wheeler, G., Ntounia-Fousara, S., Waters, J., Hajihosseini, M. K., Clark, I. and Dalmay, T. (2006). The cartilage specific microRNA-140 targets histone deacetylase 4 in mouse cells. *FEBS Lett* 580, 4214-7.

Turner, F. R. and Mahowald, A. P. (1979). Scanning electron microscopy of Drosophila melanogaster embryogenesis. III. Formation of the head and caudal segments. *Dev Biol* 68, 96-109.

van den Akker, E., Fromental-Ramain, C., de Graaff, W., Le Mouellic, H., Brulet, P., Chambon, P. and Deschamps, J. (2001). Axial skeletal patterning in mice lacking all paralogous group 8 Hox genes. *Development* 128, 1911-21.

Vega, R. B., Matsuda, K., Oh, J., Barbosa, A. C., Yang, X., Meadows, E., McAnally, J., Pomajzl, C., Shelton, J. M., Richardson, J. A. et al. (2004). Histone deacetylase 4 controls chondrocyte hypertrophy during skeletogenesis. *Cell* 119, 555-66.

Vella, M. C., Choi, E. Y., Lin, S. Y., Reinert, K. and Slack, F. J. (2004). The C. elegans microRNA let-7 binds to imperfect let-7 complementary sites from the lin-41 3'UTR. *Genes Dev* 18, 132-7.

Velleman, S. G. (2000). The role of the extracellular matrix in skeletal development. *Poult Sci* 79, 985-9.

Wada, N., Javidan, Y., Nelson, S., Carney, T. J., Kelsh, R. N. and Schilling, T. F. (2005). Hedgehog signaling is required for cranial neural crest morphogenesis and chondrogenesis at the midline in the zebrafish skull. *Development* 132, 3977-88.

Wagner, E. M., Jen, K. L., Artiss, J. D. and Remaley, A. T. (2008). Dietary alpha-cyclodextrin lowers low-density lipoprotein cholesterol and alters plasma fatty acid profile in low-density lipoprotein receptor knockout mice on a high-fat diet. *Metabolism* 57, 1046-51.

Walensky, N. A. (1965). A Study of Anterior Femoral Curvature in Man. *Anat Rec* 151, 559-70.

Walker, M. and Kimmel, C. (2007). A two-color acid-free cartilage and bone stain for zebrafish larvae. *Biotech Histochem* 82, 23-8.

Walker, M. B., Miller, C. T., Coffin Talbot, J., Stock, D. W. and Kimmel, C. B. (2006). Zebrafish furin mutants reveal intricacies in regulating Endothelin1 signaling in craniofacial patterning. *Dev Biol* 295, 194-205.

Walker, M. B., Miller, C. T., Swartz, M. E., Eberhart, J. K. and Kimmel, C. B. (2007). phospholipase C, beta 3 is required for Endothelin1 regulation of pharyngeal arch patterning in zebrafish. *Dev Biol* 304, 194-207.

Wang, B., Majumder, S., Nuovo, G., Kutay, H., Volinia, S., Patel, T., Schmittgen, T. D., Croce, C., Ghoshal, K. and Jacob, S. T. (2009). Role of microRNA-155 at early stages of hepatocarcinogenesis induced by choline-deficient and amino acid-defined diet in C57BL/6 mice. *Hepatology* 50, 1152-61.

Waxman, J. S., Keegan, B. R., Roberts, R. W., Poss, K. D. and Yelon, D. (2008). Hoxb5b acts downstream of retinoic acid signaling in the forelimb field to restrict heart field potential in zebrafish. *Dev Cell* 15, 923-34.

Wellik, D. M. (2007). Hox patterning of the vertebrate axial skeleton. *Dev Dyn* 236, 2454-63.

Wellik, D. M. (2009). Hox genes and vertebrate axial pattern. *Curr Top Dev Biol* 88, 257-78.

Wendling, O., Ghyselinck, N. B., Chambon, P. and Mark, M. (2001). Roles of retinoic acid receptors in early embryonic morphogenesis and hindbrain patterning. *Development* 128, 2031-8.

Westerfield, M. (1993). The Zebrafish Book; A guide for the laboratory use of zebrafish (Brachydanio rerio).

Westerfield, M. (1995). The Zebrafish Book. Eugene: The University of Oregon.

Wienholds, E., Kloosterman, W. P., Miska, E., Alvarez-Saavedra, E., Berezikov, E., de Bruijn, E., Horvitz, H. R., Kauppinen, S. and Plasterk, R. H. (2005). MicroRNA expression in zebrafish embryonic development. *Science* 309, 310-1.

Wightman, B., Ha, I. and Ruvkun, G. (1993). Posttranscriptional regulation of the heterochronic gene lin-14 by lin-4 mediates temporal pattern formation in C. elegans. *Cell* 75, 855-62.

Woltering, J. M. and Durston, A. J. (2006). The zebrafish hoxDb cluster has been reduced to a single microRNA. *Nat Genet* 38, 601-2.

Woltering, J. M. and Durston, A. J. (2008). MiR-10 represses HoxB1a and HoxB3a in zebrafish. *PLoS ONE* 3, e1396.

Wotton, K. R., Weierud, F. K., Dietrich, S. and Lewis, K. E. (2008). Comparative genomics of Lbx loci reveals conservation of identical Lbx ohnologs in bony vertebrates. *BMC Evol Biol* 8, 171.

Wray, G. A. (2007). The evolutionary significance of cis-regulatory mutations. *Nat Rev Genet* 8, 206-16.

Wu, X., Shi, W. and Cao, X. (2007). Multiplicity of BMP signaling in skeletal development. *Ann N Y Acad Sci* 1116, 29-49.

Yan, Y. L., Miller, C. T., Nissen, R. M., Singer, A., Liu, D., Kirn, A., Draper, B., Willoughby, J., Morcos, P. A., Amsterdam, A. et al. (2002). A zebrafish sox9 gene required for cartilage morphogenesis. *Development* 129, 5065-79.

Yan, Y. L., Willoughby, J., Liu, D., Crump, J. G., Wilson, C., Miller, C. T., Singer, A., Kimmel, C., Westerfield, M. and Postlethwait, J. H. (2005). A pair of Sox: distinct and overlapping functions of zebrafish sox9 co-orthologs in craniofacial and pectoral fin development. *Development* 132, 1069-83.

Yekta, S., Shih, I. H. and Bartel, D. P. (2004). MicroRNA-directed cleavage of HOXB8 mRNA. *Science* 304, 594-6.

Yekta, S., Tabin, C. J. and Bartel, D. P. (2008). MicroRNAs in the Hox network: an apparent link to posterior prevalence. *Nat Rev Genet* 9, 789-96.

Yu, H. H. and Moens, C. B. (2005). Semaphorin signaling guides cranial neural crest cell migration in zebrafish. *Dev Biol* 280, 373-85.

Zhang, Y., Chao, T., Li, R., Liu, W., Chen, Y., Yan, X., Gong, Y., Yin, B., Qiang, B., Zhao, J. et al. (2009). MicroRNA-128 inhibits glioma cells proliferation by targeting transcription factor E2F3a. *J Mol Med* 87, 43-51.